

# **Interference of Varicella-Zoster Virus (VZV) with the CD1 antigen presenting system on immature dendritic cells**

## **Dissertation**

zur Erlangung des akademischen Grades

doctor rerum naturalium  
(Dr. rer. nat.)

im Fach Biologie

eingereicht an der

Mathematisch-Naturwissenschaftlichen Fakultät I  
der Humboldt-Universität zu Berlin

von

Diplom-Biologin Cindy Gutzeit  
geboren am 27.01.1979 in Dresden

Präsident der Humboldt Universität zu Berlin  
Prof. Dr. Dr. h.c. Christoph Marksches

Dekan der Mathematisch-Naturwissenschaftlichen Fakultät I  
Prof. Dr. Lutz-Helmut Schön

Gutachter/in: 1. Prof. Carmen Scheibenbogen

2. Prof. Detlev H. Krüger

3. Prof. Andreas Sauerbrei

Tag der mündlichen Prüfung: 25. November 2009

## Zusammenfassung

Das strikt human pathogene Varicella-Zoster Virus (VZV) gehört zur Familie der Herpesviren und ist weltweit verbreitet. Die Seroprävalenz beträgt über 95%. Die Primärinfektion von VZV verursacht Varicellen (Windpocken), eine typische Krankheit bei Kindern, welche durch Fieber und einen disseminierten bläschenartigen Hautausschlag charakterisiert ist. Im Anschluss daran etabliert VZV eine lebenslange Latenz in sensorischen Ganglien und verursacht nach Reaktivierung Herpes Zoster (Gürtelrose). Dieser ist durch unilaterale, vesikuläre Eruptionen, meistens innerhalb eines Dermatoms, gekennzeichnet. Häufig treten nach Herpes Zoster schmerzhaftes Neuralgien auf. Seit 1995 wird ein Lebendimpfstoff aus attenuierten Virionen des VZV-Stammes V-Oka in den Vereinigten Staaten von Amerika erfolgreich eingesetzt, um Kinder gegen Varicellen zu immunisieren. Seit 2004 ist die Varicellen-Schutzimpfung für alle Kinder und Jugendlichen in Deutschland empfohlen worden. Im Gegensatz zur Infektion mit zirkulierenden virulenten VZV Stämmen tritt nach Verimpfung des Vakzin-Stammes V-Oka kein Exanthem auf. Entscheidend für die Eliminierung der VZV Infektion ist die T-Zell-vermittelte Immunität. Zudem korreliert die altersbedingte Abnahme der VZV-spezifischen T-Zell Immunität mit dem Anstieg der Inzidenz für Herpes Zoster und schmerzhaften Neuralgien.

Die Haut ist der Hauptreplikationsort von VZV. Immunologische Unterschiede zwischen virulenten VZV Stämmen und dem Vakzin-Stamm treten hier am deutlichsten auf. Diese Unterschiede wurden bisher noch nicht näher untersucht. Kutane Immunzellen, wie zum Beispiel Langerhans Zellen (LC), dermale Dendritische Zellen (DDC), inflammatorische Dendritische Zellen und intraepitheliale  $\gamma\delta$  T-Zellen sind entscheidend am Aufbau antiviraler Immunantworten beteiligt. In dieser Studie lag daher ein Fokus auf dem Vergleich von kutanen Immunantworten zwischen virulenten VZV-Stämmen und dem Vakzin-Stamm. Daher wurden klinische Isolate von VZV Genotypen, die in Europa zirkulieren, in diese Studie miteinbezogen.

In der vorliegenden Arbeit wurde das Verschwinden von LC in Hautläsionen von Herpes Zoster Patienten beobachtet. Im Gegensatz dazu, wurde eine massive Infiltration von myeloiden inflammatorischen DC nachgewiesen. Ferner wurde hier zum ersten Mal gezeigt, dass *ex vivo* isolierte LC und DDC permissiv für eine VZV Infektion sind. Von besonderer Bedeutung war die Erkenntnis, dass keine Unterschiede zwischen dem Vakzin-Stamm V-

Oka und virulentem VZV auftraten. *In vitro* Studien mit Monozyten abgeleiteten Dendritischen Zellen (DC), welche inflammatorische DC repräsentieren, zeigten, dass diese sowohl vom Vakzin-, als auch von virulentem VZV-Stamm mit gleicher Effizienz infiziert wurden. Erstaunlicherweise konnte eine signifikant erhöhte Expression von CD1c Molekülen auf VZV infizierten DC nachgewiesen werden. Funktionelle Untersuchungen mit intraepithelialen CD1c-restringierten  $\gamma\delta$  T Zellen zeigten, dass DC nach Infektion mit dem Vakzin-Stamm V-Oka phänotypisch und funktionell reiften und somit die  $\gamma\delta$  T Zellen zur IFN- $\gamma$  Sekretion stimulierten. Im Gegensatz dazu wurde die funktionelle Reifung von DC, die mit virulentem VZV infiziert waren, geblockt. Dieser Effekt war unabhängig vom Genotyp des verwendeten VZV-Stammes. Folglich wurde kein bioaktives IL-12 sezerniert, welches als entscheidendes Cytokin zum Aufbau einer antiviralen  $T_H1$  Immunantwort beiträgt. Darüber hinaus konnte gezeigt werden, dass virulentes VZV die Signalkaskade des Toll-like Rezeptors 2 (TLR2) in DC inhibiert und somit die IL-12 Produktion verhindert. Demzufolge wurde die IFN- $\gamma$  Sekretion von  $\gamma\delta$  T-Zellen verhindert.

In der vorliegenden Arbeit wurde eine neue Immunevasionsstrategie virulenter VZV Stämme entdeckt, welche erklären könnte, wie virulente VZV Stämme frühe antivirale Immunantworten umgehen und somit erfolgreich in der Haut replizieren. Zusätzlich konnte gezeigt werden, dass Kandidaten für Vakzinierungsstrategien nicht mit der Instruktion von DC interferieren sollten, um die Stimulation adaptiver Immunantworten zu gewährleisten. Daher könnten die gewonnen Erkenntnisse einen wichtigen Beitrag zur Entwicklung zukünftiger Vakzinierungsstrategien leisten.

## Summary

Varicella-zoster virus (VZV) which belongs to the family of herpesviruses is restricted to humans and distributed worldwide. The seroprevalence is over 95%. Primary infection of VZV causes chickenpox, a typical childhood disease characterized by fever and disseminated rash. Thereafter, VZV establishes a lifelong latency within sensory ganglia and can be reactivated to cause herpes zoster. This disease is characterized by lesions confined mostly to a single dermatome. A frequent complication of herpes zoster is the painful postherpetic neuralgia. Since 1995 the attenuated strain V-Oka of VZV is successfully used as vaccine in the United States of America to immunize children against VZV infection. In 2004 the vaccine was also licensed for Germany. In contrast to infection by circulating virulent VZV strains, vaccination with V-Oka remains asymptomatic. T cell mediated immunity is important to resolve VZV infection and an age related decline in VZV specific T cell mediated immunity is correlated with an increase of the incidence for herpes zoster and postherpetic neuralgia.

The skin is the major replication site of VZV and immunological differences between virulent VZV and the vaccine should become most apparent within this immune organ. However, these differences have not been elucidated so far. Cutaneous immune cells comprising epidermal Langerhans cells (LCs), dermal dendritic cells (DDCs), inflammatory dendritic cells and intraepithelial  $\gamma\delta$  T cells contribute to the induction of effective antiviral immune responses. Thus, the major focus of this study was to highlight cutaneous immune responses to virulent VZV strains as compared to the vaccine. Therefore, clinical isolates of circulating VZV genotypes in Europe were included in this study.

In this study the disappearance of LCs in skin lesions of herpes zoster patients was observed. In contrast, a strong infiltration of myeloid-derived inflammatory DCs has been detected. Furthermore, it has been shown for the first time that *ex vivo* isolated LCs and DDCs were permissive for VZV infection. Most importantly, no differences between the effects of the vaccine strain V-Oka and a virulent VZV strain have been observed. *In vitro* studies with monocyte-derived dendritic cells (DCs), reflecting inflammatory DCs, showed that they were efficiently infected by both, the vaccine and a virulent VZV strain. Intriguingly, a significant upregulation of CD1c molecules on VZV-infected DCs was observed. Func-



tional investigations using intraepithelial CD1c-restricted  $\gamma\delta$  T cells revealed that DCs infected with the vaccine virus were fully instructed to mature, thereby promoting IFN- $\gamma$  secretion of  $\gamma\delta$  T cells. In striking contrast, DCs infected with virulent VZV strains regardless of the virus genotype were efficiently blocked to mature functionally. In detail, they did not secrete bioactive IL-12 which is an instrumental cytokine for generation of antiviral T<sub>H</sub>1 responses. Moreover, virulent VZV blocked Toll-like receptor 2 (TLR2) signaling in DCs thereby preventing production of bioactive IL-12 which in turn inhibited IFN- $\gamma$  secretion by  $\gamma\delta$  T cells.

In summary, this study discovered a new immune evasion strategy of virulent VZV strains which might explain how virulent VZV strains overcome innate antiviral responses and successfully replicate within the skin thereby causing the typical rash. Moreover, the findings underline that candidate vaccines should not impair DC instruction in order to allow stimulation of powerful adaptive immune responses. Therefore, this study might have further implication for future vaccine design.

# Table of Contents

<b>Zusammenfassung .....</b>	<b>2</b>
<b>Summary .....</b>	<b>4</b>
<b>Abbreviations .....</b>	<b>8</b>
<b>1 Introduction .....</b>	<b>10</b>
1.1 Varicella-Zoster Virus (VZV) .....	10
1.2 VZV Pathogenesis .....	11
1.3 Immunity during Primary VZV Infection .....	13
1.4 Vaccination and Antiviral Therapy .....	14
1.5 Dendritic Cells: Linking Innate with Adaptive Immunity .....	16
1.6 Subsets of Dendritic Cells .....	19
1.7 Dendritic Cells of the Skin and the Induction of Viral Immune Response ...	20
1.8 Herpesviral Interference with DC Maturation and Function .....	22
1.9 Immune Evasion Mechanisms of VZV .....	23
1.10 CD1 Antigen Presentation .....	23
1.11 Viral Interference with CD1 Antigen Presentation .....	25
1.12 $\gamma\delta$ T Cells .....	25
1.13 Objectives of the Study .....	27
<b>2 Material and Methods .....</b>	<b>28</b>
2.1 Human Samples .....	28
2.1.1 Blood Samples .....	28
2.1.2 Isolation of Cutaneous Dendritic Cells .....	28
2.1.3 Skin Biopsies .....	30
2.2 Cells and Cell Lines .....	30
2.3 Cell Culture Medium .....	30
2.4 Viruses .....	31
2.5 Antibodies .....	32
2.6 Fluorescent Dyes .....	33
2.7 Chemicals .....	34
2.8 Buffers and Solutions .....	35
2.9 Kits .....	36
2.10 Equipment .....	36
2.11 Quantitative RT-PCR .....	37
2.12 Immunological Methods .....	37

2.12.1 Isolation of Monocytes from Buffy Coats .....	37
2.12.2 VZV Infection of Immature DCs.....	38
2.12.3 Flow Cytometry .....	39
2.12.4 Detection of Apoptotic Death .....	39
2.12.5 T Cell Assays .....	40
2.12.5.1 Cytokine Secretion Assay .....	40
2.12.5.2 Cytotoxicity Assay .....	40
2.12.6 ELISA.....	41
2.12.7 Immunohistochemistry .....	41
2.12.8 Immunoblot Analysis.....	42
2.13 Statistics.....	42
2.14 Software .....	42
<b>3 Results .....</b>	<b>43</b>
3.1 Propagation of VZV Strains in Fibroblasts .....	43
3.2 Distribution of DCs within Skin Lesions of Herpes Zoster Patients .....	45
3.3 VZV Infection of Cutaneous DCs.....	49
3.4 Phenotype of VZV Infected Cutaneous DCs .....	50
3.5 Transmission of VZV to Immature DCs.....	52
3.6 Phenotypic Changes of CD1 Molecules on VZV-infected iDCs .....	53
3.7 Impact of VZV induced CD1c Upregulation on Innate $\gamma\delta$ T Lymphocytes ...	55
3.8 Instruction of VZV-infected iDCs by CD1c-restricted $\gamma\delta$ T cells .....	60
3.9 Interference of VZV with the Co-Stimulatory Capacity of DCs.....	65
3.10 Block of TLR2 Signaling by Virulent VZV .....	67
<b>4 Discussion .....</b>	<b>70</b>
4.1 Role of Cutaneous DCs in VZV Pathogenesis.....	70
4.2 VZV-induced Increase in CD1c Expression on Monocyte-Derived iDCs .....	73
4.3 Impact of VZV-induced CD1c Upregulation on Intraepithelial CD1c- restricted $\gamma\delta$ T Cells.....	74
4.4 T Cell mediated Instruction of VZV-infected iDCs .....	76
4.5 Co-Stimulatory and Inhibitory Molecules provided by VZV-infected iDCs ..	78
4.6 Blocking TLR-2 Signaling in iDCs by Virulent VZV .....	79
<b>5 Reference list .....</b>	<b>83</b>
<b>Acknowledgement.....</b>	<b>98</b>
<b>Eidesstattliche Erklärung.....</b>	<b>99</b>

## Abbreviations

$\gamma\delta$	Gamma delta
APC	Antigen presenting cell
CD	Cluster of Differentiation
cDC	Conventional dendritic cell
CPE	Cytopathic effect
CTL	Cytotoxic T cell
d	Days
DAPI	4',6-Diamidino-2-phenylindol
DC	Dendritic cell
DC-SIGN	Dendritic cell-specific intercellular adhesion molecule-3-grabbing non-integrin
DDC	Dermal dendritic cell
DMSO	Dimethyl sulfoxide
DNA	Deoxyribonucleic acid
ds	Double-stranded
EDTA	Ethylenediaminetetraacetic acid
ELISA	Enzyme linked immunosorbant assay
EMEM	Eagle's Minimal Essential Medium
ER	Endoplasmatic reticulum
ERK	Extracellular signal-regulated kinase
FACS	Fluorescent-activated cell sorting
FcR	Fc receptor
FCS	Fetal calf serum
FITC	Fluorescein Isothiocyanate
g	Centrifugal force
gC	Glycoprotein C
gE	Glycoprotein E
GM-CSF	Granulocyte-macrophage colony-stimulating factor
h	Hour
HCMV	Human cytomegalovirus
HELF	Human embryonal lung fibroblasts
HIV-1	Human immunodeficiency virus type 1
HRP	Horseradish peroxidase
HSV	Herpes-simplex virus
Hu	Human
HZ	Herpes zoster
ICAM-1	Intercellular adhesion molecule 1
iDC	Immature dendritic cell
IDE	Insulin degrading enzyme
IFN	Interferon
IFN- $\gamma$	Interferon gamma
IgG	Immunoglobulin G
IL	Interleukin
IL-12p70	Interleukin 12p70 (bioactive)
IU	International Units
JNK	C-Jun N-terminal kinases

<b>JoSt</b>	Clinical isolate of VZV
<b>KSHV</b>	Kaposi's sarcoma-associated herpesvirus
<b>LC</b>	Langerhans cell
<b>LPS</b>	Lipopolysaccharide
<b>LTA</b>	Lipoteichoic acid
<b>MACS</b>	Magnetic-activated cell sorting
<b>MAP kinase</b>	Mitogen-associated protein kinase
<b>mDC</b>	Mature dendritic cell
<b>MFI</b>	Mean fluorescence intensity
<b>MHC class I</b>	Major histocompatibility complex class I
<b>MHC class II</b>	Major histocompatibility complex class II
<b>min</b>	Minute
<b>MOI</b>	Multiplicity of infection
<b>mRNA</b>	Messenger RNA
<b>NK cell</b>	Natural killer cell
<b>NKT cell</b>	Natural killer T cell
<b>ORF</b>	Open reading frame
<b>p.i.</b>	Post infection
<b>PAMP</b>	Pathogen-associated molecular pattern
<b>PBMC</b>	Peripheral blood mononuclear cell
<b>PBS</b>	Phosphate buffered saline
<b>pDC</b>	Plasmacytoid dendritic cell
<b>PE</b>	Phycoerythrin
<b>PFU</b>	Plaque forming unit
<b>PHA</b>	Phytohaemagglutinin
<b>PHN</b>	Postherpetic neuralgia
<b>PI</b>	Propidium iodide
<b>PRR</b>	Pattern recognition receptor
<b>RNA</b>	Ribonucleic acid
<b>RPMI</b>	Roswell Park Memorial Institute medium
<b>RT</b>	Room temperature
<b>RT-PCR</b>	Reverse transcriptase-polymerase chain reaction
<b>SCID</b>	Severe combined Immunodeficiency
<b>SD</b>	Standard deviation
<b>SDS-PAGE</b>	Sodium dodecyl sulphate-polyacrylamide gel electrophoresis
<b>STAT</b>	Signal transducer of activation and transcription
<b>TAP</b>	Transporter associated with antigen processing
<b>TCR</b>	T cell receptor
<b>T<sub>H</sub>1</b>	CD4 <sup>+</sup> T helper cell, producing type-1 cytokines (IL-2, IFN- $\gamma$ )
<b>T<sub>H</sub>17</b>	CD4 <sup>+</sup> T helper cell, producing IL-17
<b>T<sub>H</sub>2</b>	CD4 <sup>+</sup> T helper cell, producing type-2 cytokines (IL-4, IL-5 and IL-13)
<b>TLR</b>	Toll-like receptor
<b>TMB</b>	3,3',5,5'-Tetramethylbenzidine
<b>TNF-<math>\alpha</math></b>	Tumor necrosis factor- $\alpha$
<b>U</b>	Units
<b>V-Oka</b>	Vaccine strain V-Oka
<b>VZV</b>	Varicella-zoster virus

# 1 Introduction

## 1.1 Varicella-Zoster Virus (VZV)

Varicella-zoster virus belongs to the family *Herpesviridae* and its geographic distribution is worldwide<sup>1</sup>. In Germany the seroprevalence reaches nearly 95%. The human being is the only reservoir of VZV.

The virion measures 180 to 200 nm in diameter and is composed of an outer lipid membrane which harbors the five glycoproteins (gp) gpI (gE), gpII (gB), gpIII (gH), gpIV (gI), gpV (gC), the tegument containing viral proteins of mostly unknown function, followed by the capsid where the linear double-stranded viral DNA of ~125 kbp encoding for ~71 open reading frames (ORFs) is located<sup>2,3</sup>.

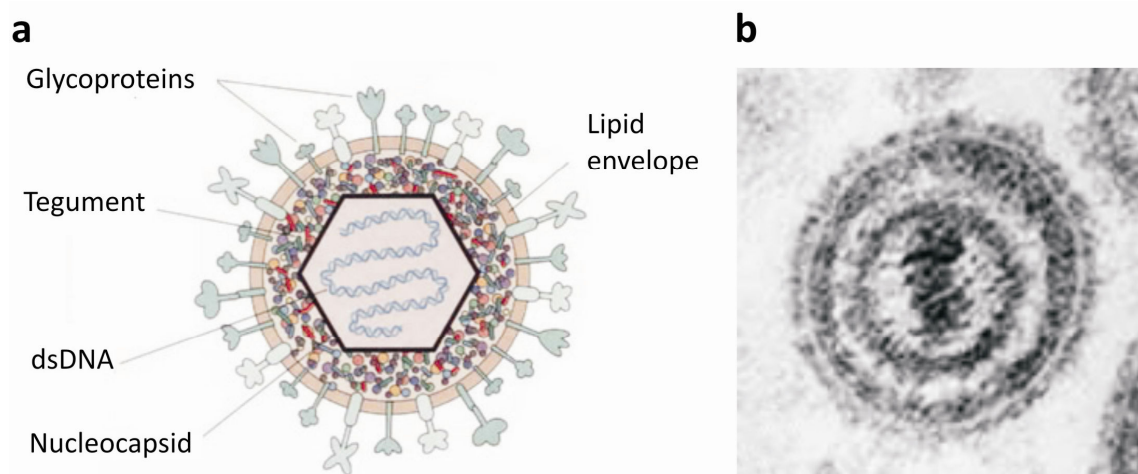


**Fig. 1: Morphology and structure of VZV.**

(a) Scheme of the virion. Within the outer membrane the glycoproteins gE, gB, gH, gI and gC are anchored. The tegument contains viral proteins and the nucleocapsid which harbors the linear double-stranded (ds) DNA. [www.bio.davidson.edu](http://www.bio.davidson.edu) (b) Electronic microscopy of VZV virion (showing the viral DNA surrounded by the capsid, embedded within the tegument and enveloped by the outer viral membrane containing the viral glycoproteins)<sup>4</sup>.

VZV binds with the glycoproteins gB, gH and gI to heparine sulfate on the cell surface, attaches to mannose 6-phosphate receptor and interacts through glycoprotein gE with the insulin degrading enzyme (IDE) to enter the host cell<sup>4-6</sup>. After fusion of the viral membrane with the host cell membrane the capsid is released into the cytoplasm and is

transported through actin and microtubules to the nuclear pore complex where the DNA is injected into the nucleus<sup>7</sup>. In the nucleus viral genes are transcribed in a cascade-like manner beginning with the immediate early (IE) genes, followed by the early (E) genes and finally the late (L) genes. Viral DNA is replicated by the rolling circle mechanism in the nucleus and the cleaved concatemers are packaged into pre-formed viral capsids. After budding from the inner nuclear membrane to the rough endoplasmic reticulum (rER) and into the cytoplasm the assembly of the virions takes place at the trans-golgi network (TGN). After wrapping of the TGN membrane the double-enveloped virions fuse with the cellular plasma membrane and release enveloped virions.

Despite the fact that VZV found in the pustular vesicles of VZV patients is highly contagious, VZV is highly cell-associated *in vitro* and no cell-free infectious virus is released into the cell culture<sup>8</sup>. This phenomenon is explained by the fact that pre-formed virions are directed to the endosomal compartment due to the presence of mannose 6-phosphate receptor where the low pH induces degradation of the viral glycoproteins<sup>4</sup>.

## 1.2 VZV Pathogenesis

Due to the fact that the replication cycle of VZV is restricted to human cells or tissues and its highly cell-associated nature, only little is known about its pathogenesis compared to other human herpesviruses like for example herpes simplex virus type-1 (HSV-1). To study the pathogenesis of VZV *in vivo* the severe combined immunodeficient (*scid/scid*) mice transplanted with human thymus/liver (T cell) or human skin xenografts known as SCID-human implant mouse model is used<sup>9</sup>.

Primary infection of naive persons leads to chickenpox which is a typical childhood disease and is characterized by a disseminated rash (Fig. 2a). Varicella is generally a mild illness; however, serious and occasionally fatal complications occur particularly in adults or immunocompromised people<sup>10-13,13</sup>. Encephalitis and fulminant hepatitis are the most severe manifestations caused by VZV<sup>13-15</sup>. Also children with apparently normal immune functions can have severe life-threatening complications due to varicella for yet unknown reason<sup>16</sup>.

After primary infection the virus establishes latency in sensory ganglia and can be reactivated to cause herpes zoster which is characterized by a rash, mostly restricted to a single dermatome (Fig. 2b)<sup>17</sup>. A severe complication of herpes zoster is the development of the very painful postherpetic neuralgia (PHN)<sup>18</sup>. The incidence for herpes zoster climbs steadily with increasing age and is believed to correlate with declining cell-mediated immunity to VZV<sup>19</sup>.

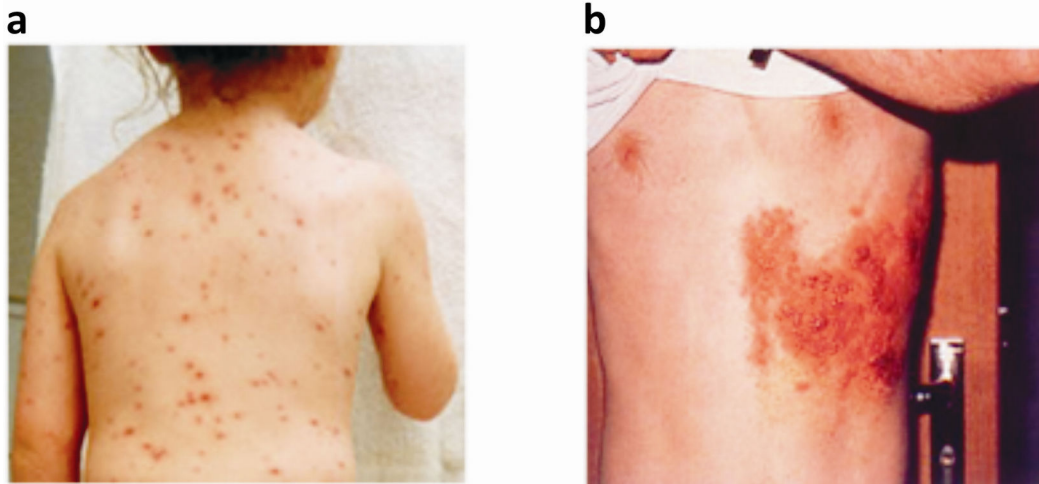


**Fig. 2: Clinical signs of chickenpox and herpes zoster.**

(a) Disseminated rash of a child after primary infection with a virulent strain of VZV. (b) Herpes zoster with a unilateral rash restricted to a single dermatome after reactivation of VZV. [www.online-praxis.com](http://www.online-praxis.com)

In the course of VZV transmission, naive persons inhale infectious virus present in aerosols or droplets of VZV-infected persons. After reaching the upper respiratory tract it is assumed that the virus infects dendritic cells (DCs) of the respiratory mucosa which transport the virus to local lymph nodes where the transmission to T cells occurs (Fig. 3)<sup>20</sup>. In the SCIDhu mouse model it could be demonstrated that VZV possesses tropism for CD4<sup>+</sup> and CD8<sup>+</sup> T cells<sup>9</sup>. Additionally, this tropism could be linked to the viral protein kinases open reading frame 47 (ORF47) and ORF66<sup>21</sup>. VZV infects preferentially tonsillar CD4<sup>+</sup> T cells which express activation, memory and skin homing markers<sup>22</sup>. In a primary viremia the virus is transported by peripheral blood mononuclear cells (PBMCs) to the replication sites liver and spleen<sup>2,23,24</sup>. In a second viremic phase the virus reaches the skin, the major replication site of VZV. The time from beginning of infection until the appearance of the typical rash is 10 to 21 days. During this prolonged incubation period the virus must circumvent



immune recognition to prevent its elimination by immune effector mechanisms of the host.

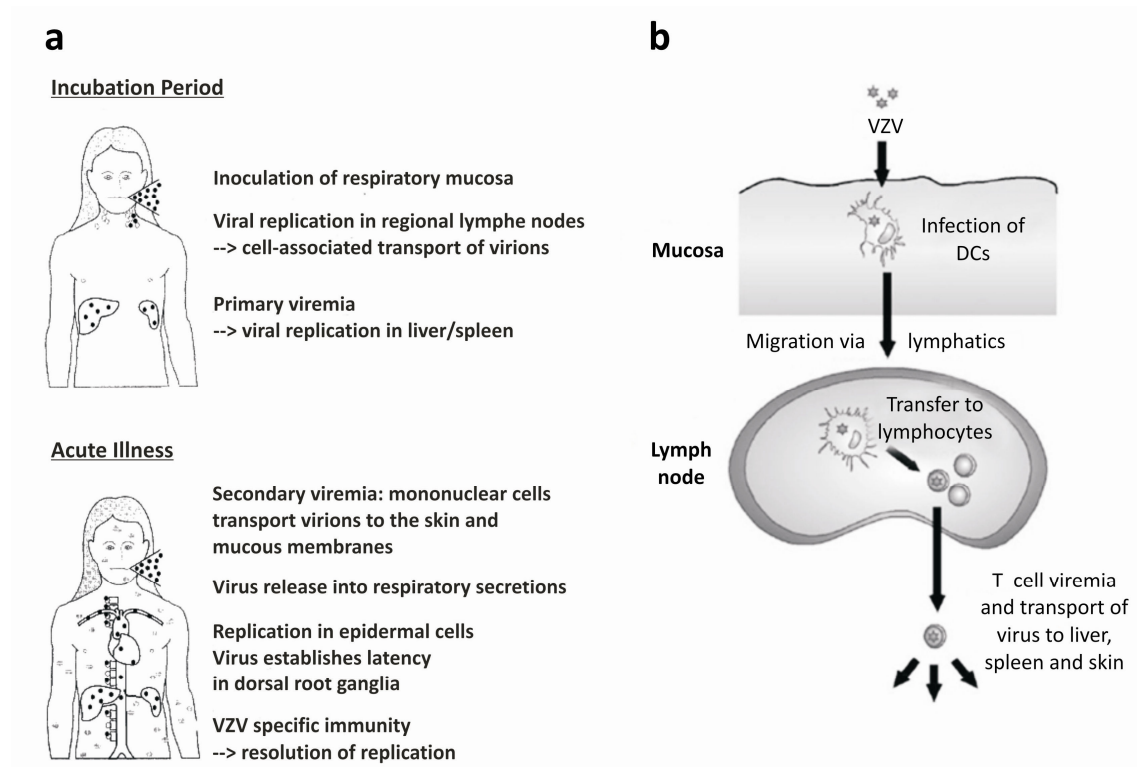


**Fig. 3: Pathogenesis of VZV.**

(a) Droplets containing infectious virions from infected person can be inhaled by naive persons. The virus replicates within regional lymph nodes and is transported cell-associated in a first viremia to liver and spleen. After a second viremia the virus is transported to the major replication site the skin. Acute illness is characterized by a disseminated rash with vesicles containing infectious virions. The virus establishes latency within dorsal root ganglia.<sup>2</sup> (b) It is assumed that the virus infects dendritic cells (DCs) of the respiratory mucosa which transport the virus to the local draining lymph nodes. There, the virus is transmitted to T cells which transport virions during a viremic phase to liver, spleen and skin<sup>2,25</sup>.

### 1.3 Immunity during Primary VZV Infection

Innate immune responses are presumed to mediate the initial control of primary VZV infection. Patients with deficiency in natural killer (NK) cells or natural killer T (NKT) cells show severe forms of varicella infections<sup>11,26,27</sup>. In the SCID-hu mouse model it could be demonstrated that uninfected epidermal cells of the skin surrounding the VZV vesicle secreted large amounts of interferon (IFN)- $\alpha$  whereas IFN- $\alpha$  secretion was inhibited in VZV-infected epithelial cells<sup>28</sup>.

Adaptive T cell responses appear to be critical for resolving primary infections and to control viral reactivation<sup>29</sup>. Interestingly, VZV specific T cell immunity is not detected till the onset of the rash, suggesting effective immune evasion mechanism in the initial phase of infection. A delay of VZV specific T cell immunity is correlated with life-threatening dissemination of the virus. The majority of epitopes recognized by the T cell receptor (TCR) on T cells and antibodies are derived from the immediate early protein 62 (IE62) and several glycoproteins of VZV. For example, cytotoxic CD8<sup>+</sup> T cells have been shown to recognize IE62 and gpl of VZV<sup>30</sup>. Additionally, it could be demonstrated that T cells recognize multiple epitopes of IE62 and gpl<sup>31</sup>.

Immunological memory to VZV is characterized by the persistence of cytotoxic T cells responsive to viral tegument and regulatory proteins encoded by ORF4, ORF10, ORF29, and ORF62<sup>32</sup>. Persistent high frequencies of VZV ORF4 protein specific CD4<sup>+</sup> T cell responses could be detected after primary infection<sup>33</sup>. Recently, it could be demonstrated that CD4<sup>+</sup> T cells directed to gpl maintain rapid effector functions even many decades after primary infection<sup>34</sup>. Additionally, CD4<sup>+</sup> T cells specific to IE63 protein of VZV were proposed to be important in the control of viral reactivation<sup>35</sup>.

VZV specific neutralizing antibodies are produced during primary infection but the course of infection of varicella appears to be uncomplicated in patients with agammaglobulinemia suggesting that the humoral immune response is less important<sup>36</sup>.

#### **1.4 Vaccination and Antiviral Therapy**

A live attenuated varicella vaccine was developed by serial passaging of clinical isolate “Oka” from a Japanese boy suffering from chickenpox<sup>37</sup>. The clinical isolate was passaged in cell culture several times using human embryo fibroblasts and guinea-pig embryo fibroblasts. This resulted in the accumulation of numerous mutations. The attenuated vaccine strain V-Oka exhibits nucleotide substitutions in several ORFs (48, 51, 52, 55, 56, 58, 59, 60, 62, 64, and 68) as well as deletions and insertions within certain regions<sup>38,39</sup>. The attenuated vaccine strain V-Oka is commercially produced by the companies Merck (VARIVAX), GlaxoSmithKline (Varilrix) and the Biken Institute in Japan (Biken varicella vaccine). The vaccine is successfully used since 1995 in the USA and since 2004 in Germany to immunize

children against varicella<sup>40</sup>. The vaccine induces protective immune responses through the induction of specific CD4<sup>+</sup> and CD8<sup>+</sup> T cells as well as neutralizing antibodies<sup>41,42</sup>. Nevertheless, in up to 5% of the healthy children vaccination causes a varicella-like rash but symptoms are milder and fewer vesicles occur. It could be demonstrated that vaccine preparations contain a mixture of VZV strains and that lesions from varicella-like rashes or herpes zoster contain only a single clone of VZV suggesting selection of a single strain during pathogenesis<sup>43,44</sup>. The majority of breakthrough varicella in immunocompetent vaccinees was linked to simultaneous infection with circulating virulent VZV strains<sup>45</sup>. Nevertheless, LaRussa *et al.* demonstrated in this study that the vaccine strain has the capacity to reactivate and cause herpes zoster in immunocompetent vaccines. Despite its potential for reactivation, a study on children with leukemia could demonstrate that immunization with the vaccine decreased the incidence for herpes zoster compared to infections with virulent VZV strains in this study group<sup>46</sup>. Recently, in a long term follow-up study, the incidence for herpes zoster in vaccinated young adults was similar to published data for the US population in the pre-vaccine era<sup>47</sup>. This suggests that despite its potential to reactivate the vaccine is efficiently controlled by yet unknown immune effector mechanisms within vaccinated population. Due to massive vaccination of children, a surveillance of vaccine induced complications and breakthrough infections is necessary.

Now, the vaccine is also tested in promising trial studies to boost the cell-mediated immunity of elderly people to decrease the incidence of herpes zoster and PHN<sup>48-50</sup>. This is important with respect to the fact that the population in industrialized countries increases in age. Additionally, it was shown that frequent exposure to varicella boosts immunity to herpes zoster<sup>51,52</sup>. These data were used to parameterize a mathematical model that estimates the impact of varicella vaccination on herpes zoster incidence. This model predicts a major epidemic of herpes zoster due to the fact that virulent VZV strains circulate less in the young population which might boost cell mediated immunity in the older population. This scenario is currently discussed although no follow-up study supports this hypothesis<sup>53,54</sup>.

For anti-viral therapy, the synthetic nucleoside analogues acyclovir, famcyclovir, valacyclovir or brivudine are commonly used<sup>55,56</sup>. It is important to treat patients within 72h after the onset of the rash to accelerate crusting of the lesions, to promote resolution of

acute pain, to diminish the risk of cutaneous and visceral complications and to prevent PHN or shorten the duration of zoster-associated pain<sup>57</sup>.

### 1.5 Dendritic Cells: Linking Innate with Adaptive Immunity

Dendritic cells (DCs) are a special subset of antigen presenting cells (APCs) which are uniquely positioned at the interface between the environment and epithelial surfaces such as the skin and the mucosa of digestive, respiratory and reproductive tracts<sup>58,59</sup>. They play an important role in both the induction of self tolerance and the priming of adaptive immune responses. For this purpose they appear in two different stages according to their phenotypic and functional properties: as immature DCs (iDCs) or as mature DCs (mDCs) (Fig. 4)<sup>60,61</sup>.

This differentiation process is induced in response to microbial or viral products, lymphocytes, cytokines, endogenous ligands or immune complexes<sup>62</sup>. To sense pathogen-associated molecular pattern (PAMP) iDCs express a set of innate pattern recognition receptors (PRRs) like the Toll-like receptors (TLRs), the retinoic-acid-inducible gene I (RIG-I) and melanoma differentiation-associated gene 5 (MDA5)<sup>63-65</sup>. Stimulation of PRRs induces the activation of intracellular signaling pathways and altered gene expression. TLRs, RIG-I and MDA5 have emerged as key sensors in recognizing viral components like nucleic acid and structural proteins produced during viral replication or viral entry and penetration<sup>66,67</sup>. Activation of PRRs leads to subsequent DC maturation. However, it becomes evident that triggering of multiple PRRs is needed to induce functional maturation of DCs, in particular marked for the production of the immune-regulating cytokine IL-12<sup>68-70</sup>. Additionally, it could be demonstrated that lymphocytes like NK cells, natural killer T (NKT) cells, conventional  $\alpha\beta$  T cells and  $\gamma\delta$  T cells can induce the maturation of iDCs<sup>71-73</sup>. Besides endogenous ligands like heat shock proteins also immune complexes through the binding to Fc receptors (FcRs) on iDCs can trigger maturation<sup>74</sup>.

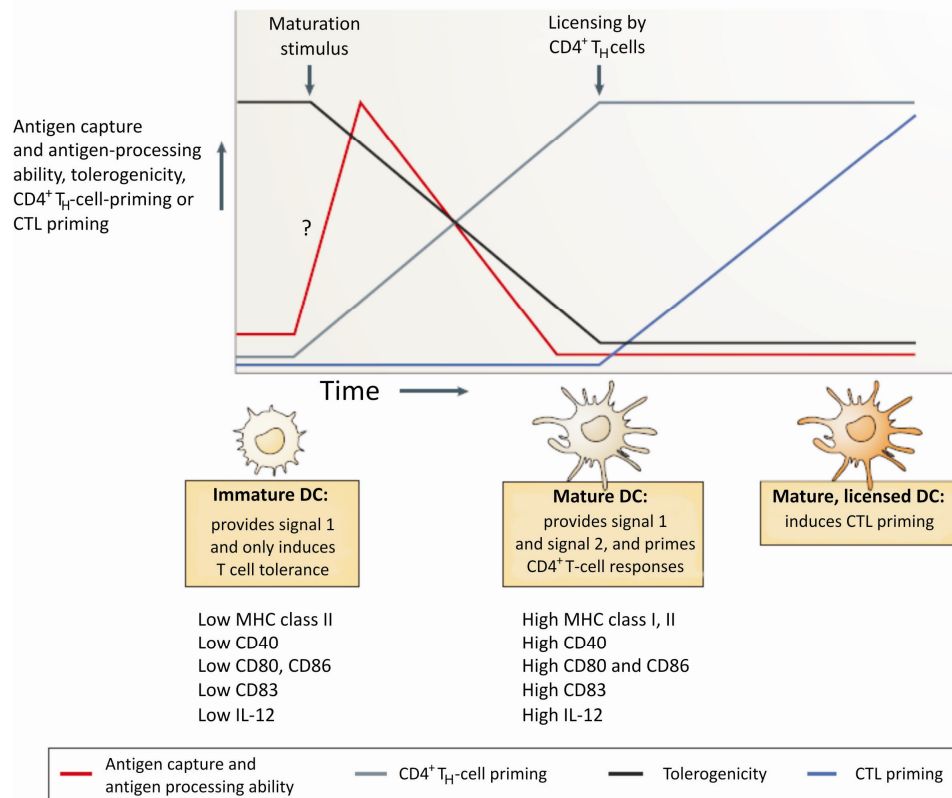


**Fig. 4: Dendritic cell maturation model.**

Dendritic cells (DCs) in the steady state are immature antigen-presenting cells (APCs) that internalize exogenous antigens and process them for MHC class II mediated presentation but cannot prime immune responses. Signal 1 is delivered through the T cell receptor (TCR) when it engages an appropriate peptide-MHC class complex. Signal 1 alone is thought to promote naive T cell inactivation by anergy, deletion or leading to tolerance. Maturation induced by danger signals leads to an increase in immunogenicity and downregulation of antigen acquisition and antigen-processing ability. Signal 2 is provided by co-stimulation through CD28 on the T cell when it engages CD80 and/or CD86 on DC. However, signal 2 is likely to be a fine balance between positive and negative co-stimulatory signals emanating from many receptors. Signal 1 and 2 induce immunity. Finally, mature DCs can be licensed by T helper (T<sub>H</sub>) cells or other cells e.g. NKT cells and  $\gamma\delta$  T cells with subsequent induction of T<sub>H</sub>-cell-dependant cytotoxic T lymphocyte (CTL) responses. Scheme of C. Reis e Sousa, 2006<sup>61</sup>, modified.

The main feature of iDCs in peripheral tissues is their capacity to capture and process antigens. Therefore, they are well suited to function as sentinels for invading pathogens. Sensing of PAMPs by PRRs induces their maturation with the following phenotypic and functional changes: up-regulation of MHC class I and II molecules, up-regulation of the co-stimulatory molecules CD40, CD80 and CD86, expression of CD83 and secretion of cytokines such as tumor necrosis factor- $\alpha$  (TNF- $\alpha$ ), interleukin-12 (IL-12), IL-10, interferon- $\alpha$  (IFN- $\alpha$ ), IFN- $\beta$  and IFN- $\gamma$ <sup>75-77</sup>. The types of cytokines produced depend on the DC subset as well as the activation stimulus. Another important aspect of the maturation process is the

change in the repertoire of chemokine receptors and the secretion of chemokines which result in different migration behavior<sup>78,79</sup>. Mature DCs migrate to local lymph nodes where they interact with naive T cells and B cells<sup>80</sup>. Due to the up-regulation of antigen presenting and co-stimulatory molecules on their cell surface, mDCs gain the capacity to stimulate efficiently naive and memory T cells and B cells and consequently initiate powerful adaptive immune responses. Mature DCs can trigger the activation of CD8<sup>+</sup> T cells by antigen presentation on MHC class I molecules whereas the T cell receptor (TCR)/CD3 complex of CD4<sup>+</sup> T cells recognizes peptides presented on MHC class II molecules<sup>81</sup>. Additional ligation of CD28 on T cells with the co-stimulatory molecules CD80 and CD86 on mDCs license the CD8<sup>+</sup> or CD4<sup>+</sup> T cells to gain full effector functions<sup>82</sup>. Activated CD8<sup>+</sup> cytotoxic T lymphocytes (CTLs) induce apoptosis through Fas ligand (FasL) in cells infected with intracellular pathogens like viruses. Furthermore, CTLs release perforin and granulysin from intracellular stored granules to form pores in the membrane of infected target cells<sup>83</sup>. Mature DCs can induce different types of CD4<sup>+</sup> helper T cells (T<sub>H</sub> cells), such as T<sub>H</sub>1, T<sub>H</sub>2, T<sub>H</sub>17 or regulatory T cells (T<sub>reg</sub>), depending on the secreted cytokine profile<sup>84,84</sup>. Secretion of IL-12 by mDCs drives the differentiation of T helper cells into T<sub>H</sub>1 cells which gain the capacity to produce IL-2, IFN- $\gamma$  and TNF- $\alpha$ . The latter's in turn activate macrophages, rendering them resistant to infection, and activate NK cells. Importantly, secretion of IL-12 by DCs and IFN- $\gamma$  by T<sub>H</sub>1 cells is regulated via positive feedback<sup>85</sup>. T<sub>H</sub>2 cells are characterized by their secretion of IL-4, IL-5, IL-13 and IL-25 which in turn induce the proliferation of B cells and their antibody class switching. The driving of T helper cells into the T<sub>H</sub>2 direction is associated with resistance to extracellular parasites like helminthes and the induction of allergic diseases. Immature DCs have been shown to induce secretion of the suppressive cytokine IL-10 by CD4<sup>+</sup> regulatory T cells<sup>86</sup>. Regulatory T cells play an important role in maintaining self-tolerance as well as in regulating immune responses. Recently, it has been demonstrated that mDCs secreting IL-6, TNF- $\alpha$  and IL-23 instructed CD4<sup>+</sup> T cells to become IL-17 secreting T helper cells (T<sub>H</sub>17 cells)<sup>87</sup>. T<sub>H</sub>17 cells play an important role in autoimmune diseases and mediate protective immunity to extracellular bacteria and fungi<sup>88</sup>.

DCs are key players of the innate immune system which drives adaptive immune responses into a certain direction by programming T cells. The dialogue between DCs and T cells is considered as a three signal integration model: Signal 1 comprising the engagement of specific peptid/lipid through MHC class I, II /CD1 molecules with the TCR/CD3 complex;

Signal 2 provides the co-stimulatory molecules CD80 and CD86 for engagement of CD28 on the T cell; and finally Signal 3 is the cytokine secreted by the DCs which determine the differentiation of the T cell into an effector T cell (CTL, T<sub>H</sub>1, T<sub>H</sub>2, T<sub>H</sub>17 or T<sub>reg</sub>)<sup>61,89</sup>.

## 1.6 Subsets of Dendritic Cells

Broadly, DCs can be divided into distinct subsets, each with specific markers and functions: plasmacytoid DCs (pDCs), conventional DCs (cDCs) and interferon-producing killer DCs (IKDCs).

Plasmacytoid DCs or interferon (IFN)-producing cells, are characterized by their ability to secrete rapidly large amounts of type I interferons (IFNs), IFN- $\alpha$  and IFN- $\beta$ , in response to stimulation by pathogens like viruses<sup>90,91</sup>.

Conventional DCs (cDCs) of myeloid origin can be phenotypically distinguished from pDCs as they express CD11c on their cell surface<sup>92</sup>. Conventional DCs can be further subdivided into three major DC populations: migratory DCs, resident DCs and monocyte-derived or inflammatory DCs<sup>93</sup>. Migratory DCs act as sentinels in peripheral tissues and migrate after uptake of antigens to local lymph nodes through lymphatics where they present these antigens to resident T and B cells<sup>94</sup>. Langerhans cells (LCs) and dermal DCs (DDCs) are examples for migratory DCs. In contrast lymphoid tissue resident DCs do not migrate through the lymph and their function and life-history are restricted to one lymphoid organ. They sample and present self and foreign antigens in that lymphoid organ. Examples include thymic and splenic cDCs. Migratory and tissue resident DCs are normally present during steady state conditions. In strong contrast, inflammatory DCs appear as a consequence of inflammation or stimuli through pathogens. They can arise from myeloid and lymphoid precursors<sup>95</sup>. Recently, it has been demonstrated that inflammatory DCs derived from monocytes control the induction of protective T<sub>H</sub>1 responses during *Leishmania* infection<sup>96</sup>.

Recently, IKDCs have been discovered which share phenotypic and functional properties of DCs and natural killer (NK) cells<sup>97</sup>. They produce substantial levels of type I interferon, IL-12 and IFN- $\gamma$ , depending on activation stimuli. By losing their NK cell like cytotoxic

potential they gain DC like antigen presenting activity and upregulate MHC class II and co-stimulatory molecules.

### **1.7 Dendritic Cells of the Skin and the Induction of Viral Immune Response**

The skin, the largest organ of the human body is comprised of distinct compartments relevant to its immune function. The epidermis, the most superficial layer, functions as physical barrier and is composed of keratinocytes, intraepithelial lymphocytes and specialized DCs so called Langerhans cells (LCs)<sup>98</sup>. The dermis is mainly composed of dermal fibroblasts and immune cells including dermal DCs (DDCs), mast cells and a small number of cutaneous lymphocyte antigen (CLA)-positive memory T cells (Fig. 5a).

Migratory cDCs in the steady state of the skin comprise immature epidermal LCs and immature DDCs which function as sentinels for invading pathogens<sup>99</sup>. LCs of the epidermis are characterized by expression of Langerin and CD1a, which function for non-peptide antigen presentation<sup>100,101</sup>. DDCs of the dermis express the mannose receptor (CD206) and DC-SIGN (CD209) for internalization of glycolipids and their sorting into the endocytotic pathway<sup>102,103</sup>.

Sensing of pathogens leads to release of cytokines and activation of epidermal cells, keratinocytes and cutaneous DCs (Fig. 5b). Activated LCs and DDCs undergo maturation and migrate to local lymph node where they present captured antigens to naive and memory T and B cells. The released cytokines and chemokines by cutaneous cells induce upregulation of E-selectin and ICAM1 which recruits additional innate immune cells from venules to the inflamed tissue. Since many years there is conflicting data regarding which type of dendritic cell, LCs or DDCs, contribute to immunity against viral infections. In the last few years several research groups demonstrated that migratory DDCs efficiently present antigens to lymph node resident T cells, therefore contributing to cutaneous immunity to viral infections, especially for herpesviral infections<sup>104-106</sup>. Which type of dendritic cell contributes to cutaneous VZV immunity has still to be elucidated even though a role for pDCs during varicella was recently discussed<sup>107</sup>. Furthermore, in skin sections from varicella and herpes zoster patients the absence of intercellular adhesion molecule-1 (ICAM-1) expression on VZV-infected keratinocytes was observed. ICAM-1 serves as adhesion mole-



cule for lymphocyte function-associated antigen 1 (LFA-1) bearing T cells<sup>108</sup>. However, VZV certainly has further evasion strategies to ensure its replication and transmission within this organ.

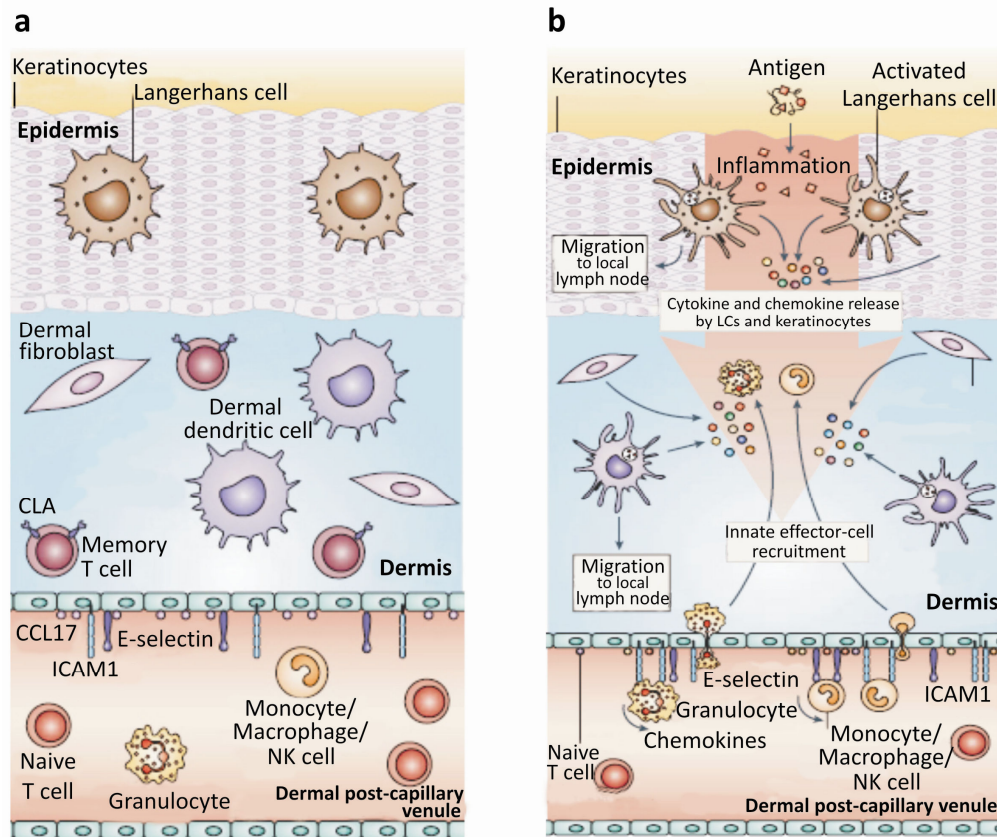


**Fig. 5: Immune surveillance in the skin.**

(a) Immune response in non-inflamed skin. The human skin is composed of three distinct compartments according to their immune function: epidermis, dermis and dermal post-capillary venules. Within the steady state the epidermis, as physical barrier, is composed amongst others of keratinocytes, Langerhans cells (LCs) and intraepithelial lymphocytes. The dermis is mainly composed of dermal fibroblasts, dermal DCs (DDCs) and a small number of cutaneous lymphocyte antigen (CLA)-positive memory T cells. Dermal post-capillary venules express low levels of E-selectin, CC-chemokine ligand 17 (CCL17) and intercellular adhesion molecule 1 (ICAM1). These support the emigration of CLA<sup>+</sup> memory T cells. (b) Immune response in inflamed skin. Pathogen invasion leads to release of primary cytokines and activation of epidermal cells, keratinocytes, LCs and DDCs. Activated LCs and DDCs mature and emigrate from the tissue to local lymph node, carrying antigen for presentation to naive and memory T cells. Released cytokines and chemokines induce upregulation of E-selectin and ICAM1 thereby directing the recruitment of additional innate immune cells.<sup>98</sup>

## 1.8 Herpesviral Interference with DC Maturation and Function

For a variety of viruses including herpes simplex virus type -1 (HSV-1), herpes simplex type-2 (HSV-2), human cytomegalovirus (HCMV) and VZV it was shown that they can infect DCs and inhibit their immune function<sup>20,25,109,110</sup>. Viral infection hijacks the biosynthetic machinery of the host cell and ensures the rapid synthesis of viral proteins, thereby providing a reservoir for viral peptides that are loaded on MHC molecules. To ensure its replication and spread viruses have evolved several evasion strategies to circumvent immune recognition. The IE protein ICP-47 of HSV-1 blocks the transporter associated with antigen processing (TAP) within the membrane of the endoplasmic reticulum (ER) and prevents CTL recognition through MHC class I molecules<sup>111,112</sup>. Moreover, HSV-1 interferes with the maturation of DCs by inhibiting upregulation of co-stimulatory molecules, cytokine secretion and responsiveness to chemokines required for migration to lymphoid organs<sup>113</sup>. Recently, it has been demonstrated that HSV-1 induces rapid induction of apoptosis in iDCs<sup>114</sup>. Furthermore, HSV-1 inhibits TCR signaling within T cells exposed to infected cells<sup>115</sup>. HSV-2 infection of murine DCs induces rapid cell death and their functional impairment<sup>116</sup>. The largest human herpesvirus HCMV also encodes for two viral proteins, U<sub>S</sub>2 and U<sub>S</sub>11, which inhibits MHC class I presentation and encodes for a viral IL-10 homologue that interferes with the function and survival of DCs<sup>109,110</sup>.

Recently it was shown that VZV can productively infect iDCs, but infection did not induce any phenotypical changes compared to mock-infected iDCs<sup>20</sup>. The viral protein kinase encoded by ORF47 was shown to be critical for viral replication in iDCs<sup>117</sup>. Furthermore, it could be demonstrated that VZV was transmitted from infected iDCs to T cells which might transport the virus through the blood stream to the replication sites liver, spleen and finally the skin<sup>20</sup>. In contrast, productive infection of mDCs induces subsequent phenotypical and functional changes: downregulation of cell surface expression of MHC class I, CD80, CD86 and CD83 but not of MHC class II molecules and reduced ability to stimulate allogeneic T cell proliferation<sup>118</sup>. It has to be mentioned that the described observations in both studies were made only with a clinical isolate of VZV (circulating in the USA) and were not compared to the vaccine response.

## 1.9 Immune Evasion Mechanisms of VZV

It could be demonstrated that VZV interferes with the classical antigen presentation through MHC class I and II molecules. The serine /threonine protein kinase ORF66 of VZV has been shown to be responsible for the retention of MHC class I molecules within the golgi compartment<sup>119-121</sup>. Moreover, VZV inhibits IFN- $\gamma$ -mediated induction of cell surface MHC class II expression on infected fibroblasts<sup>122</sup>. Recently, the interference of VZV with the activation of nuclear factor- $\kappa$  B (NF- $\kappa$ B) has been demonstrated *in vitro* and in human epidermal cells *in vivo*<sup>123</sup>.

## 1.10 CD1 Antigen Presentation

Besides the classical antigen presentation of peptides through MHC class I and II molecules a second antigen presentation system exists. CD1 molecules present lipids to CD1 restricted T cells<sup>124</sup>. In humans the CD1 gene complex is encoded on chromosome 1<sup>125</sup>. Human express five CD1 isoforms which are divided into group 1 including CD1a, CD1b and CD1c and group 2 solely comprising CD1d. Besides these cell surface expressed CD1 molecules which recirculate within endocytotic compartments, CD1e belonging to group 3 is exclusively expressed intracellularly (Fig. 6)<sup>126</sup>.

Group 1 CD1 molecules are mainly found on professional APCs, whereas CD1d is more widely expressed. *In vitro* CD1a, CD1b and CD1c molecules can be detected at high amounts on monocyte derived DCs.

Like MHC class I molecules, all CD1 molecules are heterodimers composed of an alpha chain and non-covalently linked  $\beta$ 2 microglobulin ( $\beta$ 2m). CD1 molecules can present foreign, self and synthetic glycolipids to CD1-restricted T cells<sup>127</sup>. It was shown that isoprenoid glycolipids of the outer cell wall of *Mycobacterium tuberculosis* was recognized by CD1c restricted T cells<sup>128,129</sup>. Recently, it was shown that CD1-restricted T cells have a dual reactivity for both self and foreign lipid antigens<sup>130</sup>. Interestingly, recognition of self lipids presented through CD1 molecules was recently also demonstrated for  $\gamma\delta$  T cells<sup>131</sup>.

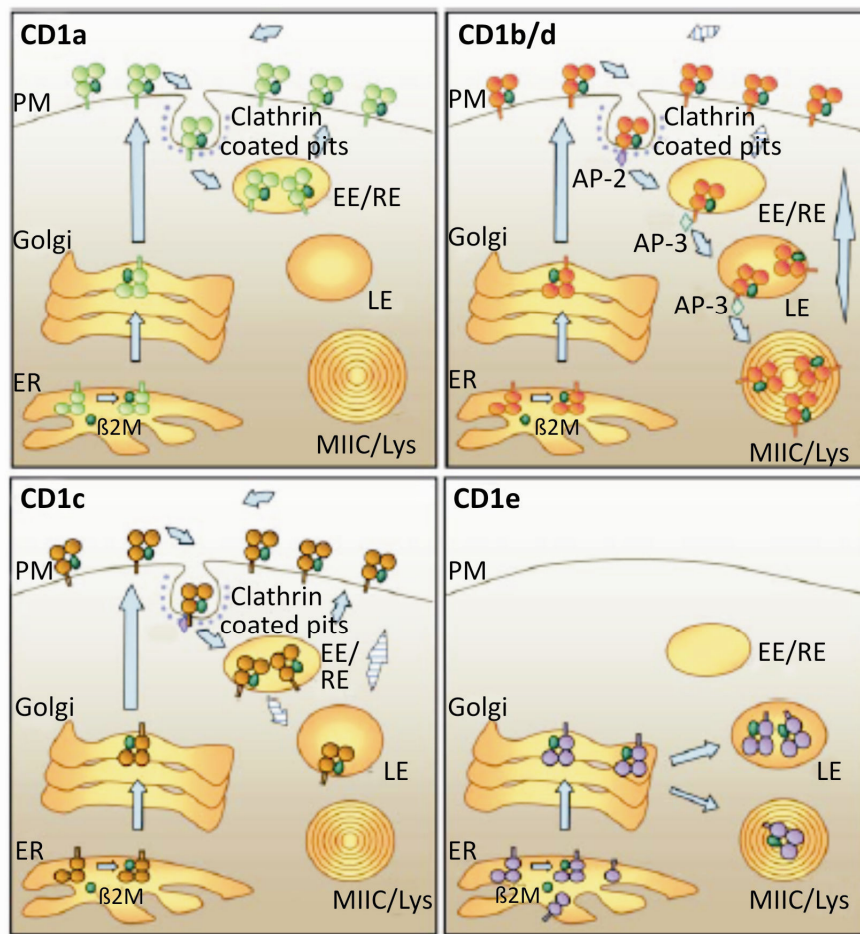


**Fig. 6: Trafficking of human CD1 molecules.**

Top left: CD1a molecules are transported in association with  $\beta 2$  microglobulin ( $\beta 2m$ ) from the endoplasmic reticulum (ER) through the secretory pathway to the plasma membrane (PM). CD1a spontaneously internalizes via clathrin-coated vesicles and recycles through early/sorting and early/recycling endosomes (EE/ER) to the PM. Top right: The cellular trafficking of CD1b and CD1d is very similar. After transport to the PM, their endocytosis into clathrin-coated pits is mediated through the interaction of their cytoplasmic tails with the cytosolic adaptor complex (AP)-2. They are delivered to early endosomes, where they access late endosomes (LE), lysosomes and the MHC class II compartments (MIIC/Lys) through their interaction with cytosolic adaptor AP-3. Bottom left: CD1c molecules are internalized via clathrin-coated vesicles through their interaction with AP-2. Most of the CD1c molecules recycle to the cell surface through EE/ER but a small fraction can be detected within LE. Bottom right: CD1e molecules remain intracellularly. In iDCs most CD1e molecules are present in the Golgi. After activation and maturation of DCs, CD1e molecules accumulate in LE and lysosomes.<sup>132</sup>

In the recent years it was shown that antigen presentation through CD1 molecules is correlated with the outcome of several diseases. It could be demonstrated that expression of group 1 CD1 molecules was strongly induced in skin lesions of patients with the tuberculoïd form of leprosy, showing active cellular immunity to infection. In strong contrast, patients with the lepromatous form did not show induction of CD1 proteins in skin lesions and lacked effective cell-mediated immunity<sup>133</sup>. Additionally, antigen presentation through

CD1a and CD1c molecules was also shown to be involved in some human autoimmune disorders<sup>134</sup>. Intriguingly, a patient who was vaccinated against VZV and developed a disseminated varicella had a deficiency in NKT cells<sup>26</sup>. This case report gives evidence that CD1 antigen presentation plays a role in VZV pathogenesis.

### 1.11 Viral Interference with CD1 Antigen Presentation

Several strategies to evade CD1 antigen presentation have been elucidated for members of the *Herpesviridae*. Recently, it was shown that HSV-1 interferes with the recirculation of CD1d molecules in APCs therefore inhibiting recognition by NKT cells<sup>135,136</sup>. For Kaposi sarcoma-associated herpesvirus (KSHV) two modulator of immune recognition (MIR) proteins were identified which blunt CD1d antigen presentation by accelerating endocytosis<sup>137</sup>. Interference with the CD1b antigen presentation on professional APCs was recently highlighted for HCMV<sup>138</sup>. Furthermore, the nef protein of human immunodeficiency virus-1 (HIV-1) blocks lipid antigen presentation by increasing the internalization of CD1d molecules from the cell surface and retaining them in the golgi compartment<sup>139</sup>.

### 1.12 $\gamma\delta$ T Cells

Gamma delta ( $\gamma\delta$ ) T cells represent a small subset of T cells that together with conventional  $\alpha\beta$  T cells and B cells use somatic DNA rearrangement to assemble the genes encoding for their defining antigen receptor. The structure of the T cell receptor (TCR) of  $\gamma\delta$  T cells is composed of a heterodimer consisting of  $\gamma$  and  $\delta$  chain. The chains are arranged by variable (V), diversity (D), junctional (J) and constant (C) gene segments. There appear to exist only six functional  $V\gamma$  genes in humans, five in the  $V\gamma 1$  family and another more distantly related  $V\gamma 2$  gene and ~8-10 distinct  $V\delta$  genes<sup>140</sup>. Despite this limited combinatorial diversity compared to conventional  $\alpha\beta$ -TCR the repertoire of  $\gamma\delta$ -TCR is greatly enhanced due to extensive junctional diversity by removal or addition of non-germline-encoded nucleotides at V-D-J junctions and alternative D segment reading frames. In contrast to  $\alpha\beta$  T cells which are

credited with immunological memory it is not known if  $\gamma\delta$  T cells carry antigen-specific memory despite expression of a memory phenotype different from  $CD8^+ \alpha\beta$  T cells<sup>141</sup>.

In humans there are two major subsets of  $\gamma\delta$  T cells which differ in their tissue distribution<sup>142</sup>. The major circulating pool of  $\gamma\delta$  T cells in human peripheral blood expresses  $V\gamma9V\delta2$  TCR chains (1% to 5%)<sup>143</sup>. These cells have been shown to recognize nonpeptide prenyl pyrophosphate intermediates in isoprenoid biosynthesis, aminobisphosphates and alkyl amines<sup>141,144</sup>.  $V\gamma9V\delta2$  T cells play an important role in immunity to both bacteria and parasites like *Mycobacterium tuberculosis* and *Plasmodium falciparum*<sup>145,146</sup>. Additionally, this  $\gamma\delta$  T cell subset has been demonstrated to kill *in vitro* many types of tumor cells through both TCR-mediated and NK receptor-mediated recognition<sup>147</sup>. Prenyl pyrophosphates are directly presented to  $V\gamma9V\delta2$  T cells, whereas recognition of bisphosphonates requires antigen presentation by APCs<sup>141</sup>. Nevertheless, activation of  $V\gamma9V\delta2$  T cells requires contact with each other or an APC.

In contrast, the majority of  $\gamma\delta$  T cells in human epithelial tissue is represented by the subset expressing  $V\delta1$  TCR chains<sup>148,149</sup>. Especially, the dermis of human skin contains  $V\delta1^+$   $\gamma\delta$  T cells which express receptors for homing to non inflamed skin<sup>150</sup>. In  $\gamma\delta$  T cell deficient mice, it could be demonstrated that skin  $\gamma\delta$  T cells provide local, nonredundant regulation of cutaneous inflammation<sup>151</sup>. It has been demonstrated that  $V\delta1^+$   $\gamma\delta$  T cells recognize stress induced MHC class I-related chain A (MICA) molecule and MICB on cells<sup>152,153</sup>. Recently, recognition of exogenous and self antigens through CD1 molecules by  $V\delta1^+$   $\gamma\delta$  T cells was shown<sup>131,154,155</sup>. Furthermore, activation and expansion of  $V\delta1^+$   $\gamma\delta$  T cells in response to lipid extracts of Gram-negative bacteria in the presence of iDCs has been shown<sup>156</sup>. The expansion of this  $\gamma\delta$  T cell subset within the periphery has also been found in HIV positive patients and in transplant recipients after infection with HCMV<sup>157,158</sup>. Activated  $V\delta1^+$   $\gamma\delta$  T cells are characterized by their immediate effector functions such as perforin- and Fas-mediated cytotoxicity and  $T_H1$ -type cytokine secretion<sup>131</sup>.

Intriguingly,  $\gamma\delta$  T cells display principal characteristics of APCs by processing and presenting antigens as well as providing co-stimulatory signals to  $\alpha\beta$  T cells<sup>159</sup>. Recently, processing and cross-presentation of microbial and tumour antigens by human  $V\delta2^+$   $\gamma\delta$  T cells to  $CD8^+ \alpha\beta$  T cells could be demonstrated with implication for further exploration in immunotherapy research<sup>160</sup>.

$\gamma\delta$  T cells interact with a variety of immune cells including DCs<sup>161</sup>. The cross-talk of DCs and  $\gamma\delta$  T cells has been shown to link innate with adaptive immune responses during microbial and viral infections<sup>162,163</sup>.  $\gamma\delta$  T cells play an important role in the induction of immunity to *Mycobacterium tuberculosis* and to certain viruses<sup>164,165</sup>. A protective role of  $\gamma\delta$  T cells in herpesviral infections has been shown in HCMV patients and in mice infected with HSV-2<sup>166,167</sup>.

### 1.13 Objectives of the Study

A main focus of this study was to investigate the interplay of VZV with innate immune cells which participate in cutaneous immunity. Little is known about VZV pathogenesis with respect to immune evasion strategies which ensure viral replication and spread within this immune organ. Therefore, punch biopsies from papovesicular lesions of immunocompetent herpes zoster patients were analyzed for the presence of immune cells which are involved during VZV pathogenesis. Furthermore, *ex vivo* isolated cutaneous DCs were tested for permissivity to VZV infection and subsequent phenotypic changes.

Another important aspect of this study was to compare for the first time innate immune responses between the vaccine and clinical isolates of genotypes circulating in Europe. A key question in this regard was whether the striking differences in the clinical outcome of infection with circulating rash inducing VZV strains on the one hand and asymptomatic infection with the vaccine on the other hand can be explained through innate immune mechanisms. Therefore, the bidirectional crosstalk of DCs and  $\gamma\delta$  T cells both potent initiators of cutaneous immunity was comparatively assessed during infection with virulent VZV strains and vaccine, respectively.

This study provides for the first time evidence that virulent VZV strains regardless of their genotype have the intrinsic potential to interfere with the phenotype and function of DCs and thereby fail to activate subsequent  $\gamma\delta$  T cell responses. Thus, this study identifies a novel immune evasion mechanism of virulent VZV which might have implications for further vaccine design.

## **2 Material and Methods**

### **2.1 Human Samples**

Ethical approval of human samples was granted by the Charité-Universitätsmedizin Berlin ethics committee (EA1/169/06). Healthy control and herpes zoster patients were recruited in cooperation with the Department of Dermatology, Venerology and Allergology of the Charité-Universitätsmedizin Berlin.

#### **2.1.1 Blood Samples**

10-20 ml of peripheral blood from healthy control and herpes zoster patients were collected using a BD Vacutainer (K2E 18.0 mg; REF 367525) blood collection system (BD Bioscience, Heidelberg, Germany). Blood was diluted 1:1 with media containing 0.2 mM EDTA and then separated by gradient centrifugation on Ficoll-Hypaque (PAA Laboratories, Marburg, Germany) with 800 g for 30min at room temperature. Peripheral blood mononuclear cells (PBMCs) were collected and stained for the appropriate cell surface markers.

#### **2.1.2 Isolation of Cutaneous Dendritic Cells**

Human epidermal LCs and DDCs were isolated from abdominal skin or foreskin from healthy volunteers. After removal of fat the skin was scaled. With a scalpel the skin was then first cut in pieces of 2 cm x 0.5 cm in size and then incised each 1-2 mm to achieve better access for further dispase I treatment. Incubation overnight at 4°C in 50 ml of dispase type I (Roche Diagnostics, Mannheim, Germany) at 0.5 mg/ml (10 g skin per 5 mg dispase I) separated the epidermis from dermal skin. Thereafter, skin streaks were placed in a petri dish with PBS (w/o  $\text{Ca}^{2+}$  and  $\text{Mg}^{2+}$ ) and epidermis was removed from dermis using forceps.

Epidermal sheets of 30 g skin were incubated in 25 ml of trypsin solution (0.25% trypsin in PBS with 5 mM  $\text{Mg}^{2+}$  and 10  $\mu\text{g/ml}$  DNase (Roche Diagnostics, Mannheim, Germany) and incubated for 15min at 37°C, 5%  $\text{CO}_2$ . Trypsin is used to achieve enzymatical cleavage of desmosomal cell-cell contacts and DNase I was added to inhibit clumping of cells by released DNA from disrupted cells. To remove cells from epidermal sheets the suspension was dispersed with a 25 ml pipette until it became unclear. The cell suspension was transferred into a 50 ml falcon



tube using a nylon cell filter and addition of 10% FCS stopped trypsin digestion. Cells were recovered by centrifugation at 260 g for 15min without break. The cell pellet was resuspended in PBS containing 10 µg/ml DNase, 5 mM Mg<sup>2+</sup> and 10% FCS and incubated for 15min at 37°C with readily opened falcon caps. After centrifugation for 5min at 260 g (with break) cells were washed twice with PBS containing 10% FCS. LCs were positively isolated from epidermal cell suspension using MACS technique and human CD1c (BDCA-1)<sup>+</sup> Dendritic Cell Isolation Kit (Miltenyi Biotec, Bergisch-Gladbach, Germany). Therefore, the pellet was resuspended in degassed ice cold MACS buffer and anti-CD1c microbeads were added according to manufacturer's instructions and cells were incubated in the refrigerator for 15min. Magnetic separation was performed using Large Cell columns. To increase purity of LCs eluted CD1c<sup>+</sup> fraction was enriched over a second Large Cell column. LCs were resuspended with a density of 1x10<sup>6</sup> cells/ml in RPMI media containing 10% FCS and GM-CSF (500 IU/ml) and directly centrifuged (160g, 45 min, RT) on mock or VZV infected fibroblast monolayers (24-well).

The dermis was first used by Sven Guhl (Department of Dermatology, Venerology and Allergology of the Charité-Universitätsmedizin Berlin) for isolation of mast cells. Dermis was cut using a scissors in very small pieces to increase cellular recovery and decrease incubation time for enzymatic digestion. The dermal pulp was incubated in 10 ml/g skin of 37°C pre-warmed PBS (Ca<sup>2+</sup> and Mg<sup>2+</sup>) containing 10% FCS, penicillin/streptomycin (10 000 U/ml), amphotericin B (2,5 µg/ml), 5 mM MgSO<sub>4</sub>, 12 mg collagenase (CellSystem, St. Katharinen, Germany) and 6.5 g hyaluronidase type I S (Sigma Aldrich, München, Germany). The suspension was incubated for 1-1.5h in a 37°C shaking waterbath. Thereafter, cell suspension was transferred in a falcon tube using two filters with a pore size of 300 µm (upper filter) and 40 µm (lower filter). The cellular filtrate was centrifuged for 15min at 350 g at 4°C the enzyme containing supernatant was re-transferred to the undigested dermal pulp for a second digestion period in 37°C shaking waterbath. This was performed for dermal pulp from abdominal skin (enzymatic digestion for two times) whereas foreskin was only digested once. The cell pellet was washed twice in PBS (w/o Ca<sup>2+</sup> and Mg<sup>2+</sup>) and once in ice cold degassed MACS buffer by centrifugation at 4°C for 10min 250 g. Mast cells from dermal suspension were isolated positively using MACS technique and the CD117 MicroBead Kit (Miltenyi Biotec, Bergisch-Gladbach, Germany). The dermal cell suspension depleted of mast cells was then used to positively isolate CD1c<sup>+</sup> DDCs using the MACS technique and human CD1c (BDCA-1)<sup>+</sup> Dendritic Cell Isolation Kit (Miltenyi Biotec, Bergisch-Gladbach, Germany). The DDCs were isolated as described above for isolation of LCs from epidermal cell suspension. CD1c<sup>+</sup> DDCs were resuspended with a density of 1x10<sup>6</sup> cells/ml in RPMI

media containing 10% FCS and GM-CSF (500 IU/ml) and directly centrifuged (160 g, 45min, RT) on mock or VZV infected fibroblast monolayers (24-well).

### 2.1.3 Skin Biopsies

4 mm punch biopsies of patients with acute herpes zoster (vesicular stage) were taken by Dr. med. Martina Ulrich (n=2). Healthy control skin was obtained from patients undergoing breast reduction surgery. Specimens were embedded in cryomolds containing tissue freezing medium, frozen in isopentane, and stored at  $-80^{\circ}\text{C}$ . 5  $\mu\text{m}$  cryosections were performed at  $-26^{\circ}\text{C}$  to  $-27^{\circ}\text{C}$  depending on the content of fatty acids in the skin. Sections were fixed with ice-cold acetone at  $-20^{\circ}\text{C}$  for 10min and then air-dried at room temperature overnight. For further investigations they were stored at  $-80^{\circ}\text{C}$ .

## 2.2 Cells and Cell Lines

**Tab. 1: Cells and Cell Lines**

Name	Source and Characteristic
HELFL	Human embryonal lung fibroblasts (Fi301)
iDCs	Human monocyte-derived immature DCs
$\gamma\delta$ T cells <sup>1</sup>	Human CD1c-restricted $\gamma\delta$ T cells <sup>131</sup> (clone JR.2.28)
CD40L cells <sup>2</sup>	Murine fibroblasts stable transfected with CD40L or control plasmid <sup>168</sup>

<sup>1</sup> kindly provided by Prof. C.T. Morita, University of Iowa College of Medicine, Division of Rheumatology, Department of Internal Medicine and Interdisciplinary Graduate Program Immunology, Iowa, USA

<sup>2</sup> kindly provided by Prof. R. Kroczeck, Robert Koch-Institut, Berlin, Germany

### 2.3 Cell Culture Medium

BioWhittaker Eagle's Minimal Essential Medium (EMEM) was purchased from Lonza (Verviers, Belgium). Roswell Park Memorial Institute 1640 (RPMI 1640) medium, Penicillin/Streptomycin, L-Glutamine, Sodium Pyruvate and MEM non essential amino acids were obtained from PAA Laboratories (Marburg, Germany). Fetal calf serum (FCS) HyClone from Perbio (Bonn, Germany) was heat-inactivated for 30min at  $56^{\circ}\text{C}$  (waterbath) and finally added to the culture medium at

a concentration of 10% or 2%. PBS for washing of cells was purchased from PAA Laboratories (Marburg, Germany). Adherent cells were collected by trypsinization at a concentration of 0.05% from Invitrogen (Karlsruhe, Germany).

EMEM or RPMI 1640 medium (500 ml)	10% or 2%	FCS
	100 mM	Hepes (only to RPMI 1640)
	2 mM	L-Glutamin
	1 mM	Sodium Pyruvate
	100 U	Penicillin
	100 µg	Streptomycin
	1x	MEM non essential amino acids

## 2.4 Viruses

Tab. 2: Viruses

VZV strain	Genotype	Source
V-Oka	J	Attenuated vaccine (V-) strain Oka “Varilrix” from GlaxoSmithKline (Rixensart, Belgium)
P-Oka	J	Parental (P)-Oka strain of VZV <sup>3</sup>
JoSt	E1	Clinical isolate of varicella patient, Germany
M1_935/05	M1	Clinical isolate of varicella patient, Germany
E2_769/05	E2	Clinical isolate of varicella patient, Germany
E1_667/05	E1	Clinical isolate of varicella patient, Germany

<sup>3</sup> The P-Oka strain of VZV was kindly provided by K. Tischer, Freie Universität Berlin, Institute of Virology, Berlin, Germany

All VZV strains were genotyped by Prof. Sauerbrei at the Institute of Virology and Antiviral Therapy of the Friedrich Schiller University of Jena (Germany) as previously published<sup>169</sup>. Partial sequencing revealed that the P-Oka strain harbored several mutations within ORF1 and ORF21 compared to the reference P-Oka strain. This is in line with the reports of K. Tischer that the isolate was already highly passaged in cell culture. Therefore, further investigations did not include the P-Oka strain of VZV.

VZV was propagated in confluent HELF monolayers (maximum after two days post seeding) consisting of VZV-infected and uninfected cells (ratio of 1:7). As inoculums VZV-infected trypsin-dispersed cells were used<sup>170</sup>. Two days post inoculation cytopathic effect (CPE) typically reached 80-100 %. VZV stocks (VZV-infected cells) were frozen in media with 10% DMSO (Roth, Germany) and stored in liquid nitrogen. The titer of VZV stocks were determined by calculation of the TCID<sub>50</sub> by the Reed-Muench formula on HELF cells and tested for mycoplasma contaminations using Venor GEM-Mykoplasmen Detektion Kit from Minerva biolabs (Berlin, Germany) according to the manufacturer's instructions.

The HSV-1 strain KOS was propagated in Vero E6 cells and kindly provided by M.J. Raftery.

## 2.5 Antibodies

The following mouse monoclonal antibodies were used for following analysis: fluorescence activated cell sorter (FACS), immunofluorescence (IF), western blot (WB) or enzyme linked immunosorbant assay (ELISA).

**Tab. 3: Primary Antibodies**

Specificity	Clone	Application	Company
<b>Actin (beta)</b>	AC-15	WB	Abcam (Hiddenhausen, Germany)
<b>CD107a</b>	H4A3	FACS	BD Biosciences (Heidelberg, Germany)
<b>CD154-PE (CD40L)</b>	TRAP1	FACS	BD Biosciences (Heidelberg, Germany)
<b>CD1a</b>	HI 149	FACS, IF	ImmunoTools (Friesoythe, Germany)
<b>CD1b</b>	4.A7.6	FACS, IF	IMMUNOTECH (Marseille, France)
<b>CD1c</b>	L161	FACS, IF	IMMUNOTECH (Marseille, France)
<b>CD206</b>	19.2	FACS, IF	BD Biosciences (München, Germany)
<b>CD209</b>		FACS, IF	Acris Antibodies (Herford, Germany)
<b>CD3</b>	UCHT1	FACS, IF	BD Biosciences (Heidelberg, Germany)
<b>CD40</b>	5C3	FACS, IF	BD Biosciences (Heidelberg, Germany)
<b>CD40-PE</b>	5C3	FACS	BD Biosciences (Heidelberg, Germany)
<b>CD83</b>	HB15e	FACS, IF	BD Biosciences (Heidelberg, Germany)
<b>CD83-FITC</b>	HB15e	FACS	BD Biosciences (Heidelberg, Germany)
<b>CD86</b>	IT2.2	FACS, IF	BD Biosciences (Heidelberg, Germany)
<b>CD86-PE-Cy5</b>	2331 (FUN-1)	FACS	BD Biosciences (Heidelberg, Germany)
<b>gE</b>	MAB8612	FACS, IF, WB	MILLIPORE (Schwalbach, Germany)
<b>IgG<sub>1</sub></b>	MOPC-21	FACS, IF	BD Biosciences (Heidelberg, Germany)
<b>IgG<sub>2b</sub></b>	MPC-11	FACS, IF	BD Biosciences (Heidelberg, Germany)
<b>p38</b>	9212	WB	Cell Signaling Technology (Danvers, USA)
<b>MAP Kinase</b>			Cell Signaling Technology (Danvers, USA)
<b>p44/42</b>	9102	WB	Cell Signaling Technology (Danvers, USA)
<b>MAP Kinase</b>			Cell Signaling Technology (Danvers, USA)
<b>Phospho-p38</b>	9211	WB	Cell Signaling Technology (Danvers, USA)
<b>MAP Kinase (Thr180/Tyr182)</b>			Cell Signaling Technology (Danvers, USA)

<b>Phospho-p44/42 MAP Kinase (Thr202/Tyr204)</b>	9101	WB	Cell Signaling Technology (Danvers, USA)
<b>Phospho-SAPK/JNK (Thr183/Tyr185)</b>	9251	WB	Cell Signaling Technology (Danvers, USA)
<b>SAPK/JNK</b>	9252	WB	Cell Signaling Technology (Danvers, USA)
<b><math>\gamma\delta</math> TCR</b>	11F2	FACS, IF	MILLIPORE (Schwalbach, Germany)

**Tab. 4: Secondary Antibodies**

<b>Specificity</b>	<b>Application</b>	<b>Company</b>
Alexa_488_IgG <sub>2b</sub>	IF	Invitrogen (Karlsruhe, Germany)
Alexa_568_IgG <sub>1</sub>	IF	Invitrogen (Karlsruhe, Germany)
Allophycocyanin-conjugated AffiniPure IgG, Fc <sub>γ</sub> subclass 2b specific	FACS	Dianova (Hamburg, Germany)
Cy5-conjugated AffiniPure IgG	FACS	Dianova (Hamburg, Germany)
FITC-conjugated AffiniPure IgG	FACS	Dianova (Hamburg, Germany)
Peroxidase conjugated Streptavidin	ELISA	Dianova (Hamburg, Germany)
Peroxidase-conjugated AffiniPure F(ab') <sub>2</sub> Fragment	WB, ELISA	Dianova (Hamburg, Germany)
R-Phycoerythrin-conjugated AffiniPure IgG	FACS	Dianova (Hamburg, Germany)
R-Phycoerythrin-conjugated AffiniPure IgG Fc <sub>γ</sub> subclass 1 specific	FACS	Dianova (Hamburg, Germany)

## 2.6 Fluorescent Dyes

**Tab. 5: Fluorescent Dyes**

<b>Specificity</b>	<b>Application</b>	<b>Company</b>
AnnexinV (sc-4252)	FACS	Santa Cruz Biotechnology (Heidelberg, Germany)
DAPI	IF	Invitrogen (Karlsruhe, Germany)
Propidium iodide (sc-3541)	FACS	Santa Cruz Biotechnology (Heidelberg, Germany)

## 2.7 Chemicals

Tab. 6: Chemicals

Name	Company
APS	Roth (Karlsruhe, Germany)
Collagenase	CellSystem (St. Katharinen, Germany)
Coomassie blue	Serva (Heidelberg, Germany)
Dispase I	Purity grade I; Roche (Mannheim, Germany)
DMSO	Roth (Karlsruhe, Germany)
DNase	Roche (Mannheim, Germany)
EDTA	AppliChem (Darmstadt, Germany)
Eosin Y solution	Merck (Darmstadt, Germany)
Ethanol	Roth (Karlsruhe, Germany)
FCS	Hyclone, Perbio Sciences (Bonn, Germany)
Formaldehyd	Merck (Darmstadt, Germany)
Hyaluronidase type I S	Sigma Aldrich (München, Germany)
Isopentane	Roth (Karlsruhe, Germany)
Isopropanol	Roth (Karlsruhe, Germany)
LPS	Sigma-Aldrich (Hamburg, Germany)
LTA	InvivoGene (San Diego, USA)
Mercaptoethanol	Merck (Darmstadt, Germany)
Methanol	Roth (Karlsruhe, Germany)
Molecular weight marker	Fermentas (St. Leon-Rot, Germany)
Monensin	Sigma-Aldrich (Hamburg, Germany)
Papanicolau's solution	Merck (Darmstadt, Germany)
PHA-L	Sigma-Aldrich (Hamburg, Germany)
Recombinant hu GM-CSF	ImmunoTools (Friesoythe, Germany)
Recombinant hu IL-4	ImmunoTools (Friesoythe, Germany)
Rotiphorese-Acrylamid	Roth (Karlsruhe, Germany)
SDS	Merck (Darmstadt, Germany)
Stop-Solution	Medac (Hamburg, Germany)
Sucofin skim milk powder	TSI (Zeven, Germany)
TEMED	Roth (Karlsruhe, Germany)
TMB-Substrate	Medac (Hamburg, Germany)
Tris-Aminomethan	Roth (Karlsruhe, Germany)
Tris-HCl	Roth (Karlsruhe, Germany)
Trypsin/EDTA	Invitrogen (Karlsruhe, Germany)
Tween-20	Roth (Karlsruhe, Germany)

## 2.8 Buffers and Solutions

Tab. 7: Buffers and Solutions

Name	Ingredients	Name	Ingredients
<b>Apoptosis buffer</b>	10 mM Hepes, pH 7.4 0.14 M NaCl 5 mM CaCl <sub>2</sub> 5% FCS 0.02% sodium azide	<b>FACS block</b>	PBS Solution 10% FCS 0.02% sodium azide
<b>Coomassie</b>	Destain solution with 2.5% coomassie-blue	<b>FACS wash</b>	PBS Solution 1% FCS 0.02% sodium azide
<b>Destain</b>	7% acetic acid 10% methanol Add H <sub>2</sub> O	<b>Fixation</b>	PBS Solution 0.37% formaldehyde
<b>Electrophoresis buffer</b>	0.06 M Tris-aminomethan 0.2 M Glycin 0.1% SDS	<b>PBS</b>	2 mM NaH <sub>2</sub> PO <sub>4</sub> 6.5 mM Na <sub>2</sub> HPO <sub>4</sub> 150 mM NaCl
<b>ELISA coating buffer</b>	100 mM Carbonat/bicarbonate buffer, pH 9.6	<b>Resolving gel</b>	0.9 M Tris-aminomethan 0.4% SDS pH 8.8
<b>ELISA blocking buffer</b>	PBS with 5% skimmed milk	<b>Stacking gel</b>	0.3 M Tris-aminomethan 0.4% SDS pH 6.8
<b>ELISA wash buffer</b>	PBS with 0.05% Tween-20	<b>Transfer buffer</b>	0.8 M Tris-aminomethan 0.4 M Glycin 20% Methanol pH 8.0

## 2.9 Kits

Tab. 8: Kits

Name	Company
BCA Protein Assay Kit	Pierce (Rockford, USA)
CD1c (BDCA-1) <sup>+</sup> Dendritic Cell Isolation Kit, hu	Miltenyi Biotech (Bergisch-Gladbach, Germany)
Complete Protease Inhibitor Cocktail	Tablets, Roche (Mannheim, Germany)
IFN- $\gamma$ ELISA	ImmunoTools (Friesoythe, Germany)
IL-12p70 ELISA	Ready-SET-Go, eBioscience (EW Breda, Netherland)
MACS columns	Large cell, LD and MS, Miltenyi Biotech (Bergisch-Gladbach, Germany)
Monocyte Isolation Kit II	Miltenyi Biotech (Bergisch-Gladbach, Germany)
mRNA Isolation	MagNA Pure LC mRNA Isolation Kit-I Lysis Buffer Refill, Roche (Mannheim, Germany)
Mycoplasma Detection	Venor GEM-Mykoplasmen Detektion Kit, Minerva biolabs (Berlin, Germany)

## 2.10 Equipment

Tab. 9: Equipment

Name	Type and Company
Anti-roll plate, glass	50 mm, Leica Microsystems GmbH (Nussloch, Germany)
Kodak Image Station	4000 MM, Kodak (Stuttgart, Germany)
Cell counting chamber	Neubauer improved, Roth (Karlsruhe, Germany)
Cell counting	CASY I, Schaefer System (Reutlingen, Germany)
Centrifuges	Megafuge 2.0 R, Heraeus (Hanau, Germany)
CO <sub>2</sub> Incubator	HERACell 150, Heraeus (Hanau, Germany)
Cryomolds	Tissue-Tek 4565, Sakura (Zoeterwoude, Netherlands)
Cryostat	Jung, Frigocut 2800N, Leica Microsystems Nussloch (Nussloch, Germany)
Electronic pipetor	Pipetus, Hirschmann Laborgeräte (Eberstadt, Germany)
Electrophoresis System	BIO-RAD Laboratories (München, Germany)
Flow Cytometer	FACSCalibur and FACSCanto II, BD Biosciences (Heidelberg, Germany)
Fluorescence Microscope	Olympus BX60, Carl Zeiss (Jena, Germany)
Freezing spray	Solidofix, Roth (Karlsruhe, Germany)
Microscope	Axiovert 25, Carl Zeiss (Jena, Germany)
Microscope slides	SuperFrost <i>Ultra</i> Plus, Menzel (Braunschweig, Germany)
Sterile filters	0,2 $\mu$ m, Schleicher and Schüll (Dassel, Germany) 300 $\mu$ m and 40 $\mu$ m Nylon, BD Biosciences (Heidelberg, Germany)



	many)
Sterile Workbench	HERASafe, Heraeus (Berlin, Germany)
Tissue Freezing Medium	Jung, Leica Microsystems (Nussloch, Germany)
Vortex	Vortex-Genie 2, Scientific Industries (New York, USA)
Waterbath	GFL (Burgwedel, Germany)
Whatman Paper	Schleicher and Schüll (Dassel, Germany)

---

## 2.11 Quantitative RT-PCR

Quantitative reverse transcriptase PCR (qRT-PCR) for CD1, CD40 and CD86 genes was performed using  $5 \times 10^5$  iDCs collected in 300  $\mu$ l lysis buffer from the MagnaPure mRNA isolation kit I (Roche Diagnostics, Mannheim, Germany). Messenger RNA (mRNA) was isolated with the MagnaPure-LC device by using the mRNA kit I standard protocol. The elution volume was set to 50  $\mu$ l. An aliquot of 8.2  $\mu$ l of RNA was reverse transcribed by using avian myeloblastosis virus RT and oligo dT. After the termination of the cDNA synthesis, the reaction mix was diluted to a final volume of 500  $\mu$ l and stored at  $-20^\circ\text{C}$  until PCR analysis. Primer sets specific for CD1a to CD1c, CD40 and CD86 genes and optimized for the LightCycler were developed and provided by SEARCH-LC. PCR was performed with the LightCycler FastStart DNA Sybr green kit I (Roche Diagnostics, Mannheim, Germany) according to the manufacturer's instructions. The calculated copy numbers were normalized according to the average expression of two housekeeping genes, the cyclophilin B and beta-actin. All qRT-PCR's were analyzed by T. Giese at the University of Heidelberg, Institute of Immunology (Heidelberg, Germany).

## 2.12 Immunological Methods

### 2.12.1 Isolation of Monocytes from Buffy Coats

Buffy coat preparations (~ 60 ml) were supplied by the Deutsche Rote Kreuz (Dresden, Germany) and diluted 1:1 with media containing 0.2 mM EDTA. The diluted blood was carefully layered on top of 20 ml of Ficoll-Hypaque in a 50 ml falcon tube (LSM1077, PAA Laboratories GmbH, Marburg, Germany). To separate the blood cells, tubes were centrifuged for 20min at room temperature at 800 g without brake. Thereafter, the white ring containing PBMCs was collected and washed with medium. To eliminate thrombocytes, the cells were once centri-

fuged at 200 g for 5min and the supernatant was carefully removed. The PBMCs were resuspended in 10 ml media and carefully layered on top of diluted Ficoll-Hypaque (1.4 ml PBS was added to 10 ml Ficoll-Hypaque). The tubes were centrifuged again at 800 g for 25min at room temperature and the white PBMC ring was harvested. For isolation of untouched monocytes, the Monocyte Isolation Kit II was used according to the manufacturer's instruction. The cells were washed once in cold MACS buffer and then incubated for 10min at 4°C with 200 µl of human FcR blocking reagent and 200 µl of monocyte Biotin-Antibody Cocktail containing mouse monoclonal antibodies anti human CD3, CD7, CD16, CD19, CD56, and Glycophorin A to label non-monocytes (T cells, B cells, NK cells, DCs and basophiles). Thereafter, 1 ml ice-cold MACS buffer and 400 µl Anti-Biotin MicroBeads were added to. After another incubation time of 15min at 4°C the labeled cells were adjusted to an equilibrated LS column. The untouched monocytes were collected from the flow through and washed twice in media. To differentiate monocytes into immature DCs, GM-CSF (500 IU/ml) and IL-4 (200 IU/ml) were added to the culture medium. Entire medium was replaced on day three post isolation when DCs were used for viral infection. Immature DCs were analyzed for cell surface expression of CD1a, CD1c and DC-SIGN.

### **2.12.2 VZV Infection of Immature DCs**

After 3d of differentiation, 1 to 2 x 10<sup>6</sup> immature DCs were centrifuged at 150 g for 45min at room temperature onto VZV-infected HELF monolayer (24-well plate). VZV-infected HELF monolayers showed cytopathic effects of 75-90% with a TCID<sub>50</sub> of ~ 2,7x 10<sup>4</sup> PFU/ml. Mock-infected cultures were set up as described above using uninfected HELFs. DCs were removed 24h post transmission and placed into a new T75 culture flask. After 2d post VZV transmission flow cytometry analysis and T cell assays were performed (Fig.7).

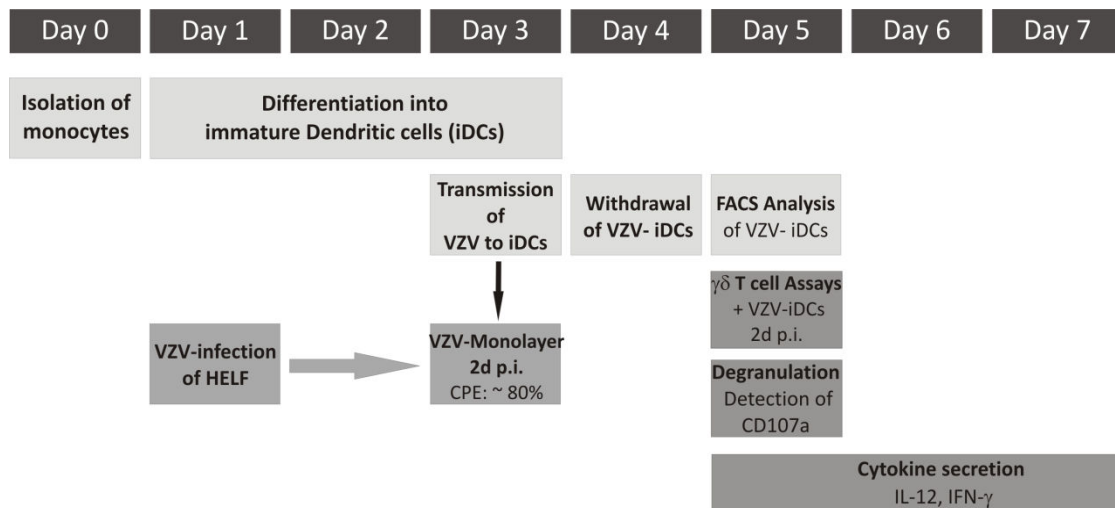


**Fig. 7: Experimental setting for phenotypic and functional analysis of VZV-infected DCs.**

Monocytes were isolated from buffy coats derived from healthy individuals and differentiated within three days into immature mo-DCs (iDCs). Human embryonic lung fibroblasts (HELFL) were infected with VZV and 2d post VZV infection iDCs were centrifuged on VZV-infected monolayers showing cytopathic effects (CPE) of about ~80%. After 24h of coculture iDCs were gently removed from the VZV monolayer and cultured for another 24h. Two days post infection VZV-infected iDCs were analyzed by flow cytometry for surface expression and used for stimulation of CD1c-restricted  $\gamma\delta$ T cells.

### 2.12.3 Flow Cytometry

To detect cell surface expression by flow cytometry cells were washed once with ice-cold FACS wash solution before being resuspended with the primary antibodies in ice-cold blocking solution for 1h. Cells were then washed with FACS wash solution and stained for 45min with secondary fluorophore-conjugated antibodies. After another washing step cells were fixed with 0.37% formaldehyde and analyzed by flow cytometry with a FACSCalibur or FACSCanto II. Data were analyzed with Cellquest Pro software.

### 2.12.4 Detection of Apoptotic Death

A characteristic early event during apoptosis is the loss in membrane asymmetry which results in the translocation of phosphatidylserine from the inner to the outer leaflet of the plasma membrane. Once exposed to the extracellular environment, phosphatidylserine can be detected through AnnexinV, a  $\text{Ca}^{2+}$ -dependent phospholipid binding protein. Due to the loss in membrane integrity in the process of cell death nucleic acids become accessible for the intercalating dye propidium iodide (PI). Staining for AnnexinV indicates early events of apoptosis whereas additional staining for propidium iodide is characteristic for later stages of apoptosis or necrosis.

During the whole staining procedure the cells must be kept in the apoptosis buffer containing 5 mM calcium. Apoptotic death was investigated using AnnexinV conjugated to the fluorophore FITC and propidium iodide.

Cells were harvested and washed once with apoptosis buffer. AnnexinV was added to the cells and incubation was performed at 4°C for 20min. After another washing step cells were kept on ice and immediately analyzed by flow cytometry. The sample was firstly analyzed for AnnexinV positive cells and thereafter propidium iodide was added to the sample. After an incubation time of 2-3min at 4°C the samples were measured for double-positive cells.

### **2.12.5 T Cell Assays**

All T cell assays were performed with the well characterized CD1c-restricted  $\gamma\delta$  T cell clone JR.2.28<sup>131</sup>. The T cell clone was cultured by periodic stimulation with PHA in the presence of irradiated EBV-transformed B cells and PBMCs as described<sup>131</sup>.

#### **2.12.5.1 Cytokine Secretion Assay**

$5 \times 10^5$  T cells were cocultured with  $5 \times 10^5$  mock or VZV-infected iDCs in a flat bottom 96-well plate. As positive control, T cells were stimulated with PHA. Supernatants were harvested after 48h of coculture and stored at -20°C. Cytokine release was determined for IFN- $\gamma$  and bioactive IL-12p70 by ELISA.

#### **2.12.5.2 Cytotoxicity Assay**

To verify cytotoxic activity of  $\gamma\delta$  T cells cell surface expression of CD107a (Lamp-1) was detected as previously described<sup>171,172</sup>. The effector-target ratio (E-T ratio) was 1:1. Therefore,  $2 \times 10^5$   $\gamma\delta$  T cells were co-cultured with  $2 \times 10^5$  mock or VZV-infected DCs in a flat bottom 96-well with a final volume of 200  $\mu$ l. The CD107a antibody (15  $\mu$ l) was directly added to the cells within the first hour of incubation at 37°C and 5% CO<sub>2</sub>. Thereafter, 5  $\mu$ l of the secretion inhibitor monensin (2 mM) was added to the wells. After a further incubation period of 4h at 37°C and 5% CO<sub>2</sub> cells were washed once with PBS and then stained with antibodies for flow cytometry analysis. To detect spontaneous degranulation of the T cells a control sample without target cells was included in every experiment.

### **2.12.6 ELISA**

To detect and quantify the cytokine concentration in unknown samples we used the two-antibody sandwich Enzyme Linked Immunosorbant Assay (ELISA). The ELISAs were performed according to the instructions of the manufacturer. Briefly, the capture antibody for the corresponding cytokine was bound overnight at 4°C by softly shaking to the 96-well flat bottom plate. After washing the plate, wells were blocked with blocking buffer for 1h at RT. Then, the plate was washed several times with washing buffer. Thereafter, the corresponding standard cytokine in appropriate dilutions and the unknown samples were applied to each well and incubated for 2h at RT (carefully shaking). After several washing steps the biotinylated detection antibody was added and allowed to bind to the cytokine during incubation time of 1h at RT under softly shaking. The enzyme horseradish peroxidase (HRP) coupled to streptavidine was added for 30min after several washing steps. Then, the substrate 3, 3', 5, 5'-tetramethylbenzidine (TMB) was added for a maximum of 30min. After incubation in the dark the reaction was stopped by adding 2N H<sub>2</sub>SO<sub>4</sub> to each well. The color density was measured at 450 nm. The cytokine concentration in unknown samples was calculated according to the standard curve of the standard antigen.

### **2.12.7 Immunohistochemistry**

Skin sections were stained for 30s with Papanicolaous solution (dilution 1:2 with H<sub>2</sub>O) and finally washed several times with tap water. Afterwards, slides were stained with Eosin solution for 2 min. After excessive washing slides were finally mounted with mounting media (Kaiser's Glyce-ringelatine with Pheno) from Merck (Darmstadt, Germany) for histology.

Skin sections from biopsies were washed once with PBS to remove acetone and then blocked for 1h at room temperature with 5% goat serum in FACS block solution. Incubation of primary antibodies was performed in a humified chamber at 37°C for 1h. Slides were washed with PBS before incubation of secondary antibodies at room temperature for 45min. In this step staining of nuclear DNA with DAPI (1/20 000) was also performed. Slides were finally covered with mounting medium from Dako (Hamburg, Germany). The stained skin sections were analyzed by fluorescence microscopy.

### 2.12.8 Immunoblot Analysis

Mock or VZV-infected iDCs (2d p.i.) were stimulated for 15min with control or CD40L-expressing adherent cells. DCs were then lysed in lysis buffer containing 0.1% NP40, 80 mM KCl, 50 mM Tris-HCl, pH 7.5, 10 mM EDTA and a protease inhibitor cocktail. Cell lysates were separated by SDS-PAGE and transferred to polyvinylidene difluoride (PVDF) membranes. Membranes were stained with the appropriate specific antibodies and visualized with an enhanced chemiluminescence system from Perbio Science (Bonn, Germany).

### 2.13 Statistics

The program SPSS 14.0 was used to perform statistics. The Wilcoxon test was used to determine the significance of differences between groups. P values of less than 0.05 were considered significant (two-tailed). The actual P values are indicated in the Box-Whisker-Plots. Boxes cover the middle 50% of the data values between the 25<sup>th</sup> and 75<sup>th</sup> percentiles, the central line being the median. Endpoint of whiskers represents true data points for smallest and biggest values.

### 2.14 Software

Tab. 10: Software

Name	Company
Adobe Photoshop	CS3 (München, Germany)
CellQuest Pro	BD Biosciences (Heidelberg, Germany)
CorelDraw	X3 (Unterschleißheim, Germany)
SPSS	14.0 (Chicago, USA)

## 3 Results

### 3.1 Propagation of VZV Strains in Fibroblasts

VZV is highly cell-associated *in vitro* and therefore propagation of the virus must be performed by coculture of VZV-infected cells with uninfected cells. VZV replication can be readily observed due to its typical plaque formation within the confluent monolayer (Fig.8). The VZV-induced cytopathic effect (CPE) in fibroblasts is characterized by syncytia formation and ballooning of the cells<sup>173</sup>.

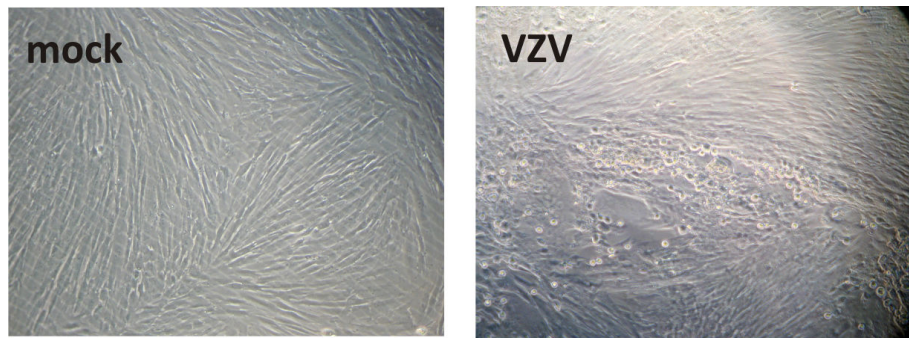


**Fig. 8: Cytopathic effect (CPE) of VZV in fibroblasts.**

Phase contrast microscopy images of mock-infected human embryonic lung fibroblasts (HELf) and VZV-infected HELf after 2d p.i. (20x magnification).

Initially, growth kinetics of attenuated vaccine strain V-Oka and clinical isolate JoSt were assessed in human embryonic lung fibroblasts (HELf). No differences in the replication capacity could be observed for both viral strains (Fig. 9a). To ensure identical titer during the transmission of VZV to iDCs the titer of a 24-well of VZV-infected HELf cells 2d p.i. was determined for each independent experiment (Fig. 9b). The titers were for the vaccine  $3.12 \times 10^4$  PFU/ml (mean) and for the JoSt strain  $3.29 \times 10^4$  PFU/ml (mean) thereby nearly identical (n=12).

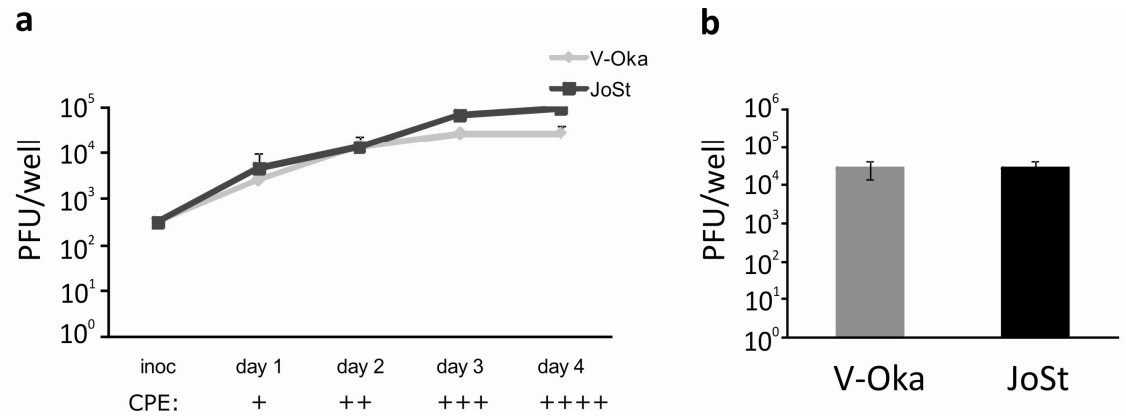


**Fig. 9: No differences in viral replication of the vaccine strain Oka (V-Oka) and a clinical isolate JoSt in cell culture.**

(a) Growth kinetic of V-Oka and JoSt infected HELFs. The titer was determined as plaque forming unit (PFU) per 24-well. Cells were infected with an inoculum of 300 PFU of cell-associated virus (VZV-infected cells) and harvested every day until four days post infection (4d p.i.). Results shown as mean  $\pm$  1 SD, were derived from three independent experiments done in duplicates for each virus. (b) The titer of VZV-infected fibroblasts (2d p.i.) within a 24-well was determined to validate equal infection of iDCs (n=12).

A main focus of this study was to compare the immunological response to vaccine strain V-Oka with that induced by clinical isolates circulating in Germany. All viral strains used were partly sequenced and genotyped (Fig. 10).

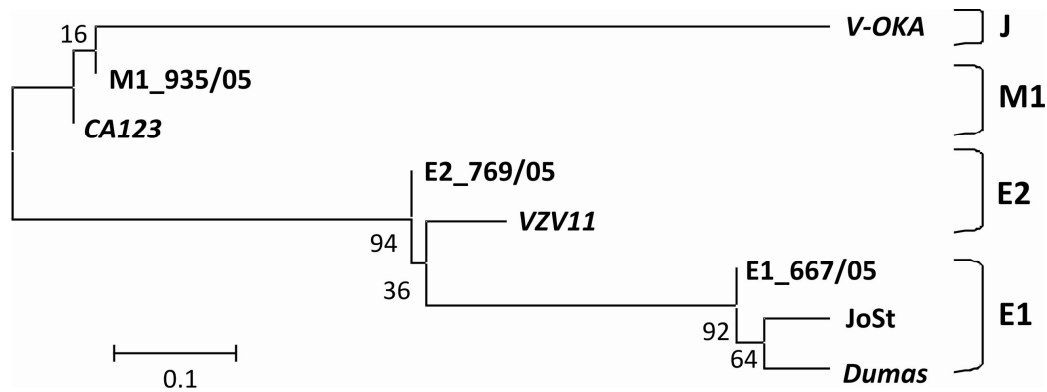


**Fig. 10: Phylogenetic tree of VZV strains.**

All VZV strains used belong to one of the following genotypes: J, M1, E2 and E1. VZV reference strains (in italics) were integrated within the phylogenetic tree. The investigated VZV strains in this study cluster in the following genotypes: the vaccine strain V-Oka clustered within genotype J, M1\_935/05 belongs to genotype M1, E2\_769/05 is representative for genotype E2 and E1\_667/05 and JoSt belongs to the genotype E1. The length of the indicated marker represents 0.1 nucleotide exchange.

The efficiency of infection of the different genotypes of VZV was assessed by immunofluorescence microscopy analysis in HELF cells (Fig. 11). VZV infection of HELF cells induced typical syncytia formation as revealed by DAPI staining. The infection was visualized



with a VZV patient serum. No differences in the infection efficiency could be observed for the clinical isolates of VZV.

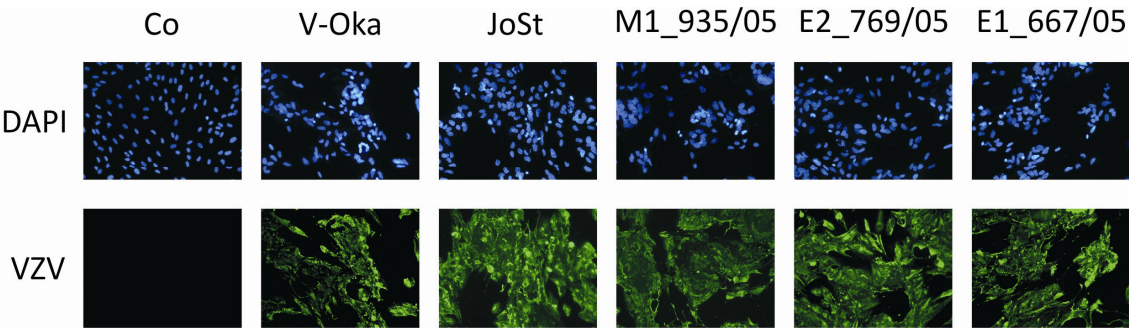


**Fig. 11: Growth of VZV clinical isolates in fibroblasts.**  
 HELFs grown on coverslides were infected with VZV clinical isolates as indicated. After 2d cells were fixed with methanol/acetone (1:1) and stained for VZV infection with a VZV patient serum (1/100). Cellular nuclei were visualized with DAPI (1/20 000). In VZV-infected cells the characteristic formation of syncytia could be observed. (10x magnification).

### 3.2 Distribution of DCs within Skin Lesions of Herpes Zoster Patients

The skin comprises distinct compartments harboring different types of DCs that function as sentinels for invading pathogens. Langerhans cells (LC) of the epidermis express on their cell surface CD1a and Langerin which capture antigen from the surrounding environment. Dermal dendritic cells (DDC) are located in the dermis and express CD1b, CD1c and DC-SIGN (DC-specific intercellular adhesion molecule-3-grabbing non-integrin) on the cell surface. To investigate which type of DC is involved during VZV pathogenesis we analyzed skin sections from punch biopsies of immunocompetent herpes zoster patients.

Frozen skin sections of healthy control and herpes zoster patients were initially stained with Papanicolaou's solution and eosin to visualize differences in tissue morphology (Fig.12). Compared to control skin herpes zoster lesions were characterized by extensive formation of multi-nucleated polykaryocytes, a gradual thickening of the epidermis, epidermal cell proliferation and cellular degeneration (Fig. 12b). In the vesicles, acantholysis (loss of intercellular connections between keratinocytes), destruction of the epidermis as well as the upper part of the dermis was observed. Additionally, local massive infiltration of inflammatory cells was detected.

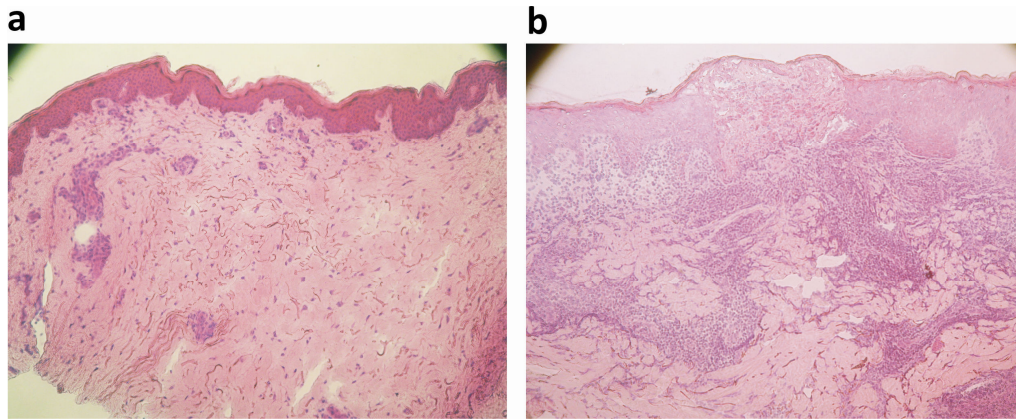


**Fig. 12: Tissue biopsies of healthy control individuals and herpes zoster patients.**

Frozen skin sections (5µm) were stained with Papanicolaou's solution and eosin to visualize morphological changes within the tissue. The epidermis is orientated upwards. (a) Skin section of healthy control. (b) Skin section of herpes zoster patient (10x magnification). Sections of one representative biopsy of two are shown.

To characterize the massive infiltration of inflammatory cells in herpes zoster lesions skin sections were assessed by immunofluorescence microscopy (Fig. 13). Staining of nuclei with the DNA-intercalating dye DAPI showed the structured organisation of the control skin. In contrast, VZV-infected tissue of herpes zoster (HZ) patients showed the typical thickening of the epidermis and locally a strong infiltration of inflammatory cells within the dermis. VZV infection was visualized by detecting the late viral gene product glycoprotein E (gE) which is the most abundantly expressed glycoprotein during VZV infection. In the herpes zoster sections staining for gE localized the VZV containing vesicle within the epidermis and dermis. As expected, no signal could be detected in the control skin. Staining for the integrin CD11c, a marker which is exclusively expressed on myeloid cells, detected the infiltration of myeloid cells within the VZV-infected tissue. CD1a and Langerin expressing LCs were evenly distributed in the epidermis of the control skin but absent in the herpes zoster skin. CD1b and CD1c expressing DDCs were evenly distributed in the upper dermis of the control skin. In strong contrast, CD1b expressing DDCs were found to strongly infiltrate herpes zoster lesions. Few CD1c expressing DDCs could be detected in close neighbourhood of the VZV vesicle.

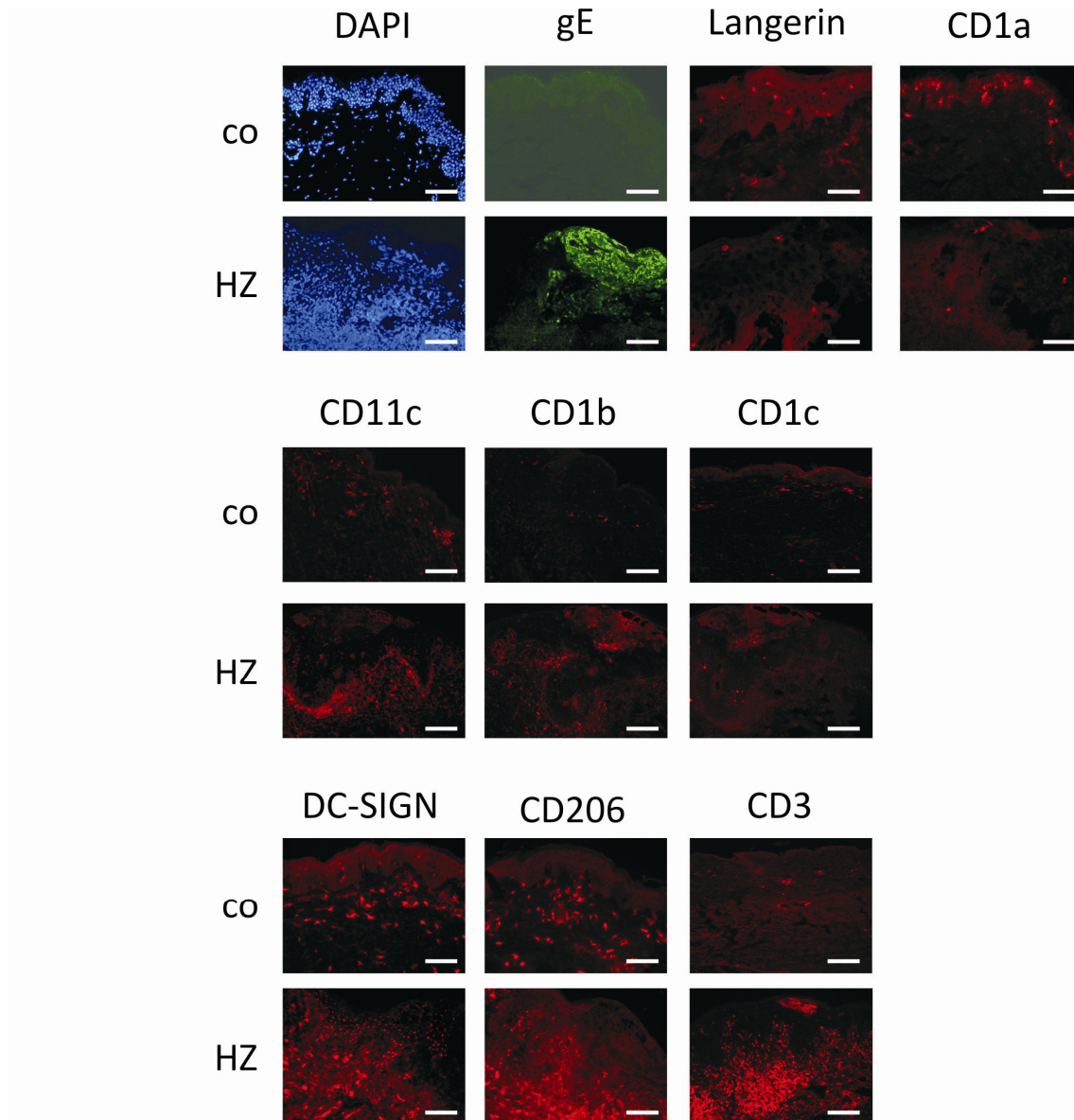


**Fig. 13: Dual immunofluorescence microscopy analysis of skin sections from control and herpes zoster (HZ) biopsies.**

Nucleic acids were stained with the DNA intercalating dye DAPI (1/20 000). All sections are orientated with the epidermis upwards. Sections were stained for viral glycoprotein E (gE), Langerhans cell markers Langerin and CD1a, CD11c as a marker of myeloid DCs, the molecules CD1b, CD1c and DC-SIGN expressed on dermal dendritic cells (DDCs), CD206 as macrophage marker and CD3 to detect T cells. One representative skin section of two biopsies is shown. White scale bar represents 200  $\mu\text{m}$ .

Intriguingly, CD1c expressing DDCs were detected in close contact to the VZV vesicle but remained undetectable in the surrounding dermis. Furthermore, staining for the marker DC-SIGN and CD206 (mannose-6 phosphate receptor) showed that the infiltrated cells within the dermis of the herpes zoster patient comprise DDCs and macrophages. Staining for CD3 showed that the infiltrated cells within the herpes zoster biopsy also con-

tained T cells. Staining for tissue-specific V $\delta$ 1  $\gamma\delta$  T cells was not possible which might be due to lack of sensitivity of the antibody used or due to emigration of  $\gamma\delta$  T cells to the local lymph node. Altogether these data provide evidence that myeloid DCs expressing CD1 molecules play a role in the cutaneous immune response against VZV.

Blood samples from herpes zoster patients in the acute phase of infection were analyzed to determine the percentage of circulating  $\gamma\delta$  T cells. Recently, a role for these cells in patients resolving cytomegalovirus infection was found<sup>166</sup>. Peripheral blood mononuclear cells (PBMCs) were stained for the expression of CD3 and  $\gamma\delta$  TCR and analyzed by flow cytometry (Fig. 14a). Slightly reduced percentages of peripheral  $\gamma\delta$  T cells were observed in herpes zoster patients compared to healthy control persons (Fig. 14b). The observed variation between 1% and 10% of  $\gamma\delta$  T cells within the control group is a common observed finding and can be explained by the donor variability.

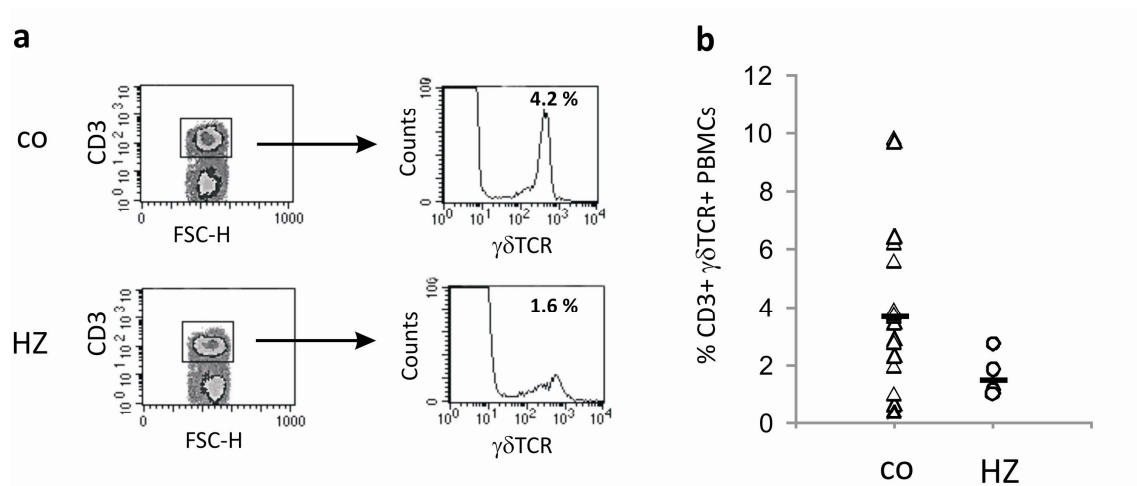


**Fig. 14: Percentage of  $\gamma\delta$  T cells in peripheral blood from healthy control and herpes zoster (HZ) patients as determined by flow cytometry.**

(a) Histograms showing  $\gamma\delta$  TCR expression on CD3<sup>+</sup> T cells. One representative experiment is shown. (b) Percentage of CD3<sup>+</sup>/ $\gamma\delta$  TCR<sup>+</sup> cells in peripheral blood mononuclear cells from healthy control (co, n=17) and herpes zoster (HZ) patients (acute phase of infection; n=4) is shown. Opened triangles and circles represent data points of patients. The median is indicated as black bar.

### 3.3 VZV Infection of Cutaneous DCs

In order to assess the question if cutaneous DCs are permissive to VZV infection, LCs and DDCs were isolated by magnetic bead technique from human skin. Staining for myeloid marker CD11c and Langerin on LCs (Fig. 15a) and CD11c and CD1c on DDCs (Fig. 15b) confirmed the purity of the preparations.

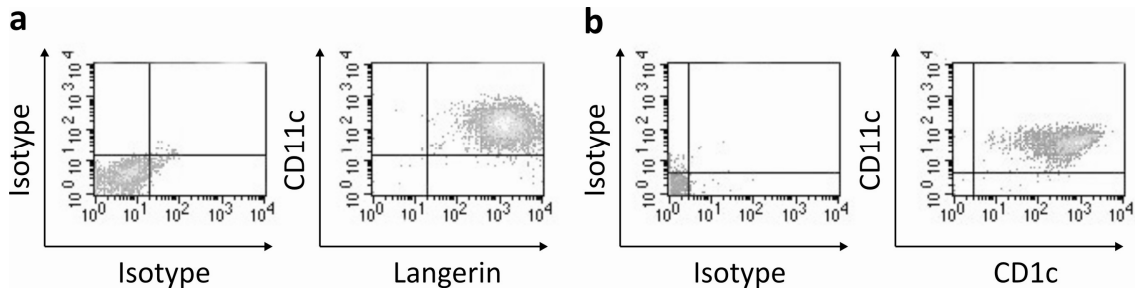


**Fig. 15: Isolation of cutaneous DCs from human skin.**

(a) LCs were isolated from epidermis and analyzed by flow cytometry for expression of CD11c and Langerin or respective isotype controls. (b) DDCs were isolated from dermis and purity was confirmed by staining for CD11c and CD1c. One representative experiment of two is shown.

Freshly isolated LCs and DDCs were used to investigate the permissivity to VZV infection. Due to the highly cell-associated nature of VZV *in vitro* LC and DDC infection was performed by coculture with VZV-infected fibroblasts. To detect and quantify the infection rate of VZV, 2d p.i. LCs and DDCs were stained for the cell surface expression of glycoprotein E (gE) (Fig. 16). Mock LCs and DDCs did not express gE on the cell surface, whereas on VZV-infected LCs and DDCs expression of gE was detected. Importantly, no differences in the efficiency of infection could be observed between the vaccine strain V-Oka and the clinical isolate JoSt.

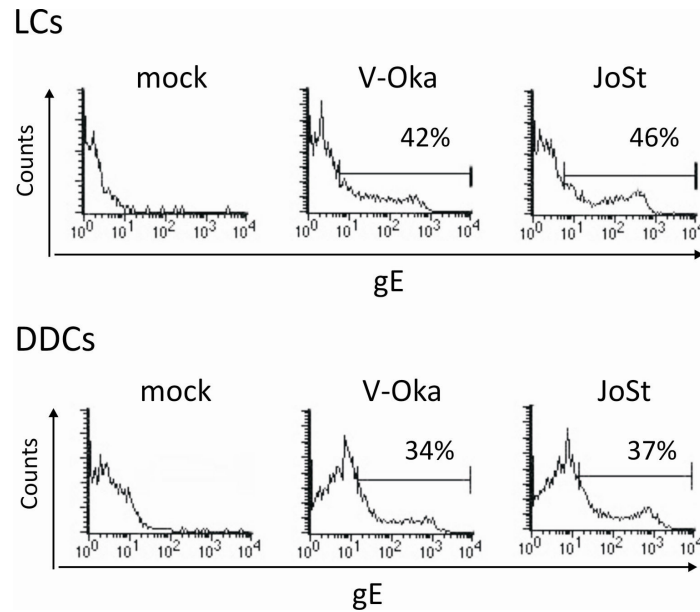


**Fig. 16: Cutaneous DCs are permissive to VZV infection.**

LCs and DDCs were cocultured with mock, V-Oka or JoSt infected iDCs and analyzed by flow cytometry 2d p.i. for cell surface expression of viral glycoprotein E (gE). Percentage of gE positive cells are indicated in the histograms. One representative experiment of two is shown.

### 3.4 Phenotype of VZV Infected Cutaneous DCs

Cutaneous migratory DCs are part of the immune surveillance system in the body's largest and most exposed interface with the environment, the skin. LCs and DDCs play a central role in host defence and are therefore well equipped to sense early invading pathogens through PRRs. After uptake of foreign antigens they undergo phenotypic and functional maturation which are characterized by expression of a set of maturation molecules like CD83, CD86 and CD40 among many others. The skin represents the major replication site of VZV. Therefore, phenotypic changes were analyzed by flow cytometry on VZV-infected LCs and DDCs (Fig. 17).

Contact of LCs with fibroblasts induced maturation in a small LC-population as cell surface expression of CD83 and CD86 on mock-infected LCs show. Furthermore, CD40 was expressed in high amounts on mock LCs. VZV infection of LCs did not induce upregulation of CD83 and CD86 on LCs. Additionally, cell surface expression of CD40 was decreased compared to mock infected LCs.



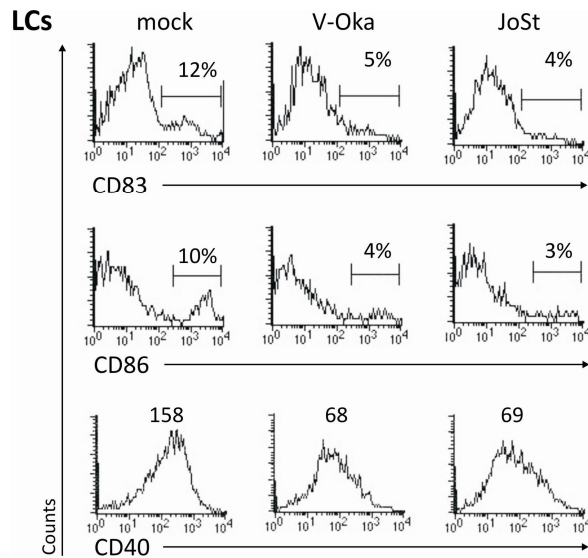


**Fig. 17: VZV does not induce phenotypic maturation on LCs.**

Mock and VZV-infected LCs were analyzed for cell surface expression of CD83, CD86 and CD40 by flow cytometry. Percentage of positive cells for CD83 and CD86 expression and MFI for CD40 expression are indicated in the histograms. One representative experiment of two is shown.

Contact of DDCs with fibroblasts or VZV infection did not induce phenotypic maturation of DDCs as cell surface staining for CD83 and CD86 demonstrated (Fig. 18). Interestingly, a decrease in CD40 cell surface expression on VZV-infected DDCs compared to mock infected DDCs was observed.

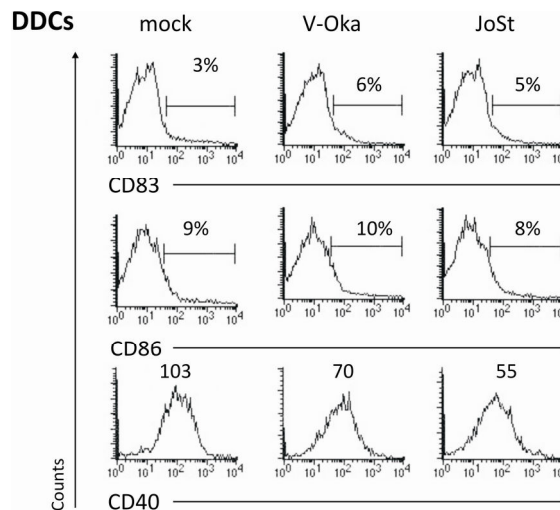


**Fig. 18: VZV infection of DDCs does not induce phenotypic maturation.**

Mock and VZV-infected DDCs were stained for cell surface expression of CD83, CD86 and CD40 and analyzed by flow cytometry. Percentage of positive cells for CD83 and CD86 expression and MFI for CD40 expression are indicated in the histograms. One representative experiment of two is shown.

Alltogether, these data provide evidence that VZV infection of cutaneous DCs did not induce phenotypic maturation and thereby prevents innate antiviral immune responses. Furthermore, VZV decreases CD40 expression on LCs and DDCs an important co-stimulatory molecule for the reciprocal crosstalk of DCs and T cells.

### 3.5 Transmission of VZV to Immature DCs

Demonstrating that cutaneous DCs are permissive to VZV infection and phenotypically modulated by VZV, further investigations were performed with monocyte-derived iDCs for several reasons. A key point is that iDCs can be differentiated from monocytes in high amounts compared to limited numbers of LCs and DDCs obtained from human skin. This is of importance because experiments with VZV are very cell consuming due to the highly cell-associated nature of VZV. Furthermore, iDCs reflect best inflammatory DCs which have been shown to differentiate from recruited monocytes into “dermal monocyte-derived DCs” during *Leishmania* infection<sup>96</sup>. Moreover, infiltration of myeloid DCs was observed in skin biopsies of herpes zoster patients and it was shown by Abendroth *et al.* that iDCs are productively infected by VZV and transmit the virus to T cells permitting viral spread<sup>20</sup>.

Before investigation of phenotype and function of VZV-infected iDCs the efficiency of infection of iDCs with the vaccine strain V-Oka and the virulent clinical isolate JoSt were analyzed. Interestingly, the morphology of iDCs changed after transmission of VZV. Compared to the single-cell morphology in the mock control, VZV-infected iDCs formed clusters (Fig. 19).

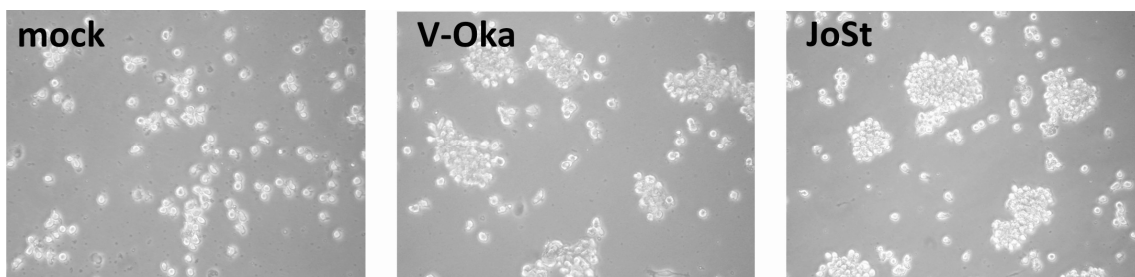


**Fig. 19: Morphology of iDCs 2d p.i. with VZV.**

Phase contrast microscopy images of mock, V-Oka and JoSt infected iDCs (10x magnification).



VZV infection by the vaccine strain V-Oka or clinical isolate JoSt was verified 2d p.i. by staining for cell surface expression of gE on iDCs (Fig. 20). Mock iDCs did not express gE on the cell surface, whereas on VZV-infected iDCs the expression of gE was detected (Fig. 20a). Interestingly, within the VZV-infected iDCs two populations (M1 and M2) were observed. The main population of VZV-infected iDCs (~75%) expressed gE in only low numbers on the cell surface (M1), whereas a minor population of less than 20% expressed high numbers of gE on the cell surface (M2, Fig. 20b). This phenomenon was observed for both VZV strains.

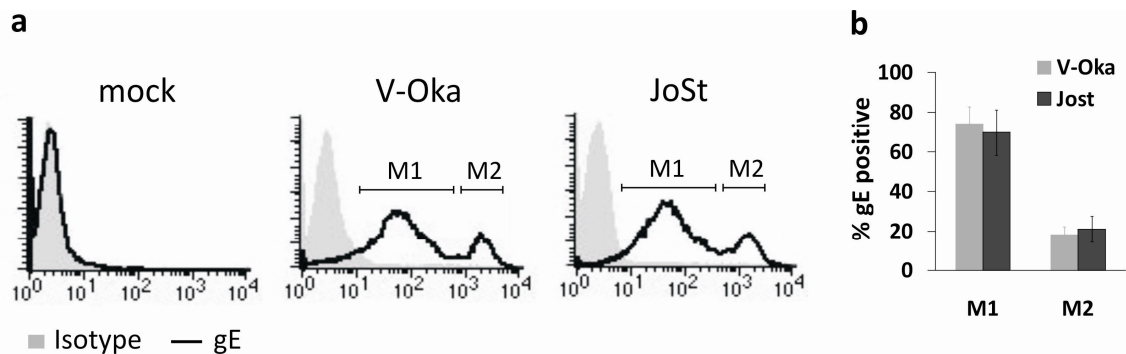


**Fig. 20: Efficiency of VZV infection of iDCs.**

(a) Flow cytometry analysis of iDCs 2d p.i. with VZV. Histograms show surface expression of viral glycoprotein E (gE) on mock, V-Oka and JoSt infected iDCs. To discriminate iDC populations with different surface density of gE after VZV infection the marker M1 and M2 were used. (B) The percentage of DCs expressing gE weakly (M1) or strongly (M2) for each DC population after infection with the VZV strain V-Oka and JoSt are shown (n=7; error bars are SD).

### 3.6 Phenotypic Changes of CD1 Molecules on VZV-infected iDCs

Recently, a case report sparked the interest on CD1 antigen presentation in the context of VZV infection. The report demonstrated a patient with a deficiency in Natural Killer T (NKT) cells who developed disseminated varicella after vaccination with the V-Oka strain<sup>26</sup>. NKT cells recognize lipid antigen through CD1d molecules. Therefore, the impact of VZV infection on CD1 antigen presentation on iDCs was assessed. For this purpose, VZV-infected iDCs 2d p.i. were stained for CD1a, CD1b, CD1c (group 1) and CD1d (group 2) molecules and analyzed by flow cytometry (Fig. 21a).

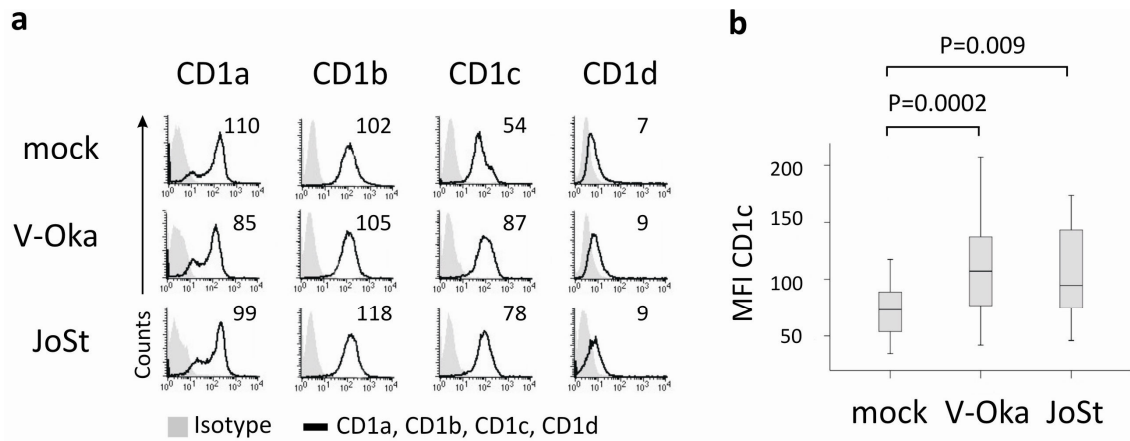


**Fig. 21: Phenotypic changes in CD1 expression on VZV-infected iDCs (2d p.i.).**

(a) Histogram plots show surface expression of CD1a, CD1b, CD1c and CD1d with indicated mean fluorescence intensities (MFI). One representative experiment out of six or more is shown. (b) Box-Whisker-Plot of MFI of CD1c surface expression on mock, V-Oka and JoSt infected iDCs (n=16). P values < 0.05 were considered significant.

No changes in CD1a, CD1b and CD1d expression on iDCs were observed after VZV infection compared to the mock control (Fig. 21a). Intriguingly, cell surface expression of CD1c was significantly enhanced on both V-Oka (P=0.0002) and JoSt (P=0.009) infected iDCs compared to the mock control (Fig. 21b). To rule out that this increase was due to enhanced transcription, quantitative real-time PCR analyses of VZV-infected iDCs were performed (Fig. 22). Analysis of group 1 CD1 transcripts pointed out that VZV infection did not interfere with the transcription of group 1 CD1 molecules. Therefore, the cell surface expression of CD1c on iDCs seems to be modulated on the protein level by VZV.

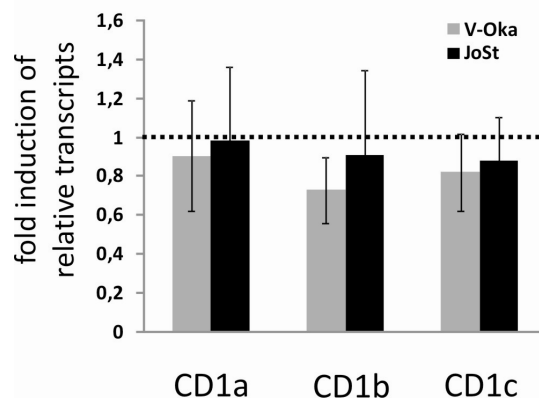


**Fig. 22: Analysis of group 1 CD1 transcripts in VZV-infected iDCs.**

The abundance of mRNA encoded by group 1 CD1 genes was determined by quantitative real-time PCR. The values are given relative to uninfected iDCs. The fold induction of transcripts in VZV-infected iDCs relative to transcripts in uninfected iDCs (stippled line) is shown. Data are delineated from three independent experiments (error bars are SD).

Altogether, these data provide evidence that lipid antigen presentation through CD1c is influenced by VZV and might have a functional impact on the reciprocal interaction of iDCs and T cells. Additionally, no differences between the vaccine and a clinical isolate of VZV regarding the infection efficiency of iDCs and their phenotypic changes could be figured out.

### **3.7 Impact of VZV induced CD1c Upregulation on Innate $\gamma\delta$ T Lymphocytes**

To study the functional impact of VZV induced CD1c upregulation, cytotoxicity and cytokine secretion assays with a well-characterized CD1c-restricted  $\gamma\delta$  T cell line were performed. Recently, it was shown that these  $\gamma\delta$  T cells recognize a yet unknown self-lipid in the context of CD1c<sup>131</sup>.

The cytotoxic potential of  $\gamma\delta$  T cells was assessed by detecting the degranulation of T cells which was shown to be essential for perforin-mediated killing<sup>171</sup>. CD107a (Lamp-1) is a lysosomal protein which is normally found within the cytotoxic granules of T cells and is detected on the cell surface of T cells after degranulation. Therefore, CD107a staining on T  $\gamma\delta$  T cells was verified to test cytotoxic activity (Fig.23). Spontaneous degranulation on  $\gamma\delta$  T cells could be observed but was less than 5% (Fig. 23b). In contrast, in the presence of mock, V-Oka and JoSt infected iDCs up to 30% of CD1c-restricted  $\gamma\delta$  T cells degranulated. However, no differences between the mock and VZV-infected iDCs could be detected.

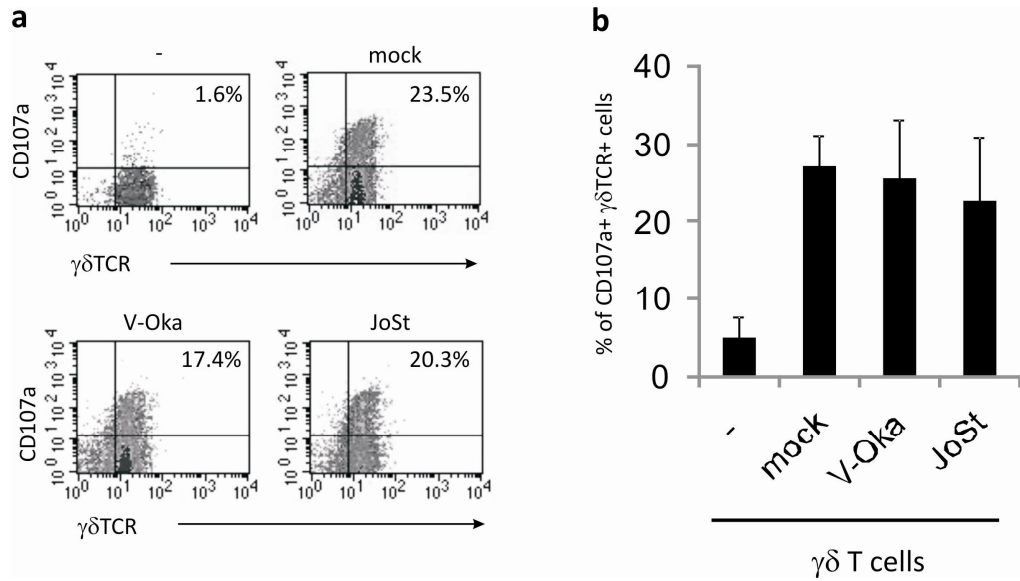


**Fig. 23: Degranulation of CD1c-restricted  $\gamma\delta$  T cell stimulated with VZV-infected iDCs.**

$\gamma\delta$  T cells were cultured alone (-) or in the presence of mock, V-Oka or JoSt infected iDCs for 6h and stained for  $\gamma\delta$ TCR and CD107a expression and analyzed by flow cytometry. (a) Dot plot showing the percentage of  $\gamma\delta$ TCR and CD107a positive cells. One representative experiment of five is shown. (b) Mean of percentages of CD1c-restricted  $\gamma\delta$  T cells expressing CD107a (n=5; error bars are SD).

Furthermore, the activation of  $\gamma\delta$  T cells was assessed by detection of secreted IFN- $\gamma$  in the presence of mock or VZV-infected iDCs (Fig. 24). These assays were carried out with clinical isolates of different VZV genotypes to rule out a genotype dependent interference of VZV with  $\gamma\delta$  T cell activation (Fig. 24a).

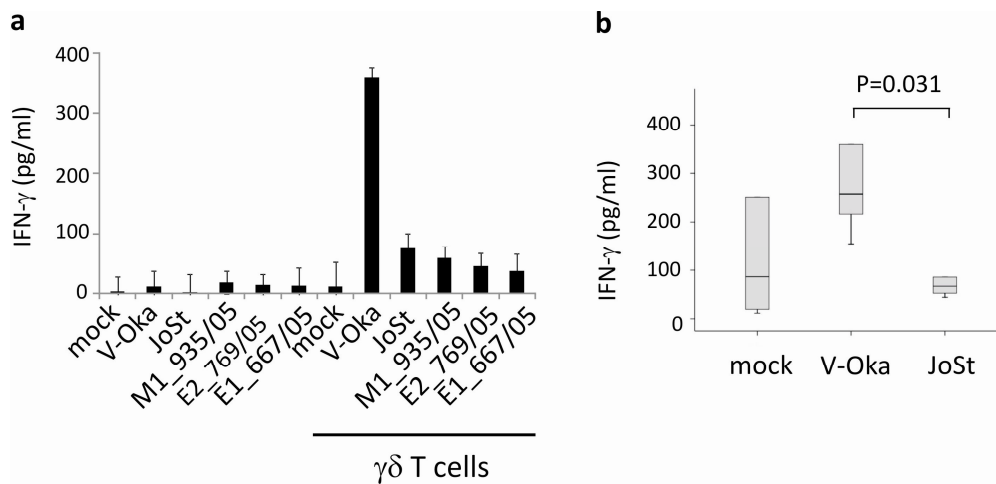


**Fig. 24: IFN- $\gamma$  secretion of CD1c-restricted  $\gamma\delta$  T cells in the presence of mock or VZV-infected iDCs.**

(a) Secreted IFN- $\gamma$  was detected in the supernatant of mock or VZV-infected iDCs in the absence or presence of CD1c-restricted  $\gamma\delta$  T cells by ELISA (48h) (n=5; error bars are SD). (b) Box-Whisker-Plot of statistical analysis of secreted IFN- $\gamma$  by CD1c-restricted  $\gamma\delta$  T cells in the presence of mock, V-Oka or JoSt infected iDCs (n=6). P value < 0.05 was considered to be significant.

Immature DCs infected with the vaccine strain V-Oka could activate  $\gamma\delta$  T cells to secrete high amounts of IFN- $\gamma$ . In striking contrast, iDCs infected with clinical isolates regardless of their genotype failed to activate CD1c-restricted  $\gamma\delta$  T cells. The IFN- $\gamma$  secretion by  $\gamma\delta$  T cells in the presence of iDCs infected with the virulent strain JoSt ( $P=0.031$ ) was significantly inhibited compared to V-Oka infected iDCs (Fig. 24b).

CD1c-restricted  $\gamma\delta$  T cells were cocultured with mock or VZV-infected iDCs in the presence of a blocking antibody directed against CD1c or the respective isotype control to verify the specificity for CD1c (Fig. 25). Anti-CD1c antibodies but not the respective isotype control could block IFN- $\gamma$  secretion.

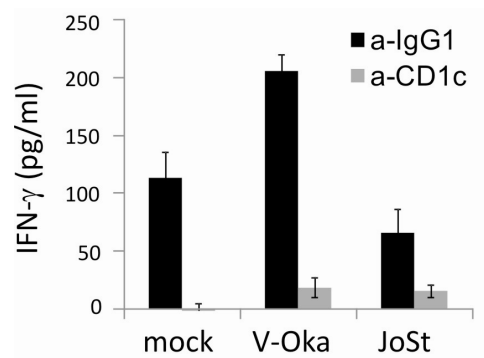


**Fig. 25: Restriction of  $\gamma\delta$  T cells for lipid antigen presentation through CD1c.**

Mock or VZV-infected iDCs were cocultured with  $\gamma\delta$ T cells for 48h in the presence of anti-CD1c antibodies or the respective isotype control (20  $\mu$ g/ml). Secreted IFN- $\gamma$  was measured in the supernatant by ELISA.

Next, the possibility that the observed functional differences were due to differences in apoptotic death of iDCs infected with VZV was assessed. For this purpose iDCs were stained by AnnexinV and propidium iodide (PI) and analyzed by flow cytometry (Fig. 26).

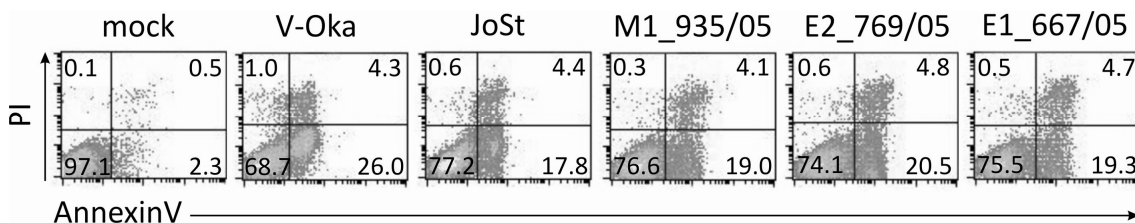


**Fig. 26: Detection of apoptotic death on mock or VZV-infected iDCs 2d post VZV infection.**

Immature DCs were double stained by AnnexinV and propidium iodide (PI). Numbers indicate the percentage of cells within each quadrant. One representative experiment out of three is shown.

In mock-infected iDCs only very low percentages of apoptotic cells could be detected (Fig. 26 and Table 1). In strong contrast, in all VZV-infected iDCs induction of apoptosis could be observed. Interestingly, no differences were seen in the vaccine-infected iDCs compared to iDCs infected with VZV clinical isolates (Table 11).

**Tab. 11: Analysis of apoptotic death in iDCs.**

The percentages of single-positive (AnnexinV) or double-positive (AnnexinV and PI) cells after mock infection (n=5), infection with V-Oka or JoSt (n=5) and with the genotypes M1, E2 and E1 (n=3) are summarized. The mean percentage and SD are shown.

	<b>% single positive iDCs (AnnexinV)</b>	<b>% double-positive iDCs (AnnexinV and PI)</b>
<b>mock</b>	<b>2.46 ± 0.69</b>	<b>0.99 ± 0.38</b>
<b>V-Oka</b>	<b>21.23 ± 4.64</b>	<b>3.00 ± 1.43</b>
<b>JoSt</b>	<b>18.51 ± 3.28</b>	<b>2.81 ± 1.21</b>
<b>M1_935/05</b>	<b>16.03 ± 6.69</b>	<b>2.02 ± 1.80</b>
<b>E2_769/05</b>	<b>17.92 ± 4.73</b>	<b>2.67 ± 1.93</b>
<b>E1_667/05</b>	<b>17.07 ± 3.94</b>	<b>2.61 ± 1.81</b>

Recently, it was shown that VZV is transmitted from infected iDCs to T cells resulting in productive T cell infection<sup>20</sup>. Furthermore, it was demonstrated that T cells infected with measles virus, a member of the *Paramyxoviridae*, are functionally impaired. Therefore, it is possible that VZV alters the function of  $\gamma\delta$  T cells after transmission from infected iDCs to  $\gamma\delta$  T lymphocytes. To test whether transmission of VZV was different for the vaccine strain V-Oka and the clinical isolate JoSt,  $\gamma\delta$  T cells were stained for the expression of gE and the  $\gamma\delta$ -T cell receptor (TCR) and analyzed by flow cytometry (Fig. 27).

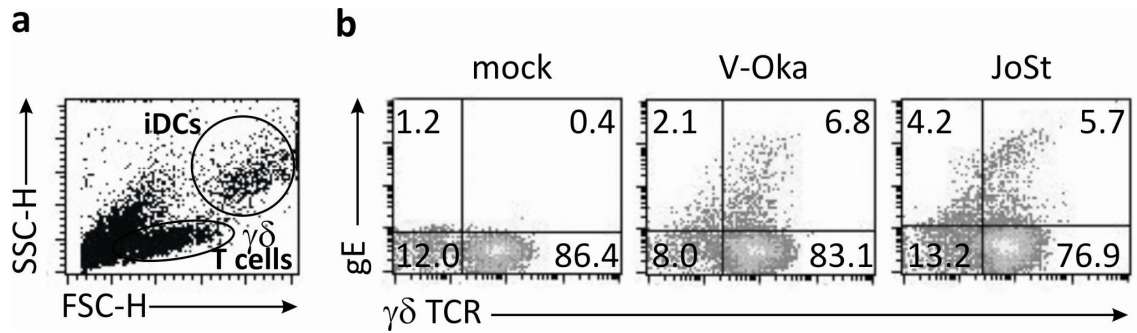


**Fig. 27: Transmission of VZV from iDCs to  $\gamma\delta$  T cells.**

(a) 2d p.i. VZV-infected iDCs were cocultured for 48h with CD1c-restricted  $\gamma\delta$  T cells and analyzed by flow cytometry. Due to differences in cellular size (FSC-H) and granularity (SSC-H)  $\gamma\delta$  T cells are distinguishable from iDCs. (b) Transmission of VZV was assessed by dual staining of gated  $\gamma\delta$  T cells for the expression of viral gE and the  $\gamma\delta$ -T cell receptor (TCR). Indicated numbers represent the percentage of cells within the quadrant. One representative experiment of five is shown.

Due to differences in cellular size (FSC-H) and granularity (SSC-H)  $\gamma\delta$  T cells could be separated from iDCs by setting a scatter gate and analyzing for surface expression of  $\gamma\delta$ -T cell receptor (TCR) and viral gE (Fig. 27a). More than 75% of the gated cells were positive for the  $\gamma\delta$ -TCR (Fig. 27b). Co-expression with gE is shown for one representative experiment (Fig. 27b). In five independent experiments  $16.8\% \pm 10.1\%$  (mean  $\pm$  SD)  $\gamma\delta$  T cells in the presence of V-Oka infected iDCs expressed gE on the cell surface. In the presence of JoSt infected iDCs  $20.5\% \pm 11.5\%$  (mean  $\pm$  SD)  $\gamma\delta$  T cells showed gE cell surface expression. Thus, no differences in the transmission rate from iDCs to  $\gamma\delta$  T cells were detected for the vaccine strain V-Oka and the clinical isolate JoSt. Both VZV strains infected T cells at only low rates in line with previously published observations<sup>174</sup>.

Next  $\gamma\delta$  T cells were stimulated with the lectin phytohaemagglutinin (PHA) in the presence of VZV-infected iDCs to test whether VZV rendered  $\gamma\delta$  T cells functionally inert. PHA was used to activate T cells independently of the presented ligand and co-stimulatory signals.

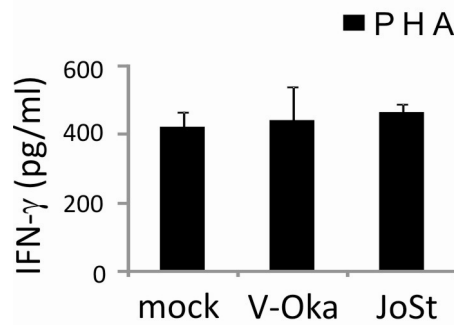


**Fig. 28: Functional integrity of  $\gamma\delta$  T cells.**

Detection of secreted IFN- $\gamma$  of PHA stimulated  $\gamma\delta$  T cells in the presence of mock or VZV-infected iDCs. One representative experiment of three is shown.

IFN- $\gamma$  secretion of  $\gamma\delta$  T cells was fully restored in the presence of iDCs infected with the clinical isolate JoSt after stimulation with PHA (Fig. 28). Altogether, these data provide evidence that the observed functional differences are due to the interference of VZV with DC function.

### 3.8 Instruction of VZV-infected iDCs by CD1c-restricted $\gamma\delta$ T cells

A hallmark of DC biology is their potential to differentiate from highly phagocytotic antigen capturing iDC into powerful T cell stimulating mDC. This differentiation process can be induced by microbial stimuli, cytokines or by innate lymphocytes. Recently, it could be demonstrated that self-reactive CD1-restricted  $\alpha\beta$  and  $\gamma\delta$  T can promote DC maturation in the absence of foreign antigens, a process which is called DC instruction<sup>72,73</sup>.

An important aim of this thesis was to investigate whether  $\gamma\delta$  T cells can license VZV-infected iDCs to mature. For this purpose, iDCs were stained for cell surface expression of the maturation marker CD83 and CD86 after coculture with  $\gamma\delta$  T cells (Fig. 29). LPS stimulated DCs were included as a positive control in the experimental setting. Immature DCs infected with the V-Oka or the clinical isolate JoSt alone expressed only low amounts of CD83 and CD86. In contrast coculture with  $\gamma\delta$  T cells or stimulation with LPS induced full maturation of VZV-infected iDCs as shown by high expression of CD83 and CD86. Interestingly, in this type of analysis no differences were observed for the vaccine strain V-Oka and the clinical isolate JoSt indicating that both V-Oka and JoSt did not interfere with phenotypic maturation.



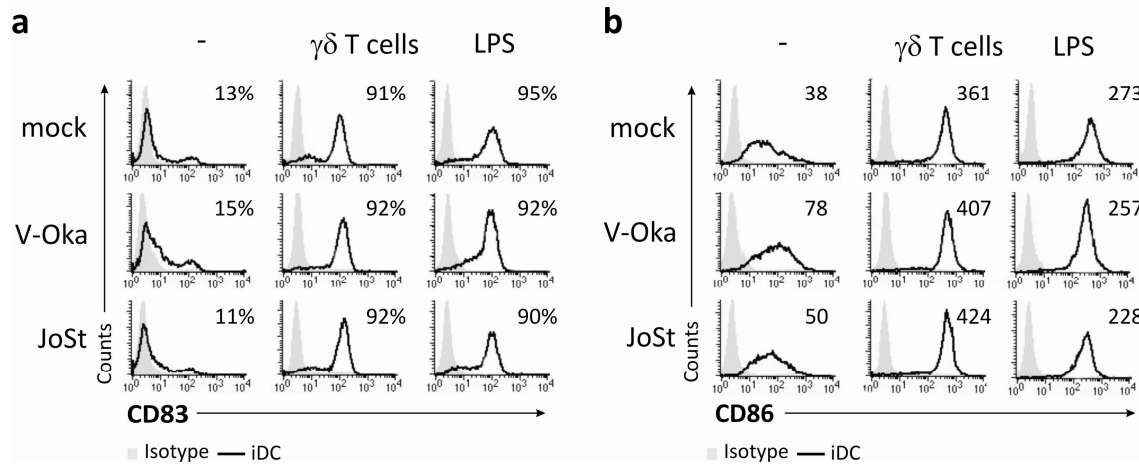


**Fig. 29: Phenotypic analysis of surface expression of CD83 and CD86 on iDCs.**

Flow cytometry analysis of surface expression of (a) CD83 and (b) CD86 on iDCs alone (-), after instruction by  $\gamma\delta$  T cells or after stimulation with LPS (48h). Numbers within the histogram plots represent percentage of positive cells (a) or mean fluorescence intensities (MFI) (b). One representative experiment of three is shown.

Functional maturation of iDCs leads to secretion of IL-12 which drives the subsequent T cell response of CD4<sup>+</sup> T helper cell into the T<sub>H</sub>1 direction<sup>175</sup>. Therefore, we quantified bioactive IL-12 (IL-12p70) within the supernatant of VZV-infected iDCs in the absence or presence of CD1c-restricted  $\gamma\delta$  T cells (Fig. 30). Interestingly, VZV infection of iDCs did not lead to secretion of bioactive IL-12 (Fig. 30a). However in the presence of  $\gamma\delta$  T cells iDCs infected with the vaccine strain V-Oka were fully licensed to secrete bioactive IL-12. In strong contrast, iDCs infected with clinical isolates of VZV inhibited the secretion of IL-12 regardless of their genotype. To evaluate the impact of IL-12 on IFN- $\gamma$  secretion,  $\gamma\delta$  T cells and VZV-infected iDCs were cocultured in the absence or presence of neutralizing anti-IL-12 antibodies and IFN- $\gamma$  secretion was quantified by ELISA (Fig. 30b). Neutralization of the secreted IL-12 blocked more than 50% of IFN- $\gamma$  secretion by  $\gamma\delta$  T cells. Therefore, it seems likely that iDCs infected with clinical isolates of VZV have an intrinsic defect to produce bioactive IL-12 which in turn lacks to fully support the reciprocal production of IFN- $\gamma$  by cocultured  $\gamma\delta$  T cells.

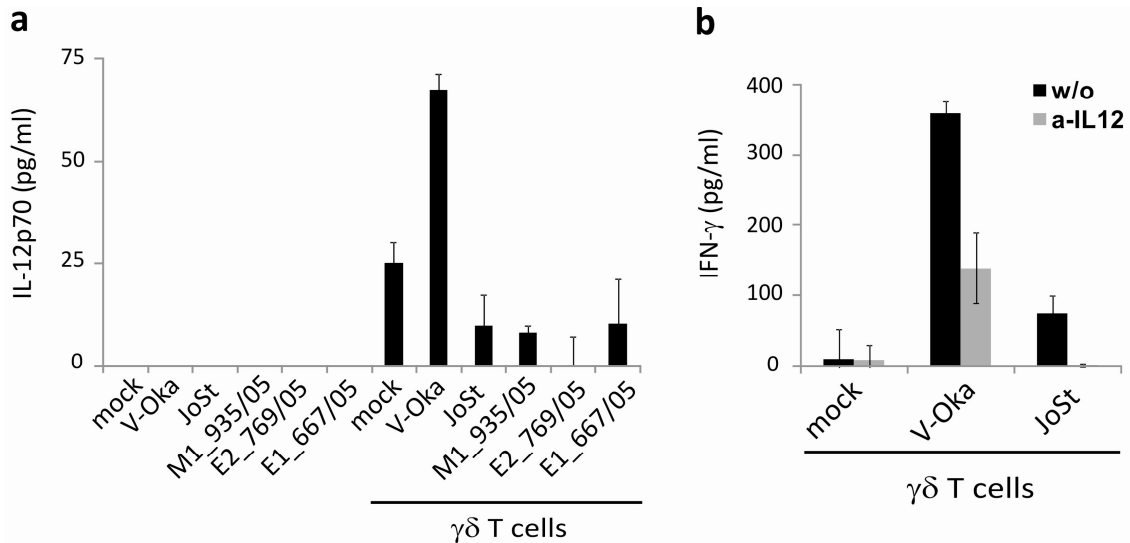


**Fig.30: Disruption of IL-12 secretion in iDCs infected with clinical isolates of VZV.**

(a) Secretion of bioactive IL-12p70 by mock or VZV-infected iDCs (2d p.i.) cultured in the absence or presence of CD1c-restricted  $\gamma\delta$  T cells was quantified by ELISA after 48 h. One representative experiment of two is shown. (b) Secretion of IFN- $\gamma$  was quantified after 48 h of coculture of mock- or VZV-infected iDCs and  $\gamma\delta$  T cells without (w/o) or in the presence of neutralizing anti-IL12 antibodies. One representative experiment of two is shown.

A powerful inducer of IL-12 secretion by iDCs is the ligation of CD40 on DCs by its CD40 ligand (CD40L) on T cells<sup>175</sup>. Signaling through CD40 activates the mitogen-activated protein kinase (MAPK) pathway, which leads to phosphorylation of c-Jun N-terminal kinases (JNK), extracellular signal-regulated kinases (ERK) and p38 mitogen-activated protein kinases (p38) and finally to IL-12 gene transcription<sup>176</sup>. The lack of IL-12 secretion by iDCs infected with clinical isolates of VZV provides evidence that VZV might interfere with the IL-12 signaling pathway. Therefore, the signal through CD40 on iDCs was provided *in trans* by coculture with a cell line which stable expressed CD40L on their cell surface<sup>168</sup>. Mock- or VZV-infected iDCs were left unstimulated or stimulated with CD40L and the lysates were analyzed by immunoblotting (Fig. 31). LPS-stimulated DCs were used as a positive control.

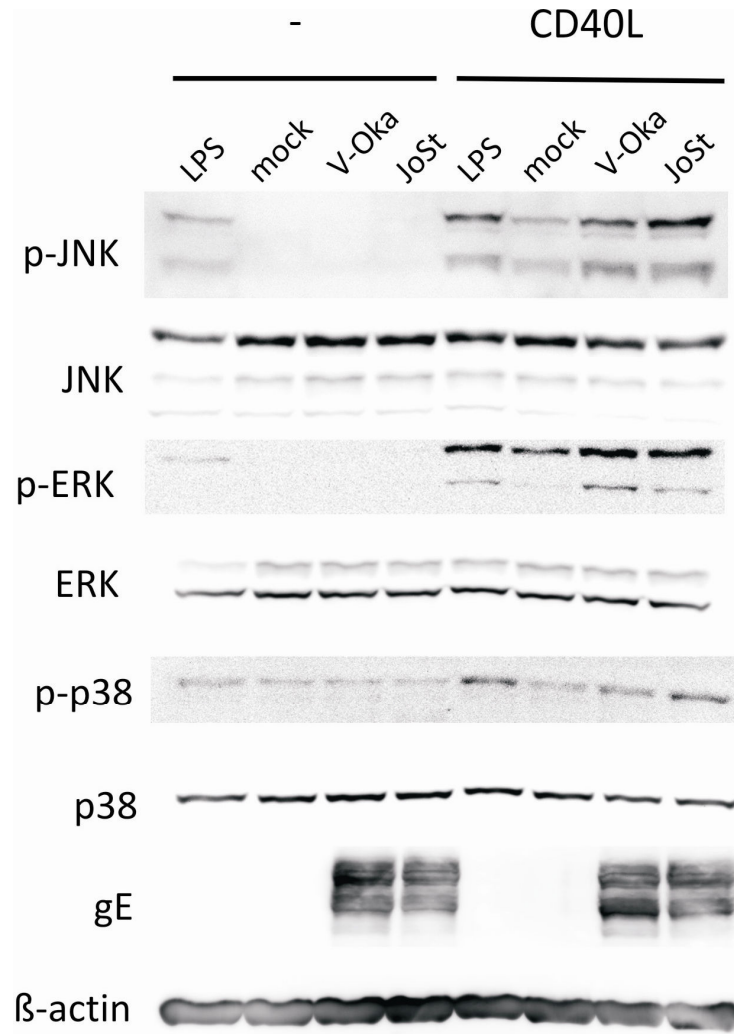


**Fig. 31: Activation of the MAPK pathway in VZV-infected iDCs.**

LPS-stimulated, mock, V-Oka and JoSt infected iDCs were cultured in the absence (-) or presence of CD40L for 15 min. Subsequently, phosphorylated MAP-kinases (p-JNK, p-ERK and p-p38) and total amounts of MAP-kinases (JNK, ERK and p38) were analyzed by western blot. VZV infection was detected by expression of viral glycoprotein E (gE) and β-actin was used as loading control. One representative experiment out of three is shown.

Phosphorylation of the MAP-kinases JNK and ERK was detected only in LPS stimulated iDCs (Fig. 31). However, low levels of phosphorylated p38 were also observed in mock, V-Oka and JoSt infected iDCs. In contrast, in the presence of CD40L-expressing cells phosphorylation of all three kinases was detectable in lysates of mock, V-Oka and JoSt infected iDCs. In conclusion, no intrinsic defect within the MAPK pathway could be observed in iDCs infected with the clinical isolate JoSt.

Secretion of IL-12 by iDCs infected with the clinical isolate JoSt was tested in the presence of a strong CD40L signal *in trans* to investigate whether these cells have an intrinsic defect (Fig. 32). Interestingly, JoSt-infected iDCs secreted as much IL-12 as vaccine-infected iDCs after stimulation with CD40L.

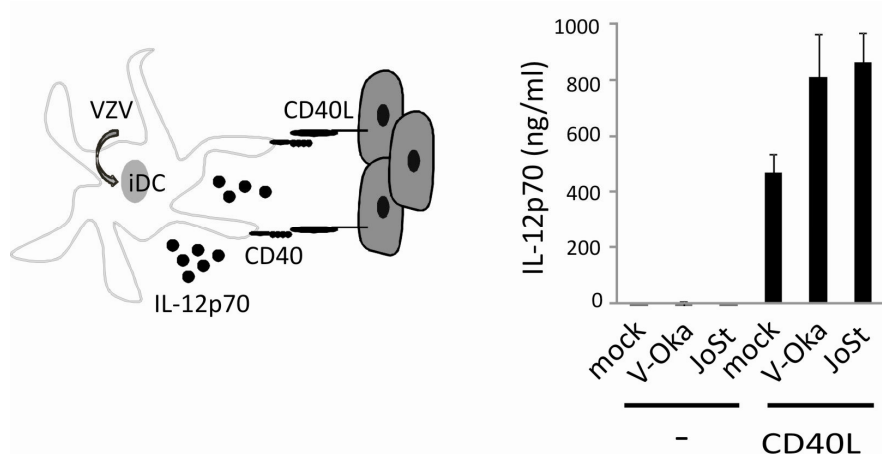


**Fig. 32: CD40-mediated rescue of IL-12 secretion in JoSt infected iDCs.**

iDCs were left unstimulated (-) or stimulated with CD40L-expressing cells for 48h and secretion of bioactive IL-12p70 was quantified by ELISA in the supernatant. One out of three independent experiments done in triplicate is shown (error bars are SD).

As IL-12 is essential for inducing IFN- $\gamma$  production by T cells, CD1c-restricted  $\gamma\delta$  T cells were added to the system and IFN- $\gamma$  was quantified by ELISA in the supernatant (Fig. 33). In this way the ability of JoSt-infected iDCs to stimulate IFN- $\gamma$  secretion by  $\gamma\delta$  T cells was fully rescued.

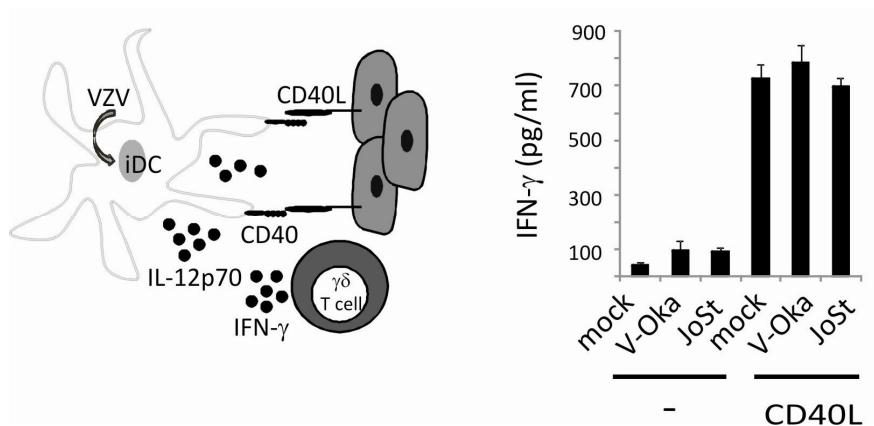


**Fig. 33: CD40-mediated restoration of IFN- $\gamma$  secretion by  $\gamma\delta$  T cells.**

iDCs were left unstimulated (-) or stimulated by CD40L-expressing cells and secretion of IFN- $\gamma$  by  $\gamma\delta$  T cells was quantified. One out of four independent experiments done in triplicates is shown (error bars are SD).

Collectively, these data suggest that iDCs infected with virulent VZV strains cannot induce CD1c-restricted  $\gamma\delta$  T cells to provide adequate CD40 signaling. In turn, lack of IL-12 secretion results in low IFN- $\gamma$  secretion by T lymphocytes.

### 3.9 Interference of VZV with the Co-Stimulatory Capacity of DCs

As co-stimulation through CD40 and CD86 on DCs is essential for full T cell activation<sup>89</sup>, cell surface expression of CD40 and CD86 on VZV-infected iDCs was investigated (Fig. 34 and 35). Flow cytometry analysis showed a significant increase in CD40 cell surface expression on iDCs infected with the vaccine V-Oka (P=0.002) compared to mock-infected iDCs and to JoSt infected iDCs (P=0.01) (Fig. 34).

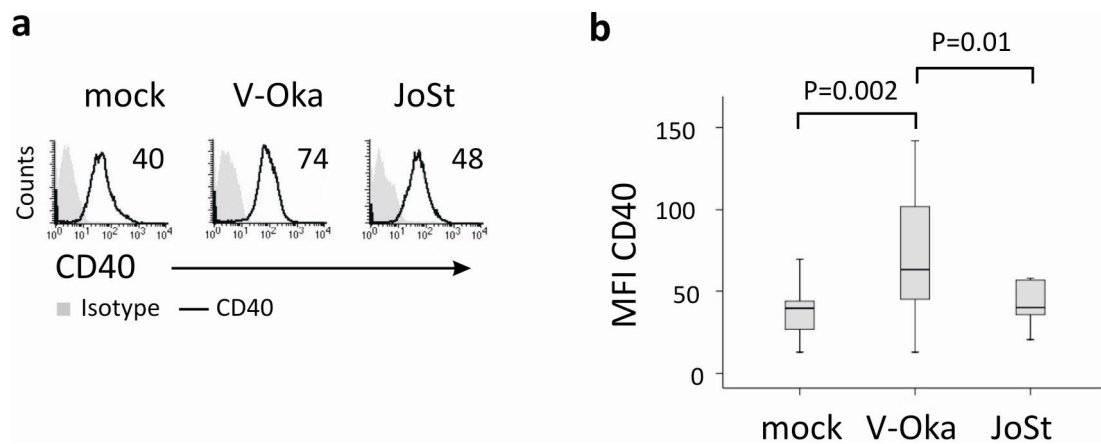


**Fig. 34: Increase in CD40 expression on iDCs infected with the vaccine V-Oka.**

(a) Histogram analysis of CD40 expression on mock, V-Oka and JoSt infected iDCs (2d p.i.). Mean fluorescence intensities (MFI) are indicated and are representative for 11 experiments. (b) Box-and-Whisker-Plot of MFI on CD40 of mock, V-Oka or JoSt infected iDCs 2d p.i. (n=11). P values < 0.05 were considered to be significant.

Additionally, analysis of CD86 expression on VZV-infected iDCs revealed that infection with the vaccine V-Oka induced a significant upregulation (P=0.002) compared to iDCs infected with the clinical isolate JoSt (Fig. 35).

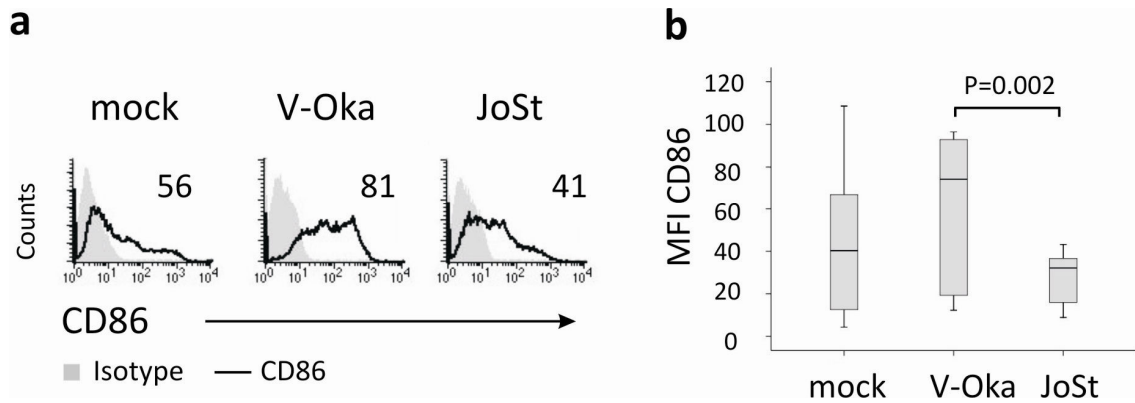


**Fig. 35: Significant increase in CD86 expression on V-Oka infected iDCs.**

(a) Histogram analysis of CD86 expression on mock, V-Oka and JoSt infected iDCs (2d p.i.). Mean fluorescence intensities (MFI) are indicated and are representative for 10 experiments. (b) Box-and-Whisker-Plot of MFI on CD86 expression on mock, V-Oka or JoSt infected iDCs 2d p.i. (n=10). P value < 0.05 was considered to be significant.

Quantitative real-time PCR analysis was used to investigate whether the observed failure of JoSt-infected iDCs to upregulate CD40 and CD86 was due to interference on the transcriptional level. As shown in figure 36, VZV did not significantly modulate CD40 and CD86 gene expression compared to mock-infected iDCs.

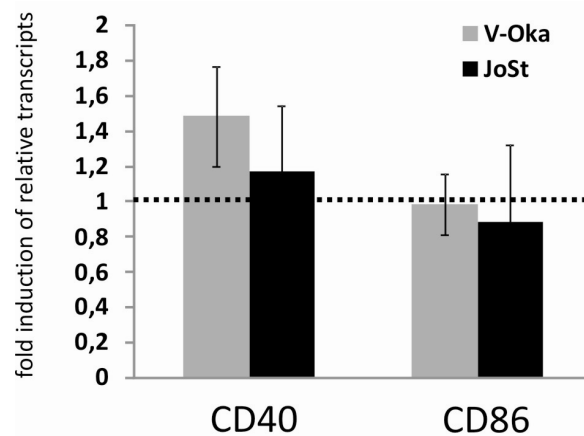


**Fig. 36: Analysis of CD40 and CD86 transcripts in VZV-infected iDCs.**

The abundance of mRNA encoded by CD40 and CD86 genes was determined by quantitative real-time PCR. The values are given relative to uninfected iDCs. The fold induction of relative transcripts in VZV-infected iDCs relative to transcripts in uninfected iDCs (stippled line) is shown. Data are delineated from three independent experiments (error bars are SD).

The reciprocal crosstalk of DCs and T cells is not only regulated by co-stimulatory signals but also influenced by the expression of co-inhibitory molecules which trigger T cell responses<sup>82</sup>. Enhanced expression of molecules of the B7-family on DCs has been shown to silence T cell responses by interaction of B7-H1 or B7-DC molecules with Programmed Death 1 (PD-1) or of B7-H2 molecules with Inducible T-cell Co-Stimulator (ICOS). Therefore,

the expression of co-inhibitory molecules of the B7-family on VZV-infected iDCs was investigated by flow cytometry (Fig. 37).

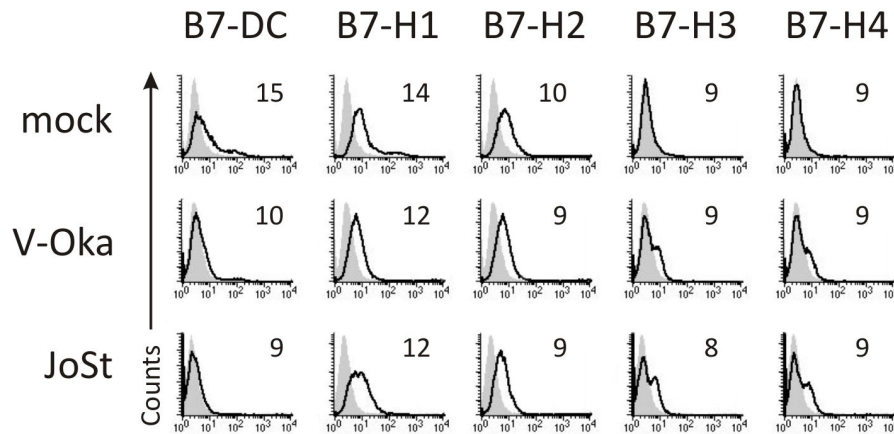


**Fig. 37: Expression of co-inhibitory molecules of the B7 family on VZV-infected iDCs.**

Histogram analysis of B7-DC, B7-H1, B7-H2, B7-H3 and B7-H4 (black curves) expression on mock, V-Oka and JoSt infected iDCs (2d p.i.). Curves in gray represent isotype control. Mean fluorescence intensities (MFI) are indicated.

However, no induction of co-inhibitory molecules of the B7-family could be detected on VZV-infected iDCs. Therefore, it is unlikely that the observed defect in IFN- $\gamma$  secretion by  $\gamma\delta$  T cells in the presence of iDCs infected with virulent strains of VZV was due to inhibitory signaling.

### 3.10 Block of TLR2 Signaling by Virulent VZV

Synergistic effects of PRR signaling are particularly important for the production of bioactive IL-12<sup>68,70,177</sup>. TLR2 has been shown to play a role in detection of herpesviruses including HSV, HCMV and VZV<sup>178-182</sup>. Therefore, we tested whether virulent VZV can interfere with TLR2 signaling. VZV-infected iDCs were stimulated through TLR2 with lipoteichoic acid (LTA) and subsequent IL-12p70 production was assessed. Moreover, to address the question if viral replication interferes with TLR signaling we compared iDCs infected with replication competent virus with that stimulated with UV inactivated virus. Additionally, HSV was included in the experimental setting to investigate if any of the observed effects are common to alpha-herpesviruses.

Viral infection of iDCs did not lead to secretion of IL-12 by iDCs (Fig. 38). However, additional stimulation with LTA provoked secretion of high amounts of IL-12 by iDCs infected with the vaccine strain V-Oka and HSV. In strong contrast, iDCs infected with the clinical isolate JoSt blocked IL-12 secretion suggesting a VZV specific interference with TLR2 signaling. Stimulation of iDCs with UV inactivated virus did not induce IL-12 secretion. Interestingly, further stimulation with LTA only induced low amounts of IL-12p70. These data provide evidence that active viral replication was critical to prime iDCs for further PRR triggering with subsequent secretion of bioactive IL-12. Moreover, these data demonstrate that virulent VZV efficiently blocked TLR2 stimulation in contrast to the vaccine strain V-Oka and HSV.

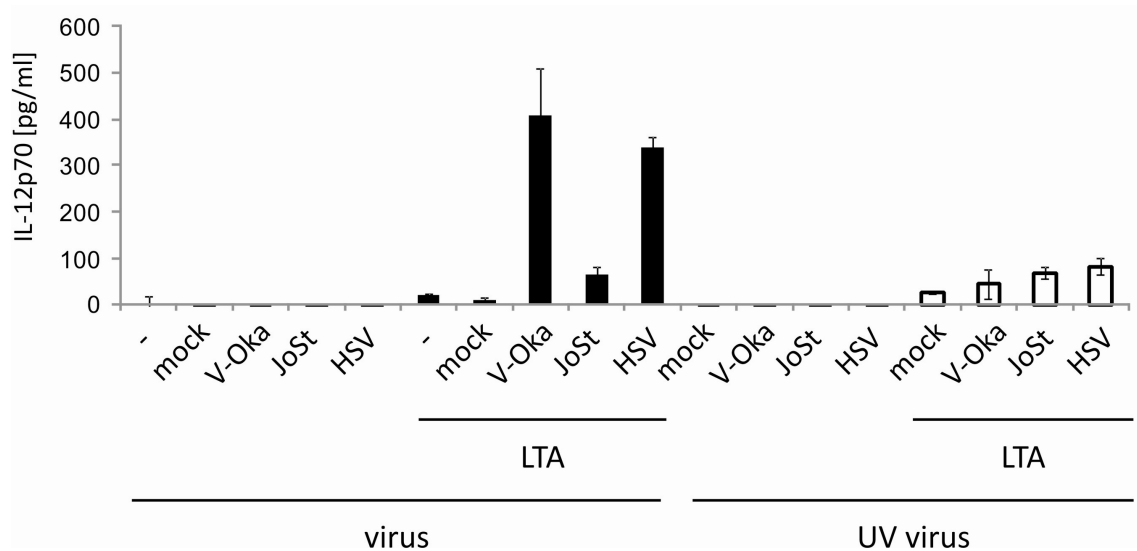


**Fig. 38: Virulent VZV blocks TLR2 signaling in mo-DCs.**

Immature DCs were left untreated (-), mock, V-Oka, JoSt or HSV infected (virus) or stimulated with UV-inactivated virus (UV virus) for 2d. Thereafter, DCs remained unstimulated or were stimulated with TLR2 agonist lipoteichoic acid (LTA) for 48h and IL-12p70 secretion was quantified by ELISA. One representative experiment out of two is shown (error bars are SD).

In summary, myeloid CD11c<sup>+</sup> DCs strongly infiltrated in skin lesions of herpes zoster patients. *Ex vivo* isolated cutaneous DCs were permissive to VZV infection and no differences in the infection efficiency between the vaccine strain V-Oka and virulent strain JoSt was observed. Similarly, monocyte-derived iDCs reflecting myeloid-derived inflammatory DCs were efficiently infected by both VZV strains without differences in the infection efficiency. Although both the vaccine strain V-Oka and the virulent strain JoSt upregulated



CD1c, only V-Oka could efficiently induce IFN- $\gamma$  secretion by CD1c-restricted  $\gamma\delta$  T cells. The observed failure of JoSt-infected iDCs to stimulate  $\gamma\delta$  T cells was neither due to an intrinsic functional defect of  $\gamma\delta$  T cells nor due to the upregulation of inhibitory molecules of the B-7 family on the surface of iDCs. Furthermore, the CD40L-induced signaling pathway leading to subsequent IL-12 production was not disturbed in VZV-infected iDCs. Virulent VZV rather blocked TLR2 signaling within iDCs thereby inhibiting secretion of bioactive IL-12.

Thus, the observed findings provide evidence that virulent VZV strains successfully interfere with functional maturation of iDCs by blocking efficiently TLR2 signaling thereby preventing stimulation of subsequent innate immune responses. This newly discovered immune evasion strategy explains why virulent VZV strains successfully replicate within the skin thereby causing the typical rash.

## 4 Discussion

Skin tropism of VZV is responsible for the most obvious clinical manifestation of VZV infection producing the vesicular cutaneous lesions that are associated with varicella and herpes zoster. Primary infection of VZV is characterized by infection of epithelial cells and DCs of the respiratory mucosa, viral transmission to T cells and subsequent viremic phases. Thereafter, the virus is transported to the skin, the major replication site of VZV. After a prolonged incubation time of 10 to 21 days the typical vesicular lesions appear<sup>183</sup>. It is assumed that this prolonged period represents the time required for VZV to overcome unrecognized but potent innate antiviral immune responses within the skin<sup>184</sup>. Until to date three different immune evasion mechanisms have been elucidated to be involved in VZV pathogenesis<sup>183</sup>. First, it has been demonstrated that the serine/threonine kinase ORF66 is responsible for downregulation of cell surface MHC class I molecules on fibroblasts by retaining them within the golgi compartment and accelerating their degradation<sup>120</sup>. In addition, VZV inhibits IFN- $\gamma$  mediated upregulation of cell surface MHC class II molecules on fibroblasts<sup>122</sup>. This escape strategy could limit primary sensitization of CD4<sup>+</sup> T cells to VZV peptides and delay the early amplification of VZV-specific CD4<sup>+</sup> helper T cells and the release of cytokines at cutaneous sites of VZV replication. As third immune evasion mechanism the interference with phenotype and function of mDCs was discovered<sup>118</sup>. Altogether, these observations underline that VZV evades adaptive T cell response by delaying clonal expansion of VZV specific CD4<sup>+</sup> and CD8<sup>+</sup> T lymphocytes.

However, detailed analysis of the interplay of VZV with cells involved in cutaneous immunity has never been investigated so far. Most importantly, immunological responses explaining the different clinical outcome of infection with the vaccine and virulent strains of VZV remain to be elucidated.

### 4.1 Role of Cutaneous DCs in VZV Pathogenesis

The skin as major immune organ of the human body contains a variety of immune cells including epidermal LCs, DDCs and intraepithelial  $\gamma\delta$  T cells. It is postulated that VZV-infected T cells transport the virus during the viremic phase to skin epithelial cells which

are subsequently infected by the virus<sup>20</sup>. It was shown in the SCID-hu mouse model that VZV replication in epithelial cells is associated with expression of a gene product that inhibits antiviral IFN- $\alpha$  production in foci of infected cells by interfering with Stat1 activation<sup>28</sup>. In the surrounding non-infected area increased levels of IFN- $\alpha$  could be detected. However, which immune cells in the skin are targeted by VZV has not been investigated so far.

LCs and DDCs are migratory DCs which are the main DC subtype in the steady-state. In contrast, inflammatory DCs transiently occur during an ongoing infection. Therefore, skin sections of herpes zoster patients were analyzed for these DC subtypes. Immunofluorescence microscopy analysis showed the disappearance of epidermal CD1a and Langerin expressing LCs. This can be explained by the emigration of LCs to local lymph nodes where they might transfer the captured antigen to resident DCs. This was recently demonstrated in HSV-1 infected mice suggesting an important role of migratory DCs which emigrate from infected skin to local lymph nodes and transfer captured antigens to resident CD8<sup>+</sup> DCs which in turn activate CD8<sup>+</sup> T cells<sup>94,104</sup>. On the other hand, migratory submucosal DCs but not LCs were shown to induce a protective T<sub>H</sub>1 response in mice after vaginal infection with HSV-2<sup>106</sup>. In sharp contrast to LCs, a strong infiltration of DCs of myeloid origin expressing CD11c, CD1c, CD1b, CD206 and CD209 in close proximity to virion containing vesicles was observed. Recently, it was demonstrated that monocytes recruited to the dermis during *Leishmania* infection locally differentiate into “dermal monocyte-derived DCs” and induce protective T<sub>H</sub>1 responses<sup>96</sup>. Therefore, it seems likely that the observed infiltrated myeloid-derived DCs in herpes zoster lesions are inflammatory DCs derived from monocytes. Interestingly, a strong infiltration of CD11c negative pDCs was detected in vesicular lesions of a varicella biopsy<sup>107</sup>. We did not stain for a specific marker of pDCs, but it is possible that different subtypes of DCs play diverse roles during systemic varicella infection or reactivation during herpes zoster.

Despite the strong infiltration of CD3 positive T cells in herpes zoster skin, detection of the intraepithelial  $\gamma\delta$  T cells within herpes zoster lesions failed. This might be due to a detection limit of the antibody used. On the other side it is possible that intraepithelial V $\delta$ 1<sup>+</sup>  $\gamma\delta$  T cells as innate immune cells emigrated early to local lymph nodes to stimulate other immune cells. A protective role for intraepithelial V $\delta$ 1<sup>+</sup>  $\gamma\delta$  T cells in HSV-2 infection was recently demonstrated in  $\gamma\delta$  T cell depleted mice<sup>185</sup>.

The percentage of  $\gamma\delta$  T cells in blood of herpes zoster patients was not significantly altered compared to percentages of healthy control donors. It has to be mentioned, that it is unlikely that V $\gamma$ 9 $\delta$ 2 T cells the major subset in peripheral blood are influenced during reactivation of VZV. However, it would be interesting to investigate the  $\gamma\delta$  T cell population during systemic varicella infection where several viremic phases occur. Especially for V $\gamma$ 9 $\delta$ 2 T cells it has been shown that they acquire the ability to function as professional APCs for naive  $\alpha\beta$  T cells<sup>159</sup>. Furthermore, cross-presentation of microbial and tumor antigens by activated V $\gamma$ 9 $\delta$ 2  $\gamma\delta$  T cells to CD8<sup>+</sup>  $\alpha\beta$  T cells has been described<sup>160</sup>.

In the SCID-hu mouse model the role of T cells as transport vehicle for viral spread during VZV pathogenesis was revealed<sup>186</sup>. Moreover, in this study the vaccine showed decreased replication in the skin compared to clinical isolates of VZV. However, vaccine strain V-Oka and virulent strains of VZV do not differ in the replication efficiency in human cell lines. This finding of our study was also observed by other research groups and suggests that cutaneous immune cells might be responsible for the observed failure of the vaccine strain to replicate efficiently in the SCID-hu mouse model. Furthermore, this hypothesis is in line with the observed finding that vaccinees do not suffer from the typical VZV rash whereas naive persons infected with clinical isolates of VZV develop disseminated varicella. Several scenarios are possible which might explain the potency of virulent VZV strains to replicate efficiently in the skin. First, it is possible that only virulent VZV strains possess the capacity to infect cutaneous immune cells and modulate their immune function thereby silencing early antiviral immune responses. Next, it is conceivable that both the vaccine and virulent VZV strains infect efficiently cutaneous immune cells but only virulent VZV strains interfere with their immune function. To test these hypotheses epidermal LCs and DDCs were isolated from human skin and tested for their permissivity to VZV infection and subsequent phenotypic changes. LCs and DDCs isolated from human skin reflecting conventional DCs during steady-state conditions were both permissive to VZV infection and no difference in the infection efficiency between both DC types was observed. More importantly, the vaccine strain V-Oka and the clinical isolate JoSt could infect these immunological important cell types equally well. Interestingly, VZV infection did not induce phenotypic maturation of LCs and DDCs as low cell surface expression of CD83 and CD86 was observed. Moreover, a decrease in cell surface expression of CD40 was detected on VZV-

infected LC and DDCs. Thus, both vaccine strain V-Oka and clinical isolate JoSt infect cutaneous DCs but only weakly modulate their phenotype.

#### **4.2 VZV-induced Increase in CD1c Expression on Monocyte-Derived iDCs**

The detected infiltration of myeloid CD11c<sup>+</sup> DCs in herpes zoster lesions suggests a role for transiently occurring inflammatory DCs in the immune response against VZV. Therefore, iDCs derived from monocytes through differentiation with IL-4 and GM-CSF *in vitro* were used for further investigations as they reflect inflammatory DCs transiently occurring during an ongoing infection (Ardavin C. personal communication).

In contrast to the low infection rates of LCs and DDCs, almost all iDCs were infected by the vaccine strain V-Oka and the clinical isolate JoSt. Importantly, as observed for LCs and DDCs no differences in the infection efficiency between both viral strains were detected. It was shown by A. Abendroth that infection of iDCs by a virulent VZV strain was not accompanied by phenotypic changes in MHC class I, MHC class II, CD86, CD40 and CD1a cell surface expression<sup>20</sup>. It has to be mentioned that in this study the infection efficiency of virulent VZV was markedly lower ( $34.4\% \pm 6.6\%$ ; mean  $\pm$  SEM). Moreover, no investigations were performed with the vaccine strain V-Oka. An aspect of our work was to assess the impact of VZV infection on CD1 antigen presentation as deficiency in CD1-restricted NKT cells has been associated with disseminated varicella after vaccination with the V-Oka strain<sup>26</sup>. Interestingly, cell surface expression of CD1c was significantly enhanced after infection with both the vaccine strain V-Oka and the clinical isolate JoSt compared to mock-infected iDCs. However, CD1a, CD1b and CD1d cell surface expression remained unaltered. The low CD1d cell surface expression can be explained by the fact that cultivation was performed with fetal calf serum which was recently demonstrated to favor group 1 CD1 expression (CD1a, CD1b and CD1c) over group 2 (CD1d) expression in contrast to human serum<sup>187</sup>. Additionally, it is well documented that monocyte-derived iDCs express only very low amounts of cell surface CD1d compared to monocytes<sup>188</sup>. Antigen presentation through CD1c was shown to be important in T cell mediated recognition of *Mycobacterium tuberculosis* infections<sup>128,129</sup>. Furthermore, clinical investigations of leprosy lesions provide evidence that the clinical outcome of this disease is determined by the CD1 antigen pre-

senting system<sup>133</sup>. This study has demonstrated a strong induction of group 1 CD1 proteins in dermal granuloma of skin biopsies from patients with the tuberculoid form of leprosy which correlates with active cellular immunity to *Mycobacterium leprae*. In contrast, in lesions from patients with the lepromatous form no induction of group 1 CD1 proteins was observed. These patients are characterized by lack of effective cellular immunity to *Mycobacterium lepra*. Quantitative real-time PCR analyses were performed to investigate if the observed increase in cell surface expression of CD1c on VZV-infected iDCs was regulated on the transcriptional or protein level. No increase in relative transcripts of CD1a, CD1b or CD1c in VZV-infected iDCs could be detected. Thus, VZV modulates CD1c cell surface expression on the protein level. This is in line with the fact that HSV-1, KHSV, HIV-1 or HCMV interfere with CD1 antigen presentation on the protein level by inhibiting trafficking or recycling of CD1 molecules<sup>189</sup>. Therefore, it is likely that the VZV-induced increase in cell surface CD1c is due to increased trafficking of CD1c to the cell surface.

#### **4.3 Impact of VZV-induced CD1c Upregulation on Intraepithelial CD1c-restricted $\gamma\delta$ T Cells**

To investigate the possibility if CD1c antigen presentation might play a role in the induction of cellular immunity to VZV functional analysis with a well characterized CD1c-restricted V $\delta$ 1<sup>+</sup>  $\gamma\delta$  T cell clone was performed. Cytokine secretion assays showed a significant decrease in IFN- $\gamma$  secretion by tissue specific CD1c-restricted  $\gamma\delta$  T cells in the presence of iDC infected with virulent VZV strains. This effect was independent of their genotype. In strong contrast,  $\gamma\delta$  T cells secreted high amounts of IFN- $\gamma$  in the presence of iDCs infected with the vaccine strain V-Oka. IFN- $\gamma$  secretion by  $\gamma\delta$  T cells was induced by antigen presentation through CD1c as demonstrated by blocking experiments. This functional difference was observed although both the vaccine strain and the VZV clinical isolate significantly increased CD1c cell surface expression. The observed finding might be explained by presentation of different lipid ligands through CD1c. As viruses hijack the host cell protein machinery it is likely that they also modulate the lipid metabolism thereby altering lipid antigen presentation through CD1 molecules. It was recently shown that HCMV regulates the host cell sphingolipid metabolism to increase viral replication<sup>190</sup>. Additionally, it has been shown

that mammalian sphingolipids are presented by all CD1 molecules to CD1-restricted T cells<sup>191</sup>. Therefore, further investigations should address the capacity of virulent VZV strains to interfere with lipid biosynthesis pathways which might ensure replication within the skin. Elucidation of such a mechanism could provide new insight into the attenuation of VZV, thereby facilitating development of new strategies for future vaccine design.

Blocking the activation of  $\gamma\delta$  T cells might be a novel immune evasion strategy of virulent VZV strains to ensure their replication and spread during primary infection and reactivation. Interference with early IFN- $\gamma$  secretion by innate  $\gamma\delta$  T cells may inhibit subsequent upregulation of MHC class II molecules on epithelial cells and fibroblasts which in turn limits immune surveillance by CD4<sup>+</sup> T cells. This is in line with the observed finding by Abenroth *et al.* that VZV infection of fibroblasts inhibited IFN- $\gamma$  mediated induction of MHC class II cell surface expression by blocking transcription of interferon regulatory factor 1 (IRF-1) and the MHC class II transactivator (CIITA)<sup>122</sup>. However, effective immune responses can be detected when the rash appears. PBMCs from varicella patients after the onset of rash secreted high amounts of IL-12, IFN- $\gamma$  and TNF- $\alpha$  which inhibited the spread of VZV within fibroblasts<sup>192</sup>. This finding provides evidence that VZV interferes only transiently with early innate immune responses to facilitate viral spread.

Many viruses including VZV possess T cell tropism. However, the observed defect in IFN- $\gamma$  secretion by CD1c-restricted T cells was not due to different transmission rates from VZV-infected iDCs to  $\gamma\delta$  T cells. Low transmission rates of only ~ 6% observed in this study are in line with low transmission rates found in another study using several VZV clinical isolates and viral mutants<sup>174</sup>. Addition of the lectin PHA to the coculture of  $\gamma\delta$  T cells and iDCs infected with virulent VZV fully restored IFN- $\gamma$  secretion by T cells. Thus, VZV does not interfere with T cell function as it was shown for measles virus infection<sup>193,194</sup>.

Furthermore, no differences in the cytotoxic potential of the CD1c-restricted  $\gamma\delta$  T cells could be observed. This might be explained by the fact that the detection of CD107a (Lamp-1) anchored in the cell membrane of cytotoxic granules on the cell surface is an early event during degranulation of T cells and does not answer the question whether VZV-infected iDCs were lysed efficiently. Therefore, the radioactive chromium release assay would be more appropriate to assess the lysis of the target cells. Unfortunately, this assay can not be performed in the Institute of Virology.

#### 4.4 $\gamma\delta$ T Cell mediated Instruction of VZV-infected iDCs

The functional integrity of  $\gamma\delta$  T cells sparked the interest on the side of the DC. Immature DCs could be infected with the vaccine strain V-Oka or the clinical isolate JoSt to the same extent. Apoptotic death of VZV-infected iDCs was evaluated to exclude the possibility that fewer iDCs are present to activate  $\gamma\delta$  T cells. Intriguingly, induction of apoptosis in VZV-infected iDCs could be detected. This is in line with reports showing induction of apoptosis in iDCs infected with HSV-1 and HCMV<sup>114,195</sup>. Importantly, no differences between the vaccine and any virulent strain of VZV could be observed. Virus-induced apoptosis represents an efficient means for providing non-infected bystander DCs with viral antigens for cross-presentation to CD8<sup>+</sup> T cells. Additionally, induction of apoptosis was observed *in vitro* in a VZV-infected subpopulation of PBMCs supporting our findings<sup>196</sup>.

A hallmark of DC biology is their differentiation from an antigen sampling iDC into a potent antigen presenting mDC which activates T cells<sup>59</sup>. Recently, it has been demonstrated for both CD1-restricted  $\alpha\beta$  and  $\gamma\delta$  T cells that they can induce maturation of iDCs<sup>72,73</sup>. This T cell-mediated DC instruction has important implications for controlling subsequent polarization of acquired immunity. VZV infection of iDCs alone did not induce phenotypic and functional maturation of iDCs as only low cell surface expression of CD83 and CD86 and no secretion of bioactive IL-12 (IL-12p70) was observed. In contrast, coculture with CD1c-restricted  $\gamma\delta$  T cells induced a fully mature phenotype of VZV-infected DCs with even higher expression of CD86 on VZV-infected iDCs compared to LPS-stimulated control DCs. Thus, CD1-restricted  $\gamma\delta$  T cells were able to phenotypically mature iDCs during an ongoing viral infection. Surprisingly, only vaccine-infected iDCs could be instructed functionally by CD1c-restricted  $\gamma\delta$  T cells to secrete bioactive IL-12. In strong contrast, functional instruction of iDCs infected with virulent VZV strains by  $\gamma\delta$  T cells failed (Fig. 40). This defect was independent of the VZV genotype used. So far this is the first description of a viral interference with T cell mediated DC instruction.



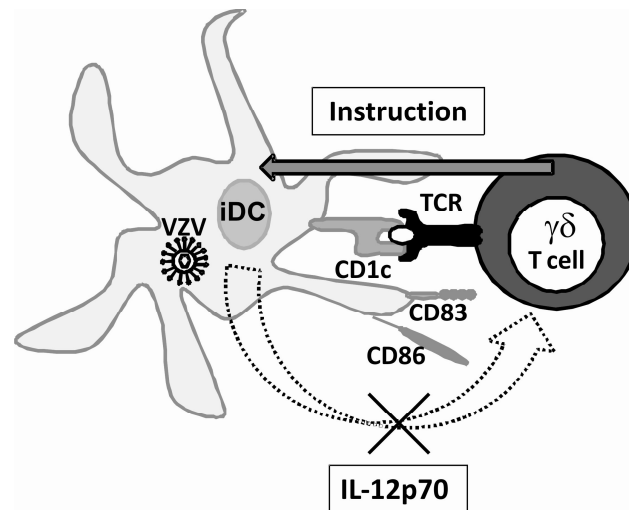


**Fig. 40: Scheme of  $\gamma\delta$  T cell-mediated instruction of iDCs infected with virulent VZV.**

CD1c-restricted  $\gamma\delta$  T cells instruct VZV-infected iDCs to mature phenotypically, shown by cell surface expression of CD83 and CD86. However, functional instruction which results in secretion of bioactive IL-12 failed in iDCs infected with virulent VZV strains.

Neutralization experiments with anti-IL-12 antibodies revealed the positive feed-back loop between IL-12 secretion by DCs and IFN- $\gamma$  secretion by T cells. Neutralization of secreted IL-12 by iDCs infected with the vaccine strain V-Oka reduced subsequent IFN- $\gamma$  secretion by CD1c-restricted  $\gamma\delta$  T cells providing evidence that IL-12p70 is critical for activation of  $\gamma\delta$  T cells. Moreover, this finding suggests that iDCs infected with virulent VZV strains are somehow intrinsically blocked to produce bioactive IL-12. The production of bioactive IL-12 consisting of covalently linked p35 and p40 subunits is facilitated by stimulation through CD40L expressed on activated T cells<sup>197</sup>. Triggering of CD40 molecule on iDCs through CD40L expressed on T cells triggers the MAPK pathway leading to subsequent IL-12 production<sup>59,84</sup>. However, VZV did not interfere with the activation of MAP kinases JNK, ERK and p38 which might have explained the deficiency in IL-12 secretion. This finding suggested that the interaction between CD40 on DCs and CD40L on T cells, which is required for induction of IL-12 secretion, was interrupted. Indeed, by providing CD40L *in trans* by a CD40L-expressing cell line iDCs infected with the clinical isolate JoSt secreted as much IL-12 as the vaccine-infected iDCs. Additionally, this rescue of IL-12 secretion also restored the secretion of high amounts of IFN- $\gamma$  by  $\gamma\delta$  T cells in the presence of iDCs infected with the clinical isolate JoSt. Therefore,  $\gamma\delta$  T cells cocultured with VZV-infected iDCs were tested for upregulation of CD40L on the cell surface. Unfortunately, staining for cell surface expressed CD40L on  $\gamma\delta$  T cells failed. However, it has to be mentioned that staining for CD40L on T

cells is difficult due to its weakly expression in general. Therefore, a failure in upregulation of CD40L on  $\gamma\delta$  T cells cannot be excluded. On the other hand it is possible that a T cell stimulatory signal provided by the DCs is somehow abrogated by infection with virulent VZV.

#### **4.5 Co-Stimulatory and Inhibitory Molecules provided by VZV-infected iDCs**

The observed findings pointed out to have a closer look on cell surface expression of the co-stimulatory molecules CD40 and CD86 on VZV-infected iDCs. Interestingly, iDCs infected with the clinical isolate JoSt significantly inhibited cell surface expression of CD40 and CD86 compared to vaccine-infected iDCs. This is in contrast to the finding observed on VZV-infected LCs and DDCs where both viral VZV strains induced a decrease in cell surface expression of CD40. However, it has to be mentioned that monocyte-derived DCs resemble inflammatory DCs which transiently arise during inflammation, for example in skin lesions of herpes zoster patients. Therefore, it is likely that virulent VZV strains modulate the phenotype of this DC subset massively infiltrating the skin during ongoing viral replication. Furthermore, iDCs infected with virulent VZV still express abundant CD40 on the cell surface which is probably sufficient to provide a T cell stimulating signal.

Moreover, VZV-infected iDCs were stained for cell surface expression of co-inhibitory molecules of the B7-CD28 family<sup>82</sup>. Ligation through B7-DC and B7-H1 with programmed cell death (PD-1) on effector T cells or B7-H4 with B and T lymphocyte attenuator (BTLA) induces suppression of T cell activation. Recently, it could be demonstrated that in chronically infected HIV-1 and HCV patients B7-H1 was upregulated on myeloid derived DCs. This correlated with disease progression in HIV-1 and B7-H1 is a marker for chronic inflammation in HCV pathogenesis<sup>198,199</sup>. Therefore, selective upregulation of inhibitory molecules of the B7-family might explain the block in IFN- $\gamma$  by  $\gamma\delta$  T cells in the presence of iDCs infected with virulent VZV strains. However, no upregulation of the above mentioned co-inhibitory molecules could be observed on VZV-infected cells.

#### 4.6 Blocking TLR-2 Signaling in iDCs by Virulent VZV

It has been demonstrated that production of bioactive IL-12 by DCs can be amplified by T cell derived signals, but must be initiated by innate signals<sup>200</sup>. Thus, CD40 ligation by T cells alone is not sufficient to induce IL-12p70 secretion by DCs. Signaling through PRRs is mandatory for production of bioactive IL-12<sup>201</sup>. Recent findings give evidence that synergistic stimulation of TLRs is necessary to induce bioactive IL-12 production by DCs<sup>68</sup>. Furthermore, it has been demonstrated that stimulation of a single TLR favors IL-23 over IL-12 secretion by myeloid-derived DC<sup>68,69</sup>.

Recognition of pathogens by DCs is largely dependent on TLRs. Members of the TLR family have been shown to sense a variety of viruses by recognizing viral genomes within endosomes through TLR3 (double stranded RNA), TLR7, TLR8 (single stranded RNA), and TLR9 (CpG) or by recognizing viral structural components at the cell surface through TLR2 and TLR4<sup>66</sup>. Especially, the TLR2 pathway has been shown to play an important role in sensing herpesviral infections. Glycoproteins B and H of HCMV are directly recognized by TLR2 and induce secretion of inflammatory cytokines through NF- $\kappa$ B in permissive cells<sup>180,181</sup>. Interaction of HSV-1 with TLR2 contributes to lethal encephalitis in mice which is dependent on the adaptor molecule MyD88<sup>178,179</sup>. Moreover, it was shown that TLR2 is activated in monocytes in response to VZV infection<sup>182</sup>. Therefore, we tested the hypothesis if virulent VZV targets TLR signaling in iDCs thereby blocking subsequent IL-12 production.

Stimulation of iDCs with replication competent or UV-inactivated virus alone did not induce secretion of bioactive IL-12. By contrast, additional stimulation with TLR2 agonist LTA induced low levels of IL-12p70 in iDCs stimulated with UV-inactivated virus and much higher amounts of IL-12p70 in iDCs infected with the vaccine strain V-Oka or HSV. In sharp contrast, triggering TLR2 pathway in iDCs infected with clinical isolate JoSt induced only negligible amounts of IL-12p70 as observed with UV-inactivated virus. These findings demonstrate that synergistic stimulation of different PRRs in iDCs is crucial to trigger bioactive IL-12 production. This is in line with reports describing strong synergistic effects of TLR ligands on IL-12 production by DCs<sup>68</sup>. Moreover, the data provide evidence that viral replication is essential to prime iDCs for further stimulation through TLRs as stimulation with UV-inactivated virus is not sufficient for high IL-12 production. It has to be mentioned that UV-light modifies viral genome which inhibits viral replication. However, the first steps of viral

life cycle comprising adsorption and penetration of virions into the host cell remained unaltered. Therefore, it is likely that a factor synthesized during viral replication of virulent VZV is responsible for blocking subsequent TLR2 signaling (Fig.41).

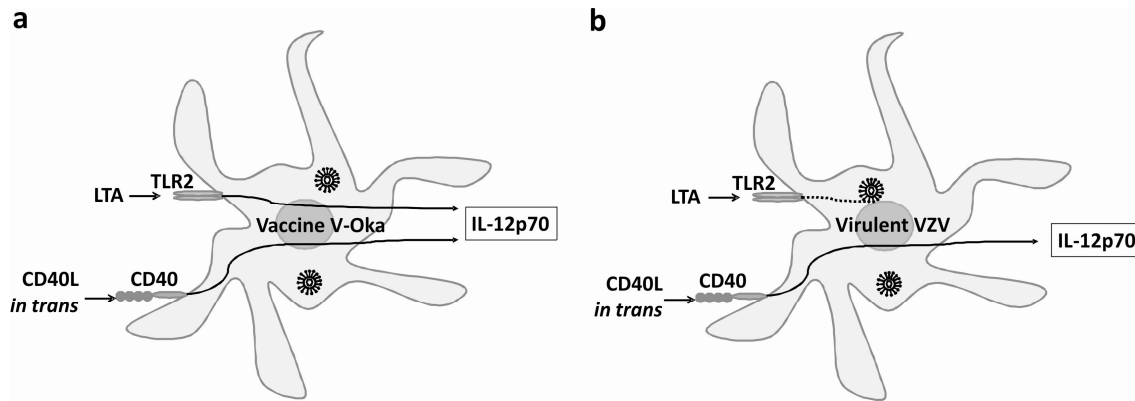


**Fig. 41: Scheme showing the interference of VZV with IL-12p70 secretion in iDCs.**

(a) The vaccine strain V-Oka primes DCs for further stimulation through TLR2 and CD40 which lead to subsequent IL-12p70 production. (b) In contrast, virulent VZV blocks TLR2 signaling thereby preventing bioactive IL-12 production. However, strong stimulation through CD40 by providing CD40L *in trans* promote IL-12 production.

Interestingly, VZV-infected iDCs stimulated with LTA secreted higher amounts of bioactive IL-12 as compared to iDCs after instruction by CD1c-restricted  $\gamma\delta$  T cells. Moreover, providing CD40L *in trans* induced the highest amount of IL-12p70 by VZV-infected DCs. These observations indicate that on the one hand CD1c-restricted  $\gamma\delta$  T cells stimulate VZV-infected iDCs through CD40 only weakly. This might explain the difficulties to stain for CD40L on CD1c-restricted  $\gamma\delta$  T cells after coculture with VZV-infected iDCs by flow cytometry. Furthermore, the experiments with CD40L *in trans* revealed that the CD40-CD40L signaling pathway was not disturbed in VZV-infected iDCs. However, stimulation of VZV-infected iDCs with LTA showed that only virulent VZV blocks TLR2 signaling. It seems likely that virulent VZV interferes with a universal adaptor molecule involved in several TLR signaling pathways. For example, TNF receptor associated factor 6 (TRAF6) which is involved in TLR2, TLR4, TLR5, TLR7, TLR8 and TLR9 signaling<sup>66</sup>.

Bioactive IL-12 is a heterodimeric cytokine composed of covalently linked p35 and p40 subunits. Interestingly, the p40 subunit is also part of the cytokine IL-23 which is required for expansion and survival of  $T_H17$  cells. Moreover, myeloid-derived DCs differentially produce IL-23 and IL-12 in response to TLR agonists<sup>69</sup>. This study demonstrated that

several TLR agonists alone induce IL-23 expression, whereas multiple signals are required for commitment to IL-12 production. Furthermore, *Peiser et al.* demonstrated that LCs stimulated through TLR2 acquired the capacity to polarize T<sub>H</sub>17 cells<sup>202</sup>. Therefore, it would be worth to investigate more closely the cytokine profile of VZV-infected iDCs after stimulation through TLR2. It might be possible that virulent VZV blocks IL-12p35 secretion thereby favoring IL-23 over IL-12p70 production.

Another research group has demonstrated that VZV activates inflammatory cytokines in human monocytes and macrophages via TLR2<sup>182</sup>. Primarily, it has to be mentioned that in this study the vaccine strain V-Oka was not included in the experimental setting allowing the comparative validation of the TLR2 activating potential of VZV. Furthermore, only the secretion of IL-6 and IL-8 by human monocytes was assessed. Moreover, it was mentioned that active viral replication was not necessary for activation of NF-κB-driven reporter gene construct. Therefore, it might be possible that in this experimental setting a block in TLR2 signaling by VZV could not be detected.

Another important aspect is that viral replication is not sufficient to activate iDCs to secrete bioactive IL-12 but additional TLR stimulation is mandatory. This is in line with the general observed finding that live vaccines are more powerful inducers of immunity as compared to inactivated vaccines.

Altogether, further investigations should address the question which adaptor molecule in the TLR2 signaling pathway is blocked by virulent VZV strains compared to the vaccine. This might be a promising field which gives further insight in the pathogenicity of VZV strains and their potency to replicate successfully within the skin.

In summary, these data provide evidence that virulent VZV strains prevent functional maturation of iDCs by blocking TLR2 signaling and bioactive IL-12 secretion. In turn early T<sub>H</sub>1 responses are prevented and thereby virulent VZV strains facilitate their replication and spread in the skin. In contrast, the vaccine strain V-Oka fully support functional maturation of iDCs and subsequent activation of T cells. However, the molecular mechanisms underlying attenuation of the vaccine strain are not yet understood. Therefore, it might be worth to reveal the factor of virulent VZV strains which blocks TLR2 signaling. This finding has practical consequences as novel vaccination strategies have to verify that the candidate vaccines do not disrupt the dialogue between innate cells and DCs.

Finally, this finding might be of relevance for preventing herpes zoster in people with increasing age which show a decline in cell-mediated immunity that correlates with an increased risk to develop herpes zoster. Several studies have shown that frequent exposure to circulating virulent VZV strains boost immunity to VZV and therefore reduces the risk for herpes zoster<sup>52</sup>. Promising vaccination studies with V-Oka as a zoster vaccine markedly reduced morbidity from herpes zoster and postherpetic neuralgia among older adults<sup>48-50</sup>.

## 5 Reference list

1. Quinlivan, M. *et al.* The molecular epidemiology of varicella-zoster virus: evidence for geographic segregation. *J. Infect. Dis.* **186**, 888-894 (2002).
2. Arvin, A.M. Varicella-zoster virus. *Clin. Microbiol. Rev.* **9**, 361-& (1996).
3. Quinlivan, M. & Breuer, J. Molecular studies of Varicella zoster virus. *Rev. Med. Virol.* **16**, 225-250 (2006).
4. Chen, J.J., Zhu, Z.L., Gershon, A.A. & Gershon, M.D. Mannose 6-phosphate receptor dependence of varicella zoster virus infection in vitro and in the epidermis during varicella and zoster. *Cell* **119**, 915-926 (2004).
5. Zhu, Z.L., Gershon, M.D., Ambron, R., Gabel, C. & Gershon, A.A. Infection of Cells by Varicella-Zoster Virus - Inhibition of Viral Entry by Mannose 6-Phosphate and Heparin. *Proc. Natl. Acad. Sci. USA* **92**, 3546-3550 (1995).
6. Li, Q.X., Ali, M.A. & Cohen, J.I. Insulin degrading enzyme is a cellular receptor mediating varicella-zoster virus infection and cell-to-cell spread. *Cell* **127**, 305-316 (2006).
7. Kuhn, M., Desloges, N., Rahaus, M. & Wolff, M.H. Varicella-zoster virus infection influences expression and organization of actin and alpha-tubulin but does not affect lamin A and vimentin. *Intervirology* **48**, 312-320 (2005).
8. Shiraki, K. & Takahashi, M. Virus-Particles and Glycoproteins Excreted from Cultured-Cells Infected with Varicella-Zoster Virus (VZV). *J. Gen. Virol.* **61**, 271-275 (1982).
9. Moffat, J.F., Stein, M.D., Kaneshima, H. & Arvin, A.M. Tropism of varicella-zoster virus for human CD4+ and CD8+ T lymphocytes and epidermal cells in SCID-hu mice. *J. Virol.* **69**, 5236-5242 (1995).
10. Nikkels, A.F. *et al.* Distribution of varicella zoster virus and herpes simplex virus in disseminated fatal infections. *J. Clin. Pathol.* **49**, 243-248 (1996).
11. Etzioni, A. *et al.* Fatal varicella associated with selective natural killer cell deficiency. *J. Pediatr.* **146**, 423-425 (2005).
12. Robertson, S., Newbigging, K., Carman, W., Jones, G. & Isles, C. Fulminating varicella despite prophylactic immune globulin and intravenous acyclovir in a renal transplant recipient: should renal patients be vaccinated against VZV before transplantation? *Clin. Transplant.* **20**, 136-138 (2006).

13. Springfield,C. *et al.* Fatal varicella in an immunocompromised adult associated with a European genotype E2 variant of varicella zoster virus. *J. Clin. Virol.* **44**, 70-73 (2009).
14. Miyazaki,Y. *et al.* VZV vasculopathy associated with myelo-radiculoganglio-meningo-encephalitis: an autopsy case of an immunocompetent 66-year-old male. *J. Neurol. Sci.* **275**, 42-45 (2008).
15. Natoli,S. *et al.* A novel mutation of varicella-zoster virus associated to fatal hepatitis. *J. of Clin.Virol.* **37**, 72-74 (2006).
16. Scheifele,D.W., Law,B., Halperin,S.A. & Tam,T. Seven fatal varicella infections in children were potentially avoidable: A report from IMPACT centres from 2000 to 2005. *Paediatr. Child Health* **11**, 413-415 (2006).
17. Gilden,D.H., Mahalingam,R., Cohrs,R.J. & Tyler,K.L. Herpesvirus infections of the nervous system. *Nat. Clin. Pract. Neurol.* **3**, 82-94 (2007).
18. Steiner,I., Kennedy,P.G. & Pachner,A.R. The neurotropic herpes viruses: herpes simplex and varicella-zoster. *Lancet Neurol.* **6**, 1015-1028 (2007).
19. Levin,M.J. *et al.* Decline in varicella-zoster virus (VZV)-specific cell-mediated immunity with increasing age and boosting with a high-dose VZV vaccine. *J. Infect. Dis.* **188**, 1336-1344 (2003).
20. Abendroth,A., Morrow,G., Cunningham,A.L. & Slobedman,B. Varicella-zoster virus infection of human dendritic cells and transmission to T cells: implications for virus dissemination in the host. *J. Virol.* **75**, 6183-6192 (2001).
21. Moffat,J.F. *et al.* The ORF47 and ORF66 putative protein kinases of varicella-zoster virus determine tropism for human T cells and skin in the SCID-hu mouse. *Proc. Natl. Acad. Sci. U. S. A* **95**, 11969-11974 (1998).
22. Ku,C.C., Padilla,J.A., Grose,C., Butcher,E.C. & Arvin,A.M. Tropism of varicella-zoster virus for human tonsillar CD4(+) T lymphocytes that express activation, memory, and skin homing markers. *J. Virol.* **76**, 11425-11433 (2002).
23. Mainka,C., Fuss,B., Geiger,H., Hofelmayr,H. & Wolff,M.H. Characterization of viremia at different stages of varicella-zoster virus infection. *J. Med. Virol.* **56**, 91-98 (1998).
24. Koenig,A. & Wolff,M.H. Infectibility of separated peripheral blood mononuclear cell subpopulations by varicella-zoster virus (VZV). *J. Med. Virol.* **70 Suppl 1**, S59-S63 (2003).
25. Bosnjak,L., Jones,C.A., Abendroth,A. & Cunningham,A.L. Dendritic cell biology in herpesvirus infections. *Viral Immunol.* **18**, 419-433 (2005).
26. Levy,O. *et al.* Disseminated varicella infection due to the vaccine strain of varicella-zoster virus, in a patient with a novel deficiency in natural killer T cells. *J. Infect. Dis.* **188**, 948-953 (2003).



27. Vossen,M.T.M. *et al.* Absence of circulating natural killer and primed CD8(+) cells in life-threatening varicella. *J. Infect. Dis.* **191**, 198-206 (2005).
28. Ku,C.C. *et al.* Varicella-zoster virus transfer to skin by T cells and modulation of viral replication by epidermal cell interferon-alpha. *J. Exp. Med.* **200**, 917-925 (2004).
29. Arvin,A.M., Koropchak,C.M., Williams,B.R.G., Grumet,F.C. & Fong,S.K.H. Early Immune-Response in Healthy and Immunocompromised Subjects with Primary Varicella-Zoster Virus-Infection. *J. Infect. Dis.* **154**, 422-429 (1986).
30. Arvin,A.M. *et al.* Equivalent Recognition of A Varicella-Zoster Virus Immediate Early Protein (IE62) and Glycoprotein-I by Cytotoxic Lymphocytes-T of Either CD4+ or CD8+ Phenotype. *J. Immunol.* **146**, 257-264 (1991).
31. Bergen,R.E., Sharp,M., Sanchez,A., Judd,A.K. & Arvin,A.M. Human T cells recognize multiple epitopes of an immediate early/tegument protein (IE62) and glycoprotein I of varicella zoster virus. *Viral Immunol.* **4**, 151-166 (1991).
32. Arvin,A.M. *et al.* Memory cytotoxic T cell responses to viral tegument and regulatory proteins encoded by open reading frames 4, 10, 29, and 62 of varicella-zoster virus. *Viral Immunol.* **15**, 507-516 (2002).
33. Jones,L., Black,A.P., Malavige,G.N. & Ogg,G.S. Persistent high frequencies of varicella-zoster virus ORF4 protein-specific CD4+ T cells after primary infection. *J. Virol.* **80**, 9772-9778 (2006).
34. Malavige,G.N., Jones,L., Black,A.P. & Ogg,G.S. Rapid effector function of varicella-zoster virus glycoprotein I-specific CD4+ T cells many decades after primary infection. *J. Infect. Dis.* **195**, 660-664 (2007).
35. Jones,L., Black,A.P., Malavige,G.N. & Ogg,G.S. Phenotypic analysis of human CD4+ T cells specific for immediate-early 63 protein of varicella-zoster virus. *Eur. J. Immunol.* **37**, 3393-3403 (2007).
36. Brunell,P.A., Gershon,A.A., Uduman,S.A. & Steinberg,S. Varicella-Zoster Immunoglobulins During Varicella, Latency, and Zoster. *J. Infect. Dis.* **132**, 49-54 (1975).
37. Takahashi,M. Current Status and Prospects of Live Varicella Vaccine. *Vaccine* **10**, 1007-1014 (1992).
38. Yamanishi,K. Molecular analysis of the Oka vaccine strain of varicella-zoster virus. *J. Infect. Dis.* **197 Suppl 2**, S45-S48 (2008).
39. Argaw,T. *et al.* Nucleotide sequences that distinguish Oka vaccine from parental Oka and other varicella-zoster virus isolates. *J. Infect. Dis.* **181**, 1153-1157 (2000).
40. Gershon,A.A., Arvin,A.M., Levin,M.J., Seward,J.F. & Schmid,D.S. Varicella vaccine in the United States: a decade of prevention and the way forward. *J. Infect. Dis.* **197 Suppl 2**, S39-S40 (2008).

41. Watson,B. Humoral and cell-mediated immune responses in children and adults after 1 and 2 doses of varicella vaccine. *J. Infect. Dis.* **197 Suppl 2**, S143-S146 (2008).
42. Frey,C.R. *et al.* Identification of CD8+ T cell epitopes in the immediate early 62 protein (IE62) of varicella-zoster virus, and evaluation of frequency of CD8+ T cell response to IE62, by use of IE62 peptides after varicella vaccination. *J. Infect. Dis.* **188**, 40-52 (2003).
43. Quinlivan,M.L., Gershon,A.A., Steinberg,S.P. & Breuer,J. Rashes occurring after immunization with a mixture of viruses in the Oka vaccine are derived from single clones of virus. *J. Infect. Dis.***190**, 793-796 (2004).
44. Quinlivan,M.L. *et al.* Natural selection for rash-forming genotypes of the varicella-zoster vaccine virus detected within immunized human hosts. *Proc. Natl. Acad. Sci. USA* **104**, 208-212 (2007).
45. LaRussa,P., Steinberg,S.P., Shapiro,E., Vazquez,M. & Gershon,A.A. Viral strain identification in varicella vaccinees with disseminated rashes. *Pediatr. Infect. Dis. J.* **19**, 1037-1039 (2000).
46. Hardy,I., Gershon,A.A., Steinberg,S.P. & LaRussa,P. The incidence of zoster after immunization with live attenuated varicella vaccine. A study in children with leukemia. Varicella Vaccine Collaborative Study Group. *N. Engl. J. Med.* **325**, 1545-1550 (1991).
47. Hambleton,S., Steinberg,S.P., Larussa,P.S., Shapiro,E.D. & Gershon,A.A. Risk of herpes zoster in adults immunized with varicella vaccine. *J. Infect. Dis.* **197 Suppl 2**, S196-S199 (2008).
48. Oxman,M.N. *et al.* A vaccine to prevent herpes zoster and postherpetic neuralgia in older adults. *N. Engl. J. Med.* **352**, 2271-2284 (2005).
49. Levin,M.J. *et al.* Varicella-zoster virus-specific immune responses in elderly recipients of a herpes zoster vaccine. *J. Infect. Dis.* **197**, 825-835 (2008).
50. Oxman,M.N. & Levin,M.J. Vaccination against Herpes Zoster and Postherpetic Neuralgia. *J. Infect. Dis.* **197 Suppl 2**, S228-S236 (2008).
51. Thomas,S.L., Wheeler,J.G. & Hall,A.J. Contacts with varicella or with children and protection against herpes zoster in adults: a case-control study. *Lancet* **360**, 678-682 (2002).
52. Brisson,M., Gay,N.J., Edmunds,W.J. & Andrews,N.J. Exposure to varicella boosts immunity to herpes-zoster: implications for mass vaccination against chickenpox. *Vaccine* **20**, 2500-2507 (2002).
53. Edmunds,W.J. & Brisson,M. The effect of vaccination on the epidemiology of varicella zoster virus. *J. Infect.* **44**, 211-219 (2002).
54. Edmunds,W.J., Brisson,M., Gay,N.J. & Miller,E. Varicella vaccination: a double-edged sword? *Commun. Dis. Public Health* **5**, 185-186 (2002).

55. Mueller,N.H., Gilden,D.H., Cohrs,R.J., Mahalingam,R. & Nagel,M.A. Varicella zoster virus infection: clinical features, molecular pathogenesis of disease, and latency. *Neurol. Clin.* **26**, 675-97, viii (2008).
56. Miwa,N. *et al.* Comparative efficacy of acyclovir and vidarabine on the replication of varicella-zoster virus. *Antiviral Res.* **65**, 49-55 (2005).
57. Johnson,R.W., Wasner,G., Saddier,P. & Baron,R. Herpes zoster and postherpetic neuralgia: optimizing management in the elderly patient. *Drugs Aging* **25**, 991-1006 (2008).
58. Banchereau,J. & Steinman,R.M. Dendritic cells and the control of immunity. *Nature* **392**, 245-252 (1998).
59. Banchereau,J. *et al.* Immunobiology of dendritic cells. *Annu.Rev. Immunol.* **18**, 767-+ (2000).
60. Wilson,N.S., El Sukkari,D. & Villadangos,J.A. Dendritic cells constitutively present self antigens in their immature state in vivo and regulate antigen presentation by controlling the rates of MHC class II synthesis and endocytosis. *Blood* **103**, 2187-2195 (2004).
61. Reis e Sousa. Dendritic cells in a mature age. *Nat. Rev. Immunol.* **6**, 476-483 (2006).
62. Schuurhuis,D.H., Fu,N., Ossendorp,F. & Melief,C.J.M. Ins and outs of dendritic cells. *Int. Arch. Allergy Immunol.* **140**, 53-72 (2006).
63. Takeda,K. & Akira,S. Toll-like receptors. *Curr. Protoc. Immunol.* **Chapter 14**, Unit (2007).
64. Eisenacher,K., Steinberg,C., Reindl,W. & Krug,A. The role of viral nucleic acid recognition in dendritic cells for innate and adaptive antiviral immunity. *Immunobiology* **212**, 701-714 (2007).
65. Bowie,A.G. & Unterholzner,L. Viral evasion and subversion of pattern-recognition receptor signalling. *Nat. Rev. Immunol.* **8**, 911-922 (2008).
66. Xagorari,A. & Chlichlia,K. Toll-like receptors and viruses: induction of innate antiviral immune responses. *Open. Microbiol. J.* **2**, 49-59 (2008).
67. Pichlmair,A. & Sousa,C.R.E. Innate recognition of viruses. *Immunity* **27**, 370-383 (2007).
68. Napolitani,G., Rinaldi,A., Bertoni,F., Sallusto,F. & Lanzavecchia,A. Selected Toll-like receptor agonist combinations synergistically trigger a T helper type 1-polarizing program in dendritic cells. *Nat. Immunol.* **6**, 769-776 (2005).
69. Roses,R.E. *et al.* Differential production of IL-23 and IL-12 by myeloid-derived dendritic cells in response to TLR agonists. *J. Immunol.* **181**, 5120-5127 (2008).
70. Trinchieri,G. & Sher,A. Cooperation of Toll-like receptor signals in innate immune defence. *Nat. Rev. Immunol.* **7**, 179-190 (2007).

71. Reschner,A., Hubert,P., Delvenne,P., Boniver,J. & Jacobs,N. Innate lymphocyte and dendritic cell cross-talk: a key factor in the regulation of the immune response. *Clin. Exp. Immunol.* **152**, 219-226 (2008).
72. Vincent,M.S. *et al.* CD1-dependent dendritic cell instruction. *Nat. Immunol.* **3**, 1163-1168 (2002).
73. Leslie,D.S. *et al.* CD1-mediated gamma/delta T cell maturation of dendritic cells. *J. Exp. Med.* **196**, 1575-1584 (2002).
74. Valentiniis,B. *et al.* Human recombinant heat shock protein 70 affects the maturation pathways of dendritic cells in vitro and has an in vivo adjuvant activity. *J. Leukoc. Biol.* **84**, 199-206 (2008).
75. Steinman,R.M. & Banchereau,J. Taking dendritic cells into medicine. *Nature* **449**, 419-426 (2007).
76. Steinman,R.M. Dendritic cells: understanding immunogenicity. *Eur. J. Immunol.* **37 Suppl 1**, S53-S60 (2007).
77. Steinman,R.M. & Hemmi,H. Dendritic cells: translating innate to adaptive immunity. *Curr. Top. Microbiol. Immunol.* **311**, 17-58 (2006).
78. Lukacs-Kornek,V., Engel,D., Tacke,F. & Kurts,C. The role of chemokines and their receptors in dendritic cell biology. *Front Biosci.* **13**, 2238-2252 (2008).
79. Dieu,M.C. *et al.* Selective recruitment of immature and mature dendritic cells by distinct chemokines expressed in different anatomic sites. *J. Exp. Med.* **188**, 373-386 (1998).
80. Celli,S., Garcia,Z., Beuneu,H. & Bousso,P. Decoding the dynamics of T cell-dendritic cell interactions in vivo. *Immunol. Rev.* **221**, 182-187 (2008).
81. Guermonprez,P., Valladeau,J., Zitvogel,L., Thery,C. & Amigorena,S. Antigen presentation and T cell stimulation by dendritic cells. *Annu. Rev. Immunol.* **20**, 621-667 (2002).
82. Sharpe,A.H. & Freeman,G.J. The B7-CD28 superfamily. *Nat. Rev. Immunol.* **2**, 116-126 (2002).
83. Catalfamo,M. & Henkart,P.A. Perforin and the granule exocytosis cytotoxicity pathway. *Curr. Opin. Immunol.* **15**, 522-527 (2003).
84. Moser,M. & Murphy,K.M. Dendritic cell regulation of TH1-TH2 development. *Nat. Immunol.* **1**, 199-205 (2000).
85. Vieira,P.L., de Jong,E.C., Wierenga,E.A., Kapsenberg,M.L. & Kalinski,P. Development of Th1-inducing capacity in myeloid dendritic cells requires environmental instruction. *J. Immunol.* **164**, 4507-4512 (2000).

86. Jonuleit,H., Schmitt,E., Schuler,G., Knop,J. & Enk,A.H. Induction of interleukin 10-producing, nonproliferating CD4(+) T cells with regulatory properties by repetitive stimulation with allogeneic immature human dendritic cells. *J. Exp. Med.* **192**, 1213-1222 (2000).
87. LeibundGut-Landmann,S. *et al.* Syk- and CARD9-dependent coupling of innate immunity to the induction of T helper cells that produce interleukin 17. *Nat. Immunol.* **8**, 630-638 (2007).
88. Fouser,L.A., Wright,J.F., Dunussi-Joannopoulos,K. & Collins,M. Th17 cytokines and their emerging roles in inflammation and autoimmunity. *Immunol. Rev.* **226**, 87-102 (2008).
89. Corthay,A. A three-cell model for activation of naive T helper cells. *Scand. J. Immunol.* **64**, 93-96 (2006).
90. McKenna,K., Beignon,A.S. & Bhardwaj,N. Plasmacytoid dendritic cells: Linking innate and adaptive immunity. *J. Virol.* **79**, 17-27 (2005).
91. Diebold,S.S. *et al.* Viral infection switches non-plasmacytoid dendritic cells into high interferon producers. *Nature* **424**, 324-328 (2003).
92. Lopez-Bravo,M. & Ardavin,C. In vivo induction of immune responses to pathogens by conventional dendritic cells. *Immunity*. **29**, 343-351 (2008).
93. Masson,F., Mount,A.M., Wilson,N.S. & Belz,G.T. Dendritic cells: driving the differentiation programme of T cells in viral infections. *Immunol. Cell Biol.* **86**, 333-342 (2008).
94. Allan,R.S. *et al.* Migratory dendritic cells transfer antigen to a lymph node-resident dendritic cell population for efficient CTL priming. *Immunity*. **25**, 153-162 (2006).
95. Manz,M.G., Traver,D., Miyamoto,T., Weissman,I.L. & Akashi,K. Dendritic cell potentials of early lymphoid and myeloid progenitors. *Blood* **97**, 3333-3341 (2001).
96. Leon,B., Lopez-Bravo,M. & Ardavin,C. Monocyte-derived dendritic cells formed at the infection site control the induction of protective T helper 1 responses against Leishmania. *Immunity*. **26**, 519-531 (2007).
97. Caminschi,I. *et al.* Putative IKDCs are functionally and developmentally similar to natural killer cells, but not to dendritic cells. *J. Exp. Med.* **204**, 2579-2590 (2007).
98. Kupper,T.S. & Fuhlbrigge,R.C. Immune surveillance in the skin: Mechanisms and clinical consequences. *Nat. Rev. Immunol.* **4**, 211-222 (2004).
99. Valladeau,J. & Saeland,S. Cutaneous dendritic cells. *Semin. Immunol.* **17**, 273-283 (2005).
100. Hunger,R.E. *et al.* Langerhans cells utilize CD1a and langerin to efficiently present non-peptide antigens to T cells. *J. Clin. Invest.* **113**, 701-708 (2004).

101. Mizumoto,N. & Takashima,A. CD1a and langerin: acting as more than Langerhans cell markers. *J. Clin. Invest.* **113**, 658-660 (2004).
102. Ebner,S. *et al.* Expression of C-type lectin receptors by subsets of dendritic cells in human skin. *Int. Immunol.* **16**, 877-887 (2004).
103. Mathers,A.R. & Larregina,A.T. Professional antigen-presenting cells of the skin. *Immunol. Res.* **36**, 127-136 (2006).
104. Allan,R.S. *et al.* Epidermal viral immunity induced by CD8 alpha(+) dendritic cells but not by Langerhans cells. *Science* **301**, 1925-1928 (2003).
105. Belz,G.T. *et al.* Cutting edge: conventional CD8 alpha+ dendritic cells are generally involved in priming CTL immunity to viruses. *J. Immunol.* **172**, 1996-2000 (2004).
106. Zhao,X.Y. *et al.* Vaginal submucosal dendritic cells, but not Langerhans cells, induce protective th1 responses to herpes simplex virus-2. *J. Exp.Med.***197**, 153-162 (2003).
107. Gerlini,G., Mariotti,G., Bianchi,B. & Pimpinelli,N. Massive recruitment of type I interferon producing plasmacytoid dendritic cells in varicella skin lesions. *J. Invest Dermatol.* **126**, 507-509 (2006).
108. Nikkels,A.F., Sadzot-Delvaux,C. & Pierard,G.E. Absence of intercellular adhesion molecule 1 expression in varicella zoster virus-infected keratinocytes during herpes zoster - Another immune evasion strategy? *Am. J .Dermatopathol.* **26**, 27-32 (2004).
109. Raftery,M.J. *et al.* Shaping phenotype, function, and survival of dendritic cells by cytomegalovirus-encoded IL-10. *J. Immunol.* **173**, 3383-3391 (2004).
110. Raftery,M.J. *et al.* Targeting the function of mature dendritic cells by human cytomegalovirus: a multilayered viral defense strategy. *Immunity.* **15**, 997-1009 (2001).
111. Fruh,K. *et al.* A viral inhibitor of peptide transporters for antigen presentation. *Nature* **375**, 415-418 (1995).
112. Hill,A. *et al.* Herpes simplex virus turns off the TAP to evade host immunity. *Nature* **375**, 411-415 (1995).
113. Salio,M., Cella,M., Suter,M. & Lanzavecchia,A. Inhibition of dendritic cell maturation by herpes simplex virus. *Eur. J. Immunol.* **29**, 3245-3253 (1999).
114. Muller,D.B., Raftery,M.J., Kather,A., Giese,T. & Schonrich,G. Frontline: Induction of apoptosis and modulation of c-FLIPL and p53 in immature dendritic cells infected with herpes simplex virus. *Eur. J. Immunol.* **34**, 941-951 (2004).
115. Sloan,D.D. *et al.* Inhibition of TCR signaling by herpes simplex virus. *J. Immunol.* **176**, 1825-1833 (2006).

116. Jones,C.A. *et al.* Herpes simplex virus type 2 induces rapid cell death and functional impairment of murine dendritic cells in vitro. *J. Virol.* **77**, 11139-11149 (2003).
117. Hu,H. & Cohen,J.I. Varicella-zoster virus open reading frame 47 (ORF47) protein is critical for virus replication in dendritic cells and for spread to other cells. *Virology* **337**, 304-311 (2005).
118. Morrow,G., Slobedman,B., Cunningham,A.L. & Abendroth,A. Varicella-zoster virus productively infects mature dendritic cells and alters their immune function. *J. Virol.* **77**, 4950-4959 (2003).
119. Cohen,J.I. Infection of cells with varicella-zoster virus down-regulates surface expression of class I major histocompatibility complex antigens. *J. Infect. Dis.* **177**, 1390-1393 (1998).
120. Abendroth,A., Lin,I., Slobedman,B., Ploegh,H. & Arvin,A.M. Varicella-zoster virus retains major histocompatibility complex class I proteins in the Golgi compartment of infected cells. *J. Virol.* **75**, 4878-4888 (2001).
121. Eisfeld,A.J., Yee,M.B., Erazo,A., Abendroth,A. & Kinchington,P.R. Downregulation of class I major histocompatibility complex surface expression by varicella-zoster virus involves open reading frame 66 protein kinase-dependent and -independent mechanisms. *J. Virol.* **81**, 9034-9049 (2007).
122. Abendroth,A. *et al.* Modulation of major histocompatibility class II protein expression by varicella-zoster virus. *J. Virol.* **74**, 1900-1907 (2000).
123. Jones,J.O. & Arvin,A.M. Inhibition of the NF-kappa B pathway by varicella-zoster virus in vitro and in human epidermal cells in vivo. *J. Virol.* **80**, 5113-5124 (2006).
124. Barral,D.C. & Brenner,M.B. CD1 antigen presentation: how it works. *Nat. Rev. Immunol.* **7**, 929-941 (2007).
125. Calabi,F. & Milstein,C. The molecular biology of CD1. *Semin. Immunol.* **12**, 503-509 (2000).
126. Moody,D.B. & Porcelli,S.A. Intracellular pathways of CD1 antigen presentation. *Nat. Rev. Immunol.* **3**, 11-22 (2003).
127. Moody,D.B. The surprising diversity of lipid antigens for CD1-restricted T cells. *Adv. Immunol.* **89**, 87-139 (2006).
128. Moody,D.B. *et al.* CD1c-mediated T-cell recognition of isoprenoid glycolipids in Mycobacterium tuberculosis infection. *Nature* **404**, 884-888 (2000).
129. Beckman,E.M. *et al.* CD1c restricts responses of mycobacteria-specific T cells - Evidence for antigen presentation by a second member of the human CD1 family. *J. Immunol.* **157**, 2795-2803 (1996).

130. Vincent,M.S., Xiong,X.W., Grant,E.P., Peng,W. & Brenner,M.B. CD1a-, b-, and c-restricted TCRs recognize both self and foreign antigens. *J. Immunol.* **175**, 6344-6351 (2005).
131. Spada,F.M. *et al.* Self-recognition of CD1 by gamma/delta T cells: implications for innate immunity. *J. Exp. Med.* **191**, 937-948 (2000).
132. Dutronc,Y. & Porcelli,S.A. The CD1 family and T cell recognition of lipid antigens. *Tissue Antigens* **60**, 337-353 (2002).
133. Sieling,P.A. *et al.* CD1 expression by dendritic cells in human leprosy lesions: Correlation with effective host immunity. *J. Immunol.* **162**, 1851-1858 (1999).
134. Roura-Mir,C. *et al.* CD1a and CD1c activate intrathyroidal T cells during Graves' disease and Hashimoto's thyroiditis. *J. Immunol.* **174**, 3773-3780 (2005).
135. Yuan,W., Dasgupta,A. & Cresswell,P. Herpes simplex virus evades natural killer T cell recognition by suppressing CD1d recycling. *Nat. Immunol.* **7**, 835-842 (2006).
136. Raftery,M.J., Winau,F., Kaufmann,S.H.E., Schaible,U.E. & Schonrich,G. CD1 antigen presentation by human dendritic cells as a target for herpes simplex virus immune evasion. *J. Immunol.* **177**, 6207-6214 (2006).
137. Sanchez,D.J., Gumperz,J.E. & Ganem,D. Regulation of CD1d expression and function by a herpesvirus infection. *J. Clin. Invest* **115**, 1369-1378 (2005).
138. Raftery,M.J. *et al.* Inhibition of CD1 Antigen Presentation by Human Cytomegalovirus. *J. Virol.* (2008).
139. Chen,N. *et al.* HIV-1 down-regulates the expression of CD1d via Nef. *Eur. J. Immunol.* **36**, 278-286 (2006).
140. Hayday,A.C. [gamma][delta] cells: a right time and a right place for a conserved third way of protection. *Annu. Rev. Immunol.* **18**, 975-1026 (2000).
141. Morita,C.T., Jin,C., Sarikonda,G. & Wang,H. Nonpeptide antigens, presentation mechanisms, and immunological memory of human Vgamma2Vdelta2 T cells: discriminating friend from foe through the recognition of prenyl pyrophosphate antigens. *Immunol. Rev.* **215**, 59-76 (2007).
142. Beetz,S., Marischen,L., Kabelitz,D. & Wesch,D. Human gamma delta T cells: candidates for the development of immunotherapeutic strategies. *Immunol. Res.* **37**, 97-111 (2007).
143. Girardi,M. Immunosurveillance and immunoregulation by gammadelta T cells. *J. Invest Dermatol.* **126**, 25-31 (2006).
144. Chien,Y.H. & Konigshofer,Y. Antigen recognition by gammadelta T cells. *Immunol. Rev.* **215**, 46-58 (2007).



145. Chen,Z.W. & Letvin,N.L. Vgamma2Vdelta2+ T cells and anti-microbial immune responses. *Microbes. Infect.* **5**, 491-498 (2003).
146. D'Ombra, M.C., Hansen, D.S., Simpson, K.M. & Schofield, L. gammadelta-T cells expressing NK receptors predominate over NK cells and conventional T cells in the innate IFN-gamma response to Plasmodium falciparum malaria. *Eur. J. Immunol.* **37**, 1864-1873 (2007).
147. Wrobel, P. *et al.* Lysis of a broad range of epithelial tumour cells by human gamma delta T cells: involvement of NKG2D ligands and T-cell receptor- versus NKG2D-dependent recognition. *Scand. J. Immunol.* **66**, 320-328 (2007).
148. Holtmeier, W. *et al.* The TCR-delta repertoire in normal human skin is restricted and distinct from the TCR-delta repertoire in the peripheral blood. *J. Invest Dermatol.* **116**, 275-280 (2001).
149. Kabelitz, D., Marischen, L., Oberg, H.H., Holtmeier, W. & Wesch, D. Epithelial defence by gamma delta T cells. *Int. Arch. Allergy Immunol.* **137**, 73-81 (2005).
150. Ebert, L.M., Meuter, S. & Moser, B. Homing and function of human skin gammadelta T cells and NK cells: relevance for tumor surveillance. *J. Immunol.* **176**, 4331-4336 (2006).
151. Girardi, M. *et al.* Resident skin-specific gammadelta T cells provide local, nonredundant regulation of cutaneous inflammation. *J. Exp. Med.* **195**, 855-867 (2002).
152. Groh, V., Steinle, A., Bauer, S. & Spies, T. Recognition of stress-induced MHC molecules by intestinal epithelial gammadelta T cells. *Science* **279**, 1737-1740 (1998).
153. Wu, J., Groh, V. & Spies, T. T cell antigen receptor engagement and specificity in the recognition of stress-inducible MHC class I-related chains by human epithelial gamma delta T cells. *J. Immunol.* **169**, 1236-1240 (2002).
154. Russano, A.M. *et al.* CD1-restricted recognition of exogenous and self-lipid antigens by duodenal gammadelta+ T lymphocytes. *J. Immunol.* **178**, 3620-3626 (2007).
155. Thedrez, A. *et al.* Self/non-self discrimination by human gammadelta T cells: simple solutions for a complex issue? *Immunol. Rev.* **215**, 123-135 (2007).
156. Das, H., Sugita, M. & Brenner, M.B. Mechanisms of Vdelta1 gammadelta T cell activation by microbial components. *J. Immunol.* **172**, 6578-6586 (2004).
157. Boullier, S., Dadaglio, G., Lefeuvre, A., Debord, T. & Gougeon, M.L. V delta 1 T cells expanded in the blood throughout HIV infection display a cytotoxic activity and are primed for TNF-alpha and IFN-gamma production but are not selected in lymph nodes. *J. Immunol.* **159**, 3629-3637 (1997).
158. Dechanet, J. *et al.* Implication of gamma delta T cells in the human immune response to cytomegalovirus. *J. Clin. Invest.* **103**, 1437-1449 (1999).

159. Brandes,M., Willimann,K. & Moser,B. Professional antigen-presentation function by human gammadelta T Cells. *Science* **309**, 264-268 (2005).
160. Brandes,M. *et al.* Cross-presenting human {gamma}{delta} T cells induce robust CD8+ {alpha}{beta} T cell responses. *Proc. Natl. Acad. Sci. U. S. A* (2009).
161. Born,W.K., Reardon,C.L. & O'Brien,R.L. The function of gammadelta T cells in innate immunity. *Curr. Opin. Immunol.* **18**, 31-38 (2006).
162. Shrestha,N. *et al.* Regulation of acquired immunity by gamma delta T-cell/dendritic-cell interactions. *Ann. N. Y. Acad. Sci.* **1062**, 79-94 (2005).
163. Eberl,M., Jomaa,H. & Hayday,A.C. Integrated immune responses to infection - cross-talk between human gamma delta T cells and dendritic cells. *Immunology* **112**, 364-368 (2004).
164. Caccamo,N. *et al.* gammadelta T cells condition dendritic cells in vivo for priming pulmonary CD8 T cell responses against Mycobacterium tuberculosis. *Eur. J. Immunol.* **36**, 2681-2690 (2006).
165. Bukowski,J.F., Morita,C.T. & Brenner,M.B. Recognition and destruction of virus-infected cells by human gamma delta CTL. *J. Immunol.* **153**, 5133-5140 (1994).
166. Lafarge,X. *et al.* Cytomegalovirus infection in transplant recipients resolves when circulating gamma delta T lymphocytes expand, suggesting a protective antiviral role. *J. Infect. Dis.* **184**, 533-541 (2001).
167. Sciammas,R., Kodukula,P., Tang,Q., Hendricks,R.L. & Bluestone,J.A. T cell receptor-gamma/delta cells protect mice from herpes simplex virus type 1-induced lethal encephalitis. *J. Exp. Med.* **185**, 1969-1975 (1997).
168. Graf,D., Korthauer,U., Mages,H.W., Senger,G. & Kroczeck,R.A. Cloning of TRAP, a ligand for CD40 on human T cells. *Eur. J. Immunol.* **22**, 3191-3194 (1992).
169. Sauerbrei,A., Zell,R., Philipps,A. & Wutzler,P. Genotypes of varicella-zoster virus wild-type strains in Germany. *J. Med. Virol.* **80**, 1123-1130 (2008).
170. Schmidt,N.J. & Lennette,E.H. Improved yields of cell-free varicella-zoster virus. *Infect. Immun.* **14**, 709-715 (1976).
171. Betts,M.R. *et al.* Sensitive and viable identification of antigen-specific CD8+T cells by a flow cytometric assay for degranulation. *J. Immunol. Methods.* **281**, 65-78 (2003).
172. Penack,O. *et al.* CD56dimCD16neg cells are responsible for natural cytotoxicity against tumor targets. *Leukemia* **19**, 835-840 (2005).
173. Cohen,J.I. Varicella-zoster virus - The virus. *Infect. Dis. Clin. North. Am.* **10**, 457-& (1996).

174. Soong,W., Schultz,J.C., Patera,A.C., Sommer,M.H. & Cohen,J.I. Infection of human T lymphocytes with varicella-zoster virus: An analysis with viral mutants and clinical isolates. *J. Virol.* **74**, 1864-1870 (2000).
175. Kelsall,B.L., Stuber,E., Neurath,M. & Strober,W. Interleukin-12 production by dendritic cells. The role of CD40-CD40L interactions in Th1 T-cell responses. *Ann. N. Y. Acad. Sci.* **795**, 116-126 (1996).
176. O'Sullivan,B. & Thomas,R. CD40 and dendritic cell function. *Crit Rev. Immunol.* **23**, 83-107 (2003).
177. Gautier,G. *et al.* A type I interferon autocrine-paracrine loop is involved in Toll-like receptor-induced interleukin-12p70 secretion by dendritic cells. *J. Exp. Med.* **201**, 1435-1446 (2005).
178. Kurt-Jones,E.A. *et al.* Herpes simplex virus 1 interaction with Toll-like receptor 2 contributes to lethal encephalitis. *Proc. Natl. Acad. Sci. U. S. A* **101**, 1315-1320 (2004).
179. Mansur,D.S. *et al.* Lethal encephalitis in myeloid differentiation factor 88-deficient mice infected with herpes simplex virus 1. *Am. J. Pathol.* **166**, 1419-1426 (2005).
180. Boehme,K.W., Guerrero,M. & Compton,T. Human cytomegalovirus envelope glycoproteins B and H are necessary for TLR2 activation in permissive cells. *J. Immunol.* **177**, 7094-7102 (2006).
181. Compton,T. *et al.* Human cytomegalovirus activates inflammatory cytokine responses via CD14 and Toll-like receptor 2. *J. Virol.* **77**, 4588-4596 (2003).
182. Wang,J.P. *et al.* Varicella-zoster virus activates inflammatory cytokines in human monocytes and macrophages via Toll-like receptor 2. *J. Virol.* **79**, 12658-12666 (2005).
183. Ann Arvin & Allison Abendroth. Human Herpesviruses; Biology, Therapy, and Immunoprophylaxis. Ann Arvin *et al.* (eds.), pp. 700-712 (Cambridge University Press, New York, 2007).
184. Jennifer Moffat, Chia-Chi Ku, Leigh Zerboni, Marvin Sommer & Ann Arvin. Human Herpesviruses; Biology, Therapy and Immunoprophylaxis. Ann Arvin *et al.* (eds.), pp. 675-688 (Cambridge University Press, New York, 2007).
185. Nishimura,H. *et al.* Intraepithelial gamma delta T cells may bridge a gap between innate immunity and acquired immunity to herpes simplex virus type. *J. Virol.* **78**, 4927-4930 (2004).
186. Moffat,J.F. *et al.* Attenuation of the vaccine Oka strain of varicella-zoster virus and role of glycoprotein C in alphaherpesvirus virulence demonstrated in the SCID-hu mouse. *J. Virol.* **72**, 965-974 (1998).
187. Leslie,D.S. *et al.* Serum lipids regulate dendritic cell CD1 expression and function. *Immunology* (2008).

188. Cao,X. *et al.* CD1 molecules efficiently present antigen in immature dendritic cells and traffic independently of MHC class II during dendritic cell maturation. *J. Immunol.* **169**, 4770-4777 (2002).
189. Van Kaer,L. & Joyce,S. Viral evasion of antigen presentation: not just for peptides anymore. *Nat. Immunol.* **7**, 795-797 (2006).
190. Machesky,N.J. *et al.* Human cytomegalovirus regulates bioactive sphingolipids. *J. Biol. Chem.* **283**, 26148-26160 (2008).
191. Lawton,A.P. & Kronenberg,M. The Third Way: Progress on pathways of antigen processing and presentation by CD1. *Immunol. Cell Biol.* **82**, 295-306 (2004).
192. Torigo,S., Ihara,T. & Kamiya,H. IL-12, IFN-gamma, and TNF-alpha released from mononuclear cells inhibit the spread of varicella-zoster virus at an early stage of varicella. *Microbiol. Immunol.* **44**, 1027-1031 (2000).
193. Klagge,I.M., Abt,M., Fries,B. & Schneider-Schaulies,S. Impact of measles virus dendritic-cell infection on Th-cell polarization in vitro. *J. Gen. Virol.* **85**, 3239-3247 (2004).
194. Muller,N. *et al.* Measles virus contact with T cells impedes cytoskeletal remodeling associated with spreading, polarization, and CD3 clustering. *Traffic.* **7**, 849-858 (2006).
195. Raftery,M.J., Schwab,M., Diesner,S., Egerer,G. & Schonrich,G. Dendritic cells cross-presenting viral antigens derived from autologous cells as a sensitive tool for visualization of human cytomegalovirus-reactive CD8+ T cells. *Transplantation* **73**, 998-1002 (2002).
196. Konig,A., Homme,C., Hauröder,B., Dietrich,A. & Wolff,M.H. The varicella-zoster virus induces apoptosis in vitro in subpopulations of primary human peripheral blood mononuclear cells. *Microbes Infect.* **5**, 879-889 (2003).
197. Trinchieri,G. Interleukin-12 and the regulation of innate resistance and adaptive immunity. *Nat. Rev. Immunol.* **3**, 133-146 (2003).
198. Wang,X. *et al.* B7-H1 up-regulation impairs myeloid DC and correlates with disease progression in chronic HIV-1 infection. *Eur. J. Immunol.* **38**, 3226-3236 (2008).
199. Chen,L. *et al.* B7-H1 up-regulation on myeloid dendritic cells significantly suppresses T cell immune function in patients with chronic hepatitis B. *J. Immunol.* **178**, 6634-6641 (2007).
200. Schulz,O. *et al.* CD40 triggering of heterodimeric IL-12 p70 production by dendritic cells in vivo requires a microbial priming signal. *Immunity.* **13**, 453-462 (2000).
201. Reis e Sousa *et al.* Regulation of dendritic cell function by microbial stimuli. *Pathol. Biol. (Paris)* **51**, 67-68 (2003).

202. Aliahmadi, E. *et al.* TLR2-activated human langerhans cells promote Th17 polarization via IL-1beta, TGF-beta and IL-23. *Eur. J. Immunol.* (2009).

## Acknowledgement

My gratitude to all people, who contributed to this work and gave me mental and scientific support throughout the years.

Thanks to my doctoral thesis supervisor Prof. Detlev H. Krüger from the Charité-Universitätsmedizin Berlin for providing excellent scientific environments and equipment at the Institute of Virology.

Thanks to my scientific supervisor Prof. Günther Schönrich, who made it possible to perform this PhD thesis in his lab at the Institute of Virology.

Thanks to Martin Raftery for your expertise, help and for all the fruitful discussions.

Special thank to all the people of “AG Schönrich” who have been my second family in the past. In more detail: Nina Lütteke, Anne Rabes, Min-Hi Lee, Angela Kather and Monika Bigalke.

Many thanks to all my girls from the “Virusanzucht”. It was always a pleasure to work with you in the lab. I will miss all of you and especially your fabulous sense of humor.

Many thanks to Matthias Peiser for the great-lab company at the end of this work and your unfailing support.

Thanks to Karsten Tischer for the enlightening VZV discussions.

Thanks to Prof. Andreas Sauerbrei, who provided me with the clinical isolates of VZV and for their genotyping.

I would like to acknowledge Dennis Ernst for your kind help and support with the cryo sections.

Also, I would like to thank supporters and friends outside of work:

Katja Wagenführ, Nina Lütteke, Anne Rabes, Sybille Böhm and Manuel Hitzler for all the fun, all the parties, the discussions about science and life, and don't forget the occasional orienteering we've shared through the years!

Zum Schluss möchte ich mich von ganzem Herzen bei meiner Familie bedanken für die uneingeschränkte Unterstützung während all der vielen Jahre des ewigen Studierens. Im Speziellen bei Dir Mama für Deine Hilfe im „normalen Leben“; bei Dir Nadia für die faszinierenden Einblicke in diese Welt; bei Dir kleiner Philip, einfach dass Du da bist; und Omi und Opi für Euer grenzenloses Vertrauen in mich und meine Fähigkeiten das Leben erfolgreich zu meistern.

## **Eidesstattliche Erklärung**

Ich erkläre, dass ich die vorliegende Arbeit selbständig und nur unter Verwendung der angegebenen Hilfsmittel angefertigt habe.

Cindy Gutzeit

Berlin, im April 2009